

5-2009

## Design and fabrication of a small prototype airframe structure

Kimberly Lynn Clark  
*University of Nevada, Las Vegas*

Follow this and additional works at: <https://digitalscholarship.unlv.edu/thesesdissertations>



Part of the [Materials Science and Engineering Commons](#), and the [Structures and Materials Commons](#)

---

### Repository Citation

Clark, Kimberly Lynn, "Design and fabrication of a small prototype airframe structure" (2009). *UNLV Theses, Dissertations, Professional Papers, and Capstones*. 1169.  
<https://digitalscholarship.unlv.edu/thesesdissertations/1169>

This Thesis is protected by copyright and/or related rights. It has been brought to you by Digital Scholarship@UNLV with permission from the rights-holder(s). You are free to use this Thesis in any way that is permitted by the copyright and related rights legislation that applies to your use. For other uses you need to obtain permission from the rights-holder(s) directly, unless additional rights are indicated by a Creative Commons license in the record and/or on the work itself.

This Thesis has been accepted for inclusion in UNLV Theses, Dissertations, Professional Papers, and Capstones by an authorized administrator of Digital Scholarship@UNLV. For more information, please contact [digitalscholarship@unlv.edu](mailto:digitalscholarship@unlv.edu).

DESIGN AND FABRICATION OF A SMALL  
PROTOTYPE AIRFRAME STRUCTURE

by

Kimberly Lynn Clark

Bachelor of Science, Mechanical Engineering  
University of Nevada, Las Vegas  
2006

A thesis submitted in partial fulfillment  
of the requirements for the

**Master of Science Degree in Materials and Nuclear Engineering**  
**Department of Mechanical Engineering**  
**Howard R. Hughes College of Engineering**

**Graduate College**  
**University of Nevada, Las Vegas**  
**May 2009**

UMI Number: 1472403

### INFORMATION TO USERS

The quality of this reproduction is dependent upon the quality of the copy submitted. Broken or indistinct print, colored or poor quality illustrations and photographs, print bleed-through, substandard margins, and improper alignment can adversely affect reproduction.

In the unlikely event that the author did not send a complete manuscript and there are missing pages, these will be noted. Also, if unauthorized copyright material had to be removed, a note will indicate the deletion.

**UMI<sup>®</sup>**

---

UMI Microform 1472403  
Copyright 2009 by ProQuest LLC  
All rights reserved. This microform edition is protected against  
unauthorized copying under Title 17, United States Code.

---

ProQuest LLC  
789 East Eisenhower Parkway  
P.O. Box 1346  
Ann Arbor, MI 48106-1346



**Thesis Approval**  
The Graduate College  
University of Nevada, Las Vegas

April 23, 2009

The Thesis prepared by

Kimberly Lynn Clark

Entitled

Design and Fabrication of a Small Prototype Airframe  
Structure

is approved in partial fulfillment of the requirements for the degree of

Master of Science in Materials and Nuclear Engineering

*Examination Committee Chair*

*Dean of the Graduate College*

*Examination Committee Member*

*Examination Committee Member*

*Graduate College Faculty Representative*

## ABSTRACT

### **Design and Fabrication of a Small Prototype Airframe Structure**

by

Kimberly Lynn Clark

Dr. Brendan O'Toole, Examination Committee Chair  
Associate Professor of Engineering  
University of Nevada, Las Vegas

This project called for a first-generation prototype aircraft with hovering capabilities that was lightweight. The focus of this study was to design a small low-cost prototype composite airframe that meets specified requirements, analyze structures using finite element analysis and mechanical testing, and construct a prototype using proven composite manufacturing techniques. One fuselage, one wing, and several engine nacelles were designed and fabricated. Several design and fabrication methods and materials were analyzed, with focus given to the nacelles, and recommendations were provided for the manufacture of the first generation airframe based on time, weight, and cost.

## TABLE OF CONTENTS

ABSTRACT.....	iii
LIST OF TABLES.....	vi
LIST OF FIGURES .....	vii
ACKNOWLEDGMENTS .....	ix
CHAPTER 1 INTRODUCTION.....	1
1.1 Objectives .....	3
CHAPTER 2 REVIEW OF RELATED LITERATURE.....	5
CHAPTER 3 COMPOSITE THEORY .....	9
3.1 Introduction to Composite Materials .....	9
3.2 Micromechanics of Composite Materials .....	11
CHAPTER 4 PROTOTYPE FABRICATION OPTIONS .....	17
4.1 Rapid Prototyping .....	17
4.2 Composite Wet Lay-up .....	22
4.3 Preimpregnated Composites (Prepreg) .....	24
CHAPTER 5 MATERIAL PROPERTIES .....	27
5.1 Rapid Prototyping Materials .....	27
5.2 Carbon Fiber/Epoxy Composites .....	27
5.2.1 Carbon Fiber/Epoxy Wet Lay-Up Procedure .....	28
5.2.2 Prepreg Lay-up Procedure .....	31
5.2.3 Specimen Preparation .....	34
5.2.4 Testing Procedure .....	36
5.2.5 Results and Analysis .....	40
5.2.6 Wet Lay-Up Unidirectional Carbon Tape.....	45
5.2.7 Conclusion .....	45
CHAPTER 6 PROTOTYPE DESIGN AND FABRICATION.....	47
6.1 Wing Design and Fabrication .....	47
6.2 Fuselage Design and Fabrication .....	53
6.3 Nacelle Design .....	57

6.4 Finite Element Analysis of Nacelle Structure.....	58
6.5 Nacelle Fabrication .....	66
6.5.1 Prepreg Nacelle Construction .....	70
6.5.2 Wet Lay-up Nacelle Construction .....	76
6.6 Nacelle Compression Testing .....	78
 CHAPTER 7 DISCUSSION AND CONCLUSIONS .....	 86
 APPENDIX I MATERIAL DATA SHEET FOR CARBON PREPREG .....	 91
 APPENDIX II STRESS VS. STRAIN PLOTS FOR PLAIN WEAVE CARBON FIBER .....	 92
 APPENDIX III STRESS VS. STRAIN PLOTS FOR PREPREG CARBON FIBER ....	97
 APPENDIX IV AXIAL VS. TRANSVERSE STRAIN PLOTS FOR PLAIN WEAVE CARBON FIBER .....	 102
 APPENDIX V AXIAL VS. TRANSVERSE STRAIN PLOTS FOR PREPREG CARBON FIBER .....	 106
 APPENDIX VI SAMPLE OPTISTRUCT REPORT FOR NACELLES .....	110
 APPENDIX VII LOAD VS. DEFLECTION PLOTS FOR NACELLES.....	112
 APPENDIX VIII SAMPLE RADIOSS 9.0 REPORT FOR NACELLES .....	116
 REFERENCES .....	118
 VITA .....	120

## LIST OF TABLES

Table 4.1	Price Quotes for Rapid Prototyping by Company and Technology .....	21
Table 5.1	Properties for Common Rapid Prototyping Materials [17-21] .....	28
Table 5.1	Maximum Tensile Stress Experienced by the Specimens .....	41
Table 5.2	Tensile Modulus Values for Carbon Composite Specimens .....	43
Table 5.3	Poisson's Ratio Values for Carbon Composite Specimens .....	44
Table 5.4	Material Properties for Wet Lay-Up Unidirectional Carbon Tape .....	45
Table 6.1	Maximum Stress and Deformation in a Nacelle Loaded Along its Centerline for Various Laminates made from Prepreg Carbon/Epoxy .....	65
Table 6.2	Maximum Stress and Deformation in a Nacelle Loaded along its Centerline for Various Laminates made from Wet Lay-Up Carbon/Epoxy.....	66
Table 6.3	Properties of PBHT-30 Foam .....	67
Table 6.4	Maximum Load, Weight, and Load to Weight Ratios of Nacelles.....	82
Table 6.5	Load Results from FEA and Experimental Analysis.....	85
Table 7.1	Estimated Material Cost for Wings .....	86
Table 7.2	Estimated Material Cost for Fuselage.....	87
Table 7.3	Estimated Material Cost for Prepreg Nacelles.....	87
Table 7.4	Estimated Material Cost for Wet Lay-Up Nacelles. * - MDF was not actually used in this project .....	88



## LIST OF FIGURES

Figure 3.1	Plain Weave (a.), Satin Weave (b.), and Unidirectional Carbon Cloth (c.) .	10
Figure 4.1	Rapid Prototyped Nacelles .....	18
Figure 4.2	Diagram of Stereolithography (SLA) Process.....	19
Figure 4.3	Diagram of Selective Laser Sintering (SLS) Process.....	19
Figure 4.4	Diagram of Fused Deposition Modeling (FDM) Process.....	20
Figure 4.5	Hand Lay-Up of Carbon Fiber Cloth.....	22
Figure 4.6	Lay-Up of a Flat Carbon Prepreg Panel .....	25
Figure 5.1	Wet Lay-Up of a Flat Carbon Fiber Panel.....	29
Figure 5.2	Vacuum-Bagged Carbon Fiber Panel with Vacuum Applied .....	30
Figure 5.3	Cutting Prepreg from the Roll (Left) and Lay-Up of Flat Panels (Right) ....	31
Figure 5.4	Prepreg Panel with Vacuum Bagging in Place.....	32
Figure 5.5	Autoclave Used to Cure the Prepreg .....	34
Figure 5.6	Diagram of Specimen as Required by ASTM D3037 (dimensions in mm). 35	
Figure 5.7	Specimen with Axial/Transverse Strain Gage in Place .....	36
Figure 5.8	MTS Testing Machine.....	37
Figure 5.9	Hydraulic Grips with Specimen in Place.....	38
Figure 5.10	Axial and Transverse Extensometers on a Specimen.....	39
Figure 5.11	Strain Gage Box .....	39
Figure 5.12	Testing and Failure of Plain Weave Carbon Fiber Specimen .....	40
Figure 5.13	Plot of Stress versus Strain for Carbon Prepreg .....	43
Figure 5.14	Plot of Poisson’s Ratio for Carbon Prepreg .....	44
Figure 5.15	Carbon Prepreg Specimens After Tensile Testing .....	46
Figure 6.1	Artist’s Rendering of VTOL UAV Prototype .....	48
Figure 6.2	Model of Wing Structure: Isometric View (Left) and Front View (Right)..	49
Figure 6.3	Wing Profile Patterns .....	50
Figure 6.4	Wing Cores Cut from Closed-Cell Foam .....	51
Figure 6.5	Assembled Wing Cores with Unidirectional Fiber Reinforcement.....	51
Figure 6.6	Lay-Up of Wing Structure.....	52
Figure 6.7	Laid Up Wing Hung to Cure .....	52
Figure 6.8	Finished Wing Structure.....	53
Figure 6.9	SolidWorks Model of Fuselage .....	54
Figure 6.10	Fuselage Frame Mock-Up Construction .....	56
Figure 6.11	Complete Fuselage Frame Mock-Up.....	57
Figure 6.12	SolidWorks Model of Original Nacelle Design .....	58
Figure 6.13	SolidWorks Model of Inner Skin of Nacelle with Engine Mount.....	58
Figure 6.14	Element Orientation in FEA Model (arrows represent 0 degree direction)	61
Figure 6.15	Ply Stacking Orientation in FEA Model .....	61
Figure 6.16	Fiber Orientation by Ply ([90/0/+45/-45/0/90] Prepreg Model).....	62

Figure 6.17	FEA Model of Nacelle Showing Loading (green) and Constrains (red)....	63
Figure 6.18	Displacement Contours for [90/0/+45/-45/0/90] Prepreg Nacelle .....	64
Figure 6.19	Displacement Contours for [0/+45/-45/0] Wet Lay-Up Nacelle.....	64
Figure 6.20	SolidWorks Model of Central Mold Piece. Final Design Shown on Right	68
Figure 6.21	SolidWorks Model of Mandrel: Assembled (Left) and Exploded View....	68
Figure 6.22	In-House CNC Mill .....	69
Figure 6.23	Nacelle Mold .....	69
Figure 6.24	Fiber Orientation for Prepreg Lay-Up.....	71
Figure 6.25	Prepreg Nacelle Lay-Up (Left) and Preparation for Cure .....	71
Figure 6.26	Prepreg Nacelle Under Vacuum (Left) and Ready for Cure in Autoclave.	72
Figure 6.27	Removal of Mold from Cured Nacelle.....	73
Figure 6.28	Damage Caused by Nacelle Removal .....	73
Figure 6.29	Surface Damage from Second Prepreg Lay-up .....	75
Figure 6.30	Finished Prepreg Nacelle.....	75
Figure 6.31	Fiber Orientation for Wet Lay-Up.....	77
Figure 6.32	Wet Lay-Up of Nacelle (Left) and Preparation for Cure .....	77
Figure 6.33	Finished Wet Lay-Up Nacelle .....	78
Figure 6.34	Compression Test Set-Up with Three-Point Bend Fixture.....	79
Figure 6.35	Compression Test of Woven Nacelle .....	80
Figure 6.36	Plot of Load Versus Deflection for Sample Specimens .....	81
Figure 6.37	Load and Constraint Locations for FEA: Isometric (left) and Front Views	83
Figure 6.38	Contour Plot of Displacement for Prepreg Nacelle.....	83
Figure 6.39	Contour Plot of Displacement for Wet Lay-Up Nacelle .....	84

## ACKNOWLEDGMENTS

I would like to thank Dr. Brendan O'Toole for acting as my advisor and providing me with the opportunity to work on this project, and my committee members for their time and support. I would also like to thank Tom Higgins and Richard Jennings for their invaluable help in fabricating the prototype airframe. I want to thank Stacy Nelson, Jagadeep Thota, and Robert O'Brien for their help in the development of my thesis. Finally, I would like to thank my friends and family who have supported me during my studies.

## CHAPTER 1

### INTRODUCTION

Prototyping is a necessary step in most manufacturing processes. The value of a prototype lies in the ability to prove design intent and spot potential issues, whether in the manufacturability or in the application of the design, that were not noticed in a computer model or drawing. It gives the designers a good feel for the appearance and functionality of the design. Unfortunately, prototyping is costly and time-consuming and is very difficult to do on a small budget and limited time schedule. It is especially difficult to develop a proper prototype or remain on schedule when the customer modifies the requirements of the product every couple months. Sometimes the prototype must be fully functional and may not go into full production; a prototype satisfying this requirement is labeled as “one-off” or single item production run.

Airframes in particular require close attention to weight. Taking payload into consideration, an aircraft frame must be constructed light enough to attain proper altitude with the given power system. A vertical take-off and landing (VTOL) airframe demands even more attention, since the weight of the aircraft plus payload cannot exceed the thrust provided by the motors; ideally the total weight should be less than the applied thrust for the aircraft to gain altitude. It is therefore important that the airframe designer knows the

payload weight for the aircraft prior to designing the airframe, since material choice and structural design are heavily reliant on this information.

Several avenues exist for developing a functional prototype. One option is to use composite materials laid up in molds or over cores to create a strong, lightweight airframe. Another is to rapid prototype the airframe, which is a quicker, less labor intensive alternative to laying up a composite prototype, but the materials are generally heavier than and not as strong and stiff as fiber reinforced composites. The method of fabrication of the prototype must be determined early on in the design, which presents a challenge. Options for composite material fabrication include:

1. *Wet lay-up without vacuum bagging*

This process is the simplest and least expensive but provides a low fiber volume fraction and thus the part is heavier than and not as strong as a vacuum bagged part or a part made from preimpregnated (prepreg) material.

2. *Wet lay-up with vacuum bagging*

Vacuum bagging a part after a hand lay-up provides better, albeit not ideal, resin consolidation.

3. *Resin infusion or resin transfer molding (RTM)*

RTM results in good resin consolidation and can be comparable to prepreg in terms of structural efficiency. It involves vacuum bagging and can be cured at room temperature or at an elevated temperature. This process requires more set-up than a wet lay-up with vacuum bag and is therefore more expensive.

4. *Prepreg*

Since the resin is mechanically applied in a prepreg material prior to use, and thus an optimal quantity of resin is used, it has the best resin consolidation of any of the processes listed. Parts created from prepreg materials generally have the best strength and stiffness to weight ratios. Prepreg is usually the most costly form of fabrication due to the pre-impregnation, the complexity of the lay-up, and the necessity of a pressurized high-temperature cure.

These processes, along with the rapid prototyping alternative, are explained in further detail in Chapters 4 and 5.

Facilities focused solely on research and design, such as universities and research laboratories, generally create one or two functional prototypes for testing and never venture into full production. Researchers can gather experience from previous projects that can be applied to new projects, which speeds up the research and design processes in those projects (this is not always the case since not all experience can be applied to every project). Universities, on the other hand, employ students to conduct a large portion of their research. Students generally cycle through every two to three years and thus new students are always being trained. Since students lack the years of experience garnered by professionals, this training time must be factored in to the time estimates for prototype production in a university setting.

## 1.1 Objectives

This thesis was developed with the intention of quantifying the previously qualitative process of small aircraft composite prototype fabrication specific to a university or a research laboratory setting. This is done by comparing the fabrication cost and time of

the prepreg and wet lay-up processes, the structural integrity of the parts, and the personnel training required to complete the lay-ups and perform mechanical testing. The entire process of fabricating a first-generation composite aircraft frame, from computer aided design (CAD) design to manufacturing, is described in this paper. The aircraft design is a quad-rotor VTOL vehicle with rotating nacelles located at the extremities of the airframe. The first prototype is only intended to demonstrate hovering capabilities (no translational flight), so the structural integrity of the fuselage and the wings is not important. However, due to their location, the nacelles may be prone to impact during flight testing. Emphasis is given to the aircraft nacelles, which epitomize the research process in this project. Therefore, several nacelles will be tested in compression to verify finite element analysis (FEA) data.

Material characterization experiments will be conducted to determine material properties for use in FEA to predict the load deflection response of the nacelles. Finite element simulations will be compared to the experimental data to determine the effectiveness of the FEA software in predicting composite material behavior. The paper concludes by summarizing the information gathered from the research and utilizing it to compare the positive and negative aspects of each prototyping method.

## CHAPTER 2

### REVIEW OF RELATED LITERATURE

Miniature (mini) unmanned aerial vehicles (UAVs) are divided into two categories: micro UAVs, with wingspans under 6 inches (DARPA target size), and man-portable UAVs [1]. The appeal of mini UAVs is their potential application in a modern war environment; i.e., smaller, remotely-piloted aircraft are ideal for urban warfare where small size and agility mean an aircraft can cruise down narrow corridors and even travel inside structures to obtain information for troops. Their utility stretches beyond military use as civilian companies are noticing the benefit to having remote surveillance equipment to monitor items that are difficult for workers to access, such as remote power lines and gas pipelines.

Smaller sizes generally require small engines, which result in a large decrease in power, necessitating a lightweight airframe. Even greater decreases in airframe weight can allow for increases in payload capacity, depending upon engine choice. Therefore, fiber-reinforced composite materials are an attractive choice for various UAV components, including the fuselage and wings.

C. Soutis [2] stated that focus on cost reduction of composite parts manufacturing is important for the future of the aircraft industry. The author touted the superiority of carbon fiber reinforced plastics (CFRPs) in aerospace manufacturing, citing high



modulus and strength properties, as well as weight reduction, versus metal alloy materials. However, Soutis mentioned that CFRP parts should not merely be manufactured in the same shape as traditional aluminum and titanium alloy components; because of the fibers' ability to take on compound curvatures and its anisotropic properties, it should be exploited to its fullest capabilities.

K. Uzawa et al [3] and M. Niitsu et al [4] also emphasized low cost in their design and construction of the HOPE-X, a space reentry aircraft. Tooling costs should be reduced as much as possible, they stated, since tooling accounts for a large amount of the overall cost of a low-production or one-off aircraft. Other keys to reducing costs are to avoid needing an autoclave for curing and to reduce the number of components. The authors were also concerned with weight and chose to omit fasteners wherever possible and instead joined parts using more composite material.

Previous mini UAV designs have been attempted. K. Kotwani [5] utilized a simple traditional airplane platform with a wingspan of 91.4 cm (3 ft) and a single dual-blade propeller. This design was lightweight, but it could only be applied in open settings and lacked any hovering capabilities. Kotwani also failed to explore the unique characteristics of the CFRP he chose; his design used simple shapes from existing aircraft originally manufactured using metal alloys.

J.R. Chou and S.W. Hsiao [6] broke down prototyping into three main steps in their creation of a composite electric scooter: CAD design and physical solid modeling, body and frame construction, and assembly of all mechanical, electrical and computer components.

Another option for prototype or tooling fabrication is rapid prototyping. O'Donnchadha et al [7] looked at selective laser sintering (SLS) as an option in manufacturing tooling. The benefit of SLS, they state, is the durability of many of the materials that can be used by the machines, which lends itself to use as a functional part, whether as tooling or as a final component in a product. The authors also point out that a single SLS machine can utilize any material resulting in a lower cost part, unlike EOS GmbH's DirectTool system, for example, which can only use one material per machine.

F. K. Chang and Z. Kutlu [8] explored the mechanical responses of unidirectional carbon prepreg cylinders under compressive loads. Since cylindrically shaped composite parts respond greater to out-of-plane loading than flat plates, for example, it is important to determine the magnitude and by what means failure occurs so that the design can compensate for the behavior. The authors studied two types of loading along the length of the cylinder: plate loading, where the cylinder was sandwiched between two solid plates, and line loading, where two thin bars compressed the cylinder along a narrow line down its length. They looked at the initial failure and maximum loads and the modes of failure of the cylinders. They tested several fiber orientations and recorded the load and the displacement for each cylinder.

Mold material selection, particularly for prepreg lay-up, is another important consideration for the project. In a study by D. L. McLarty [9], several composite mold materials were evaluated. The author listed a number of guidelines for comparing the materials, the most important being vacuum integrity, dimensional stability (determined by the material's coefficient of thermal expansion), and springback during cure. The third guideline is specific to composite materials as it is a behavior of the matrix.

It was necessary to obtain material property data via mechanical testing for the materials used in this project. In their study, Y. Tomita and M. Tempaku [10] performed tensile tests on unidirectional carbon/epoxy composites of different tensile fracture stresses to determine the failure behavior between notched and unnotched specimens. Their results showed that the material with the higher tensile fracture stress leads to higher tensile strength in the unnotched specimen but lower strength in the notched specimen than the material with the lower tensile fracture stress. The unnotched specimen with the lower fracture stress failed in a jagged manner perpendicular to the applied load while the unnotched specimen with the higher fracture stress failed parallel to the load.

M. Kawai et al [11] have shown that end tab geometry affects the strain experienced by composite specimens. Rectangular end tabs created large differences in the axial and transverse strains depending on strain gage location while oblique tabs negated the difference, showing that strain gage location was not critical.

S. R. Akanda et al [12] showed that the strain rate affects the elastic modulus and the tensile strength of fiber-reinforced epoxy composites. Their tests revealed that the elastic modulus and the tensile strength of the material increased as the strain rate increased; however, a higher strain rate led to a lower failure strain.

## CHAPTER 3

### COMPOSITE THEORY

Before delving in to the processes of composite lay-up, it is important to gain a little understanding of the theory behind composite materials since their behavior is vastly different from isotropic materials.

#### 3.1 Introduction to Composite Materials

Fiber-reinforced composites consist of strands of a reinforcing material surrounded by a matrix material that performs the task of holding the fibers together and distributing any applied loads. Typical reinforcing materials are fiberglass, carbon/graphite, and Kevlar fibers; matrix materials include plastics, metals and ceramics. The composites used in this study are carbon fiber reinforced epoxies, so the focus of this chapter will be on these composites.

Carbon fibers have a high tensile strength and elastic modulus with respect to their weight, making them an appealing option for applications that require strong, stiff, lightweight materials. The fibers are initially manufactured in single filaments and then bundled together into tows. Tow size, generally referred to by the number of filaments in each one, can range from 1,000 to 160,000 [13]. The tows are then used to create fabrics

and other performs using standard textile processes. The most common carbon fiber cloths contain 3,000 filaments per tow, referred to as 3K carbon fiber.

The fibers come from the manufacturer in many different forms depending on the application. Unidirectional fibers are laid in one direction, thus the composite strength will lie in only that direction. Plain weave carbon cloth is composed of fibers laid in the 0 and 90 degree directions, with a one over/one under weave pattern. Satin weave employs the same concept, but instead the weave pattern is two over/two under. The looser weave provides better contouring over complex geometries at the risk of the weave pulling apart during the lay-up. Unidirectional cloths are held together with a small amount of material, usually fiberglass or polyester, running perpendicular to the fibers. Examples of these are shown in Figure 3.1.

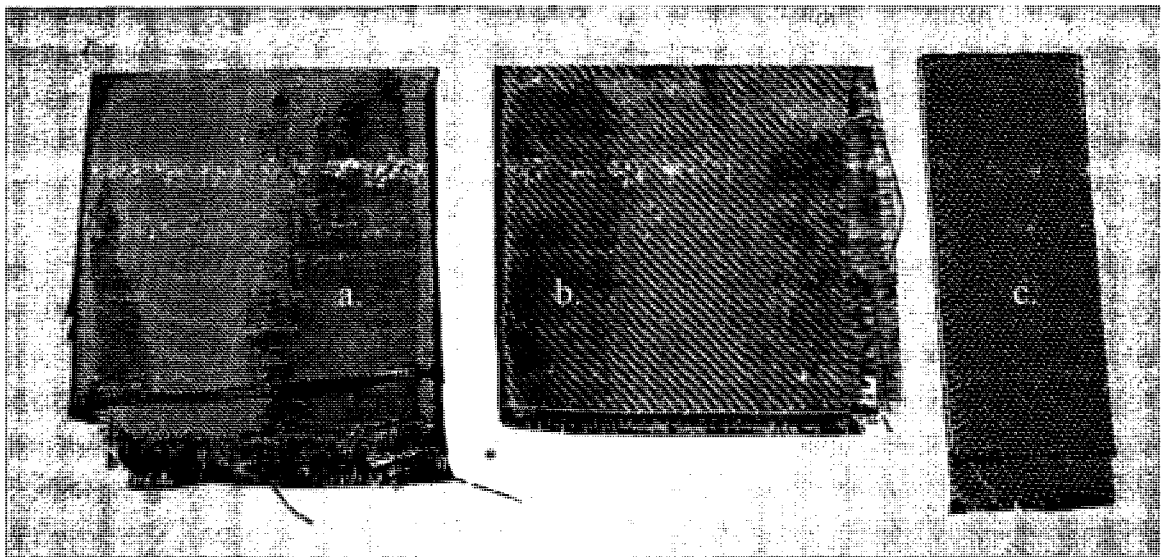


Figure 3.1 Plain Weave (a.), Satin Weave (b.), and Unidirectional Carbon Cloth (c.)

Epoxy resins fall into the class of thermoset matrices, which lies within the broader class of polymeric matrices. Thermosets cure via a chemical reaction between an epoxy and a hardener (catalyst), resulting in a material that cannot be remelted and remolded. Epoxies have good mechanical properties, are thermally stable and are very resistant to chemicals [13].

### 3.2 Micromechanics of Composite Materials

An important factor for determining composite material properties is the fiber volume fraction (FVF) of the composite. The FVF is the volume of fiber present in the composite relative to the total volume of the part. It can be found using Equation 3.1:

$$V_f = \frac{w_f / \rho_f}{w_f / \rho_f + (1 - w_f) / \rho_m} \quad \text{Eq. 3.1}$$

Where  $w_f$  and  $\rho_f$  are the weight fraction and density of the fibers, respectively, and  $\rho_m$  is the density of the matrix. The volume fraction of fibers in the composite can never be 1; the maximum FVF can be calculated by assuming that all the fibers are perfectly aligned and positioned in a closely packed hexagonal array, shown in the diagram in Figure 3.2a. Assuming that the distance between the centers of two adjacent fibers is equal to  $2r$  and the height of the triangle is  $\sqrt{3}r/2$ , the maximum FVF can be determined by dividing the area of half of the circle (amount of fibers within the triangle) by the area of the triangle as shown in Equation 3.2:

$$V_f^{\max} = \frac{\pi r^2 / 2}{2\sqrt{3}r^2 / 2} = \frac{\pi}{2\sqrt{3}} = 0.91 \quad \text{Eq. 3.2}$$

The hexagonal arrangement is an idealized packing geometry. Instead, the fibers are usually arranged in a square array, such as that shown in Figure 3.2b. In this orientation, the maximum theoretical FVF is about 79 percent.

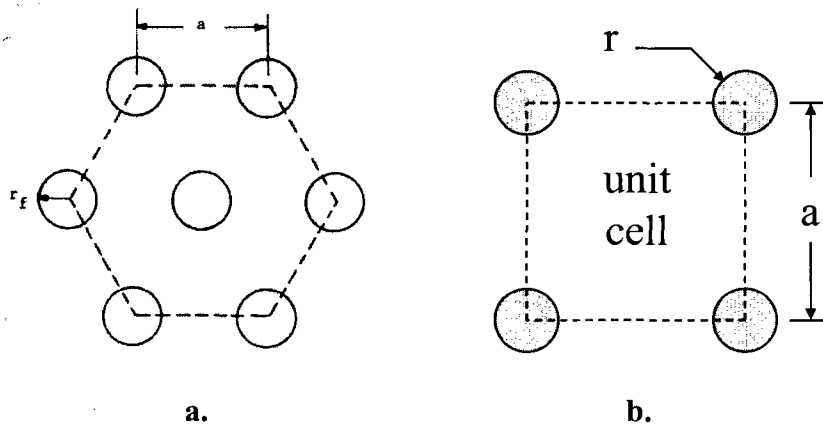


Figure 3.2 Fiber packing geometry: hexagonal array (a.) and square array (b.)

In a material with a FVF of 80 percent or more, the composite lacks enough matrix material to hold the fibers together effectively and transfer any loading. Therefore, a realistic maximum FVF is about 70 percent. The prepreg material used in this study, for example, has an average FVF of 60 percent after autoclave processing. This value is important in determining the theoretical properties of FRC materials such as elastic modulus and Poisson's ratio.

The void content of a composite is another important physical factor. Voids can drastically alter some of the mechanical properties of the composite. This value is

determined by comparing the actual density,  $\rho$ , of the composite to its theoretical density,  $\rho_c$ , as shown in Equation 3.3:

$$V_v = \frac{\rho_c - \rho}{\rho_c} \quad \text{Eq. 3.3}$$

It is best to have a void content below 2 percent to avoid altering the mechanical properties.

Materials that exhibit no change in properties depending on the orientation of the load are considered isotropic; such materials include metals, plastics, and ceramics. Continuous fiber-reinforced materials do not exhibit the same properties in all directions; they show property symmetry in up to three planes, called the principal material directions; thus they are considered orthotropic. Isotropic material properties include the Young's modulus ( $E$ ), Poisson's ratio ( $\nu$ ), and the shear modulus ( $G$ ). For an orthotropic material, these properties change depending on the principal material directions. This means that there are three values for each of these properties, for a total of nine. Thin-walled, two-dimensional unidirectional fibers are special in that these elastic constants can be reduced to  $E_1$ ,  $E_2$ ,  $\nu_{12}$ ,  $\nu_{21}$ , and  $G_{12}$ . Four of these constants are independent since  $E_2 = (\nu_{21}/\nu_{12})E_1$ . The FVF and individual properties of the fibers and the matrix can be used to estimate these values using the simplified Rule of Mixtures equations (Equations 3.4 through 3.7):



$$E_1 = E_f V_f + E_m (1 - V_f) \quad \text{Eq. 3.4}$$

$$E_2 = \frac{E_f E_m}{E_m V_f + E_f (1 - V_f)} \quad \text{Eq. 3.5}$$

$$\nu_{12} = \nu_f V_f + \nu_m (1 - V_f) \quad \text{Eq. 3.6}$$

$$\frac{1}{G_{12}} = \frac{V_f}{G_f} + \frac{(1 - V_f)}{G_m} \quad \text{Eq. 3.7}$$

Several mechanical properties are examined when selecting a composite material for a specific application. The first property is stress; this is the amount of loading experienced by the material per unit area of its cross section, shown in Equation 3.8:

$$S_x = \frac{P_x}{A} \quad \text{Eq. 3.8}$$

Where  $P_x$  is the load applied in the x-direction and  $A$  is the cross-sectional area. The ultimate tensile strength is always calculated using the largest stress value of the material under axial loading.

The elastic modulus, also known as Young's modulus when referring to the tensile modulus, is a numerical value representing a material's elasticity, or ability to deform. A

higher elastic modulus indicates a material that deforms little under stress. Equation 3.9 is generally used to find the Young's modulus, where  $\sigma_t$  is the tensile stress and  $\epsilon_t$  is the tensile strain of the specimen:

$$E = \frac{S_t}{\epsilon_t} \quad \text{Eq. 3.9}$$

The elastic modulus, like stresses, is different for each principal material direction in a composite.

Poisson's ratio is the ratio of the transverse strain versus the axial strain and therefore is a unitless value. It reveals the magnitude at which deformation in one direction affects deformation in the other direction. It can generally be calculated by Equation 3.10, where  $\epsilon_x$  is the strain in the transverse direction and  $\epsilon_y$  is the strain in the axial direction:

$$\nu = -\frac{\epsilon_x}{\epsilon_y} \quad \text{Eq. 3.10}$$

The negative sign is necessary since compression, represented as a negative value, generally occurs in one of the directions and  $\nu$  is always positive. Most materials will have a Poisson's ratio between 0 and 0.5; a value of 0 means the material will completely compress in one direction (i.e. it experiences a significant volume reduction), whereas a

value of 0.5 corresponds to a material that will experience virtually no compression (i.e. no volume change).

The elastic modulus and Poisson's ratio equations are simplified since all of the material analysis in this paper is done on specially orthotropic materials. If the loading were applied off of the axial direction, the equations for these properties would be much more involved.

Woven composites have poorer strength properties than unidirectional composites because the weave of the material creates stress concentrations at the intersections of the fiber strands. The fibers are also undulated, not straight, thus further reducing the strength and increasing the axial strain of a woven material. However, woven materials exhibit better properties in the transverse direction, where unidirectional composites are weakest.

## CHAPTER 4

### PROTOTYPE FABRICATION OPTIONS

Prototyping is an essential step in manufacturing; however, it can be costly and time-consuming. It can also require the use of complex tooling and manufacturing that may be used only once or twice. Several avenues exist for creating a one-off model, including rapid prototyping and composite wet and prepreg lay-ups, which were evaluated in this study.

#### 4.1 Rapid Prototyping

The need for quicker prototyping has led to new technologies, including three-dimensional printing, also known as rapid prototyping. Initially designed to provide visual representations of a design, rapid prototyping machines have evolved to produce functioning components using an ever-increasing range of materials. An example of a rapid prototyped part is shown in Figure 4.1. With any rapid prototyping technology, a CAD file is directly imported to the machine as a .stl file. The most common rapid prototyping technologies include stereolithography (SLA), selective laser sintering (SLS), and fused deposition modeling (FDM).

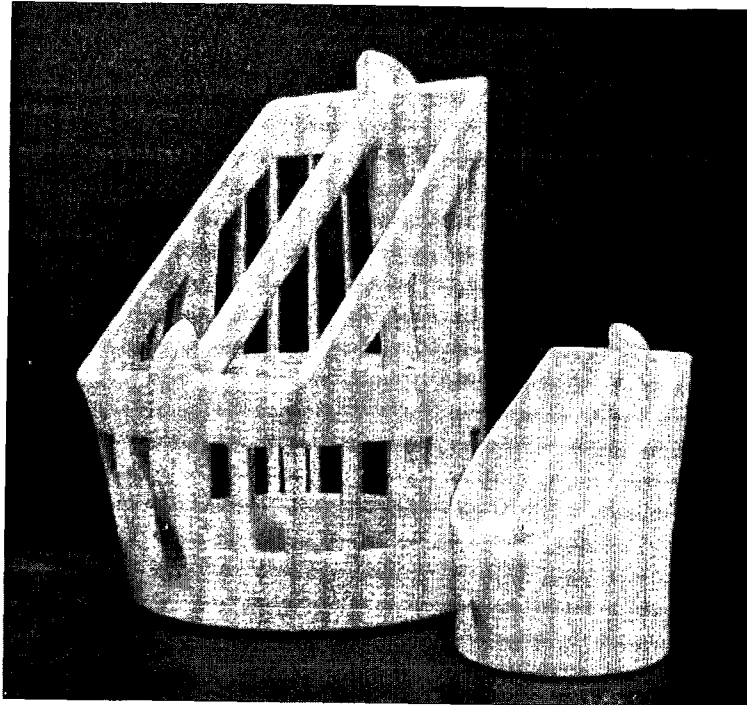


Figure 4.1 Rapid Prototyped Nacelles

In SLA, the material is held in a vat in a liquid state until it is hardened by a laser. The machine builds the part from the bottom up inside the vat, adding a new layer as the platform moves down in increments equal to the thickness of each layer. Dissolvable supports are printed into the model where necessary and then later removed. SLA machines use photopolymer resins that simulate common materials, such as ABS plastic and polypropylene [14-16]. A diagram of the SLA process is shown in Figure 4.2.

SLS is similar to SLA in the way that it builds the model in layers from the bottom up. Unlike SLA, SLS utilizes materials in powder form, allowing for a wider range of material options, including plastics, ceramics, and metals. A laser traces the cross-section of the model in the powder, fusing the particles together to create the part. The variety of materials results in parts that can be used in working prototypes or even in low-production final products [14-16]. The SLS process is depicted in Figure 4.3.

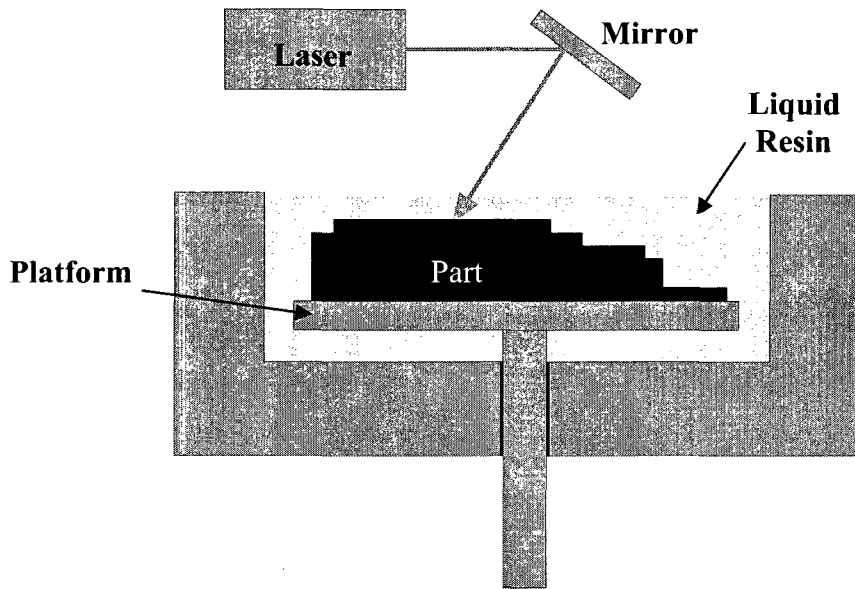


Figure 4.2 Diagram of Stereolithography (SLA) Process

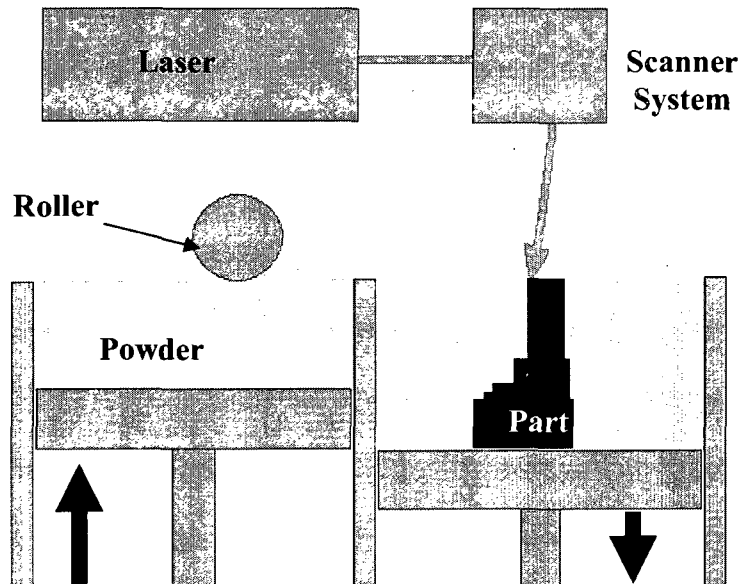


Figure 4.3 Diagram of Selective Laser Sintering (SLS) Process

FDM uses thermoplastic material fed through an extrusion head that heats the material to just above its melting temperature. Like the two aforementioned methods, the

platform moves vertically while the head moves in the horizontal plane to create the part. The part is built from the bottom up in layers similar to both SLA and SLS. FDM mostly utilizes common plastics, including ABS, polycarbonate, and polyethylene [14-16]. Figure 4.4 shows a schematic of the FDM process.

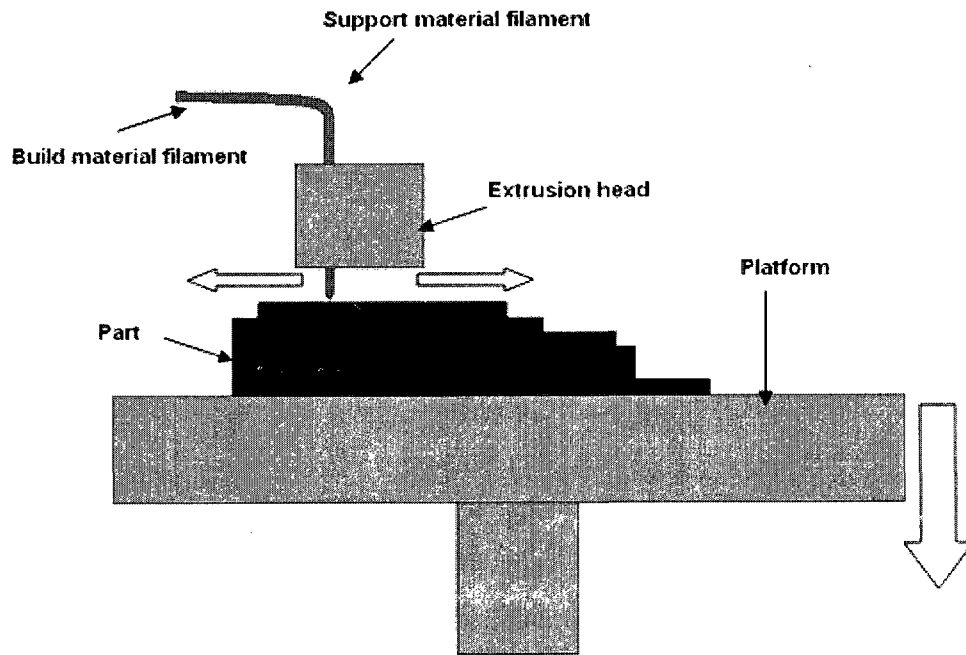


Figure 4.4 Diagram of Fused Deposition Modeling (FDM) Process

One drawback to rapid prototyping is the high capital cost, which ultimately results in high-cost products. Other drawbacks include the limited materials available versus other prototyping methods (more and more materials are becoming available every year however), the limited strength of the materials (although with certain treatments, some materials can come close in strength to cast materials), and the weight of the finished part, which is much greater than an equivalent fiber composite part, even when using plastics. While the cost is worth the time saved for companies with large budgets, other

organizations such as universities usually lack the funding to pursue this option. In the latter case, it may be more economical to create a prototype using slower but less expensive means.

At the onset of this project, rapid prototyping (RP) was considered as a fabrication option. Price quotes were obtained from several prototyping companies, which are listed in Table 4.1 (the different RP methods were explained in Chapter 2, Section 1). The quotes were based on a simple cylinder 16 inches in length with a ten inch diameter and a wall thickness of 0.125 inches, roughly the dimensions of the aircraft nacelles. The costs ranged from \$1,350 to \$4,995, with an average cost of around \$2,350. The cost was determined to be too high for the limited budget for the project; the fiber reinforced composite airframe option was therefore chosen since the design group had access to woven and prepreg carbon fiber materials and the necessary equipment to cure them. Unfortunately, this option was very time-consuming, requiring CNC-machined molds and hand lay-ups. For the small airframe project, the other prototyping options included a hand lay-up of carbon fiber cloth and a prepreg lay-up of unidirectional carbon fiber, or a combination of the two.

Table 4.1 Price Quotes for Rapid Prototyping by Company and Technology

Company	Method	Material	Cost	Notes
ProtoCAM	SLA	various	\$4,995	part made in 1 piece
	SLA	various	\$2,895	part made in 2 pieces, glued after printing
Solid Concepts	SLS	DuraForm GF	\$1,577	
	SLS	NyTek 1100	\$1,697	
	SLS	Alumide	\$1,575	
Tech, Inc.	SLA	11120	\$1,350	



## 4.2 Composite Wet Lay-up

Carbon fiber composites can be manufactured using a variety of methods. Most common in small-scale manufacturing is the hand lay-up technique, which involves manually placing the carbon cloth or strands in the desired orientation and infusing it with the matrix material (usually an epoxy resin that flows readily) using hands, brushes, squeegees, or any other efficient tool (Figure 4.5). This method is easy to set up and requires no advanced tools; however, it is time-consuming and labor-intensive and does not provide a good fiber volume fraction (FVF) due to the inability to remove much of the excess matrix material.



Figure 4.5 Hand Lay-Up of Carbon Fiber Cloth

Vacuum-bagging the part after a hand lay-up can partially alleviate the fiber volume fraction issue. While still lacking the ability to achieve an ideal FVF, vacuum-bagging

significantly reduces the amount of matrix material left in the part. The technique is more complex than a simple hand lay-up: the piece and the mold (if one is used) must be covered in a vacuum bag sealed with a special removable adhesive. A vacuum pump pulls the air and excess resin from the assembly in a set up as to not allow any pulled resin to enter the pump (usually done with a sump). The final piece has better resin consolidation than a hand lay-up piece. The hand lay-up procedure for carbon cloth is covered in detail in Chapter 5.

Resin transfer molding (RTM) is another wet lay-up option. The fiber cloth is laid onto a mold while dry, allowing for easier manipulation and thus better control over the orientation of the fibers. The part is then sealed, either with another mold piece or vacuum bagging (vacuum-assisted resin transfer molding, or VARTM), and the resin is pumped out of a vat or container and through the part. Once the fibers are saturated, the excess resin is pumped out of the mold and the part is cured. This method provides the best FVF of almost any wet lay-up method, but it is difficult to execute and even more difficult to perfect. RTM is being considered for future fabrication on this project, but was not used for the first set of components because of its complexity.

The cost of the hand lay-up manufacturing option is reasonable. US Composites, a composite material distributor from whom UNLV obtains its cloth and resin, sells its FG-CARB5750 plain weave carbon cloth from \$37 to \$47 per meter (\$34 to \$43 per yard), depending on the quantity ordered. The 635 Thin Epoxy Resin System with a 3 to 1 epoxy/hardener ratio can be purchased for \$16 per liter (\$61 per gallon) ([www.uscomposites.com](http://www.uscomposites.com)). Tooling is relatively inexpensive for wet lay-ups since heat is not required for curing. Medium density fiberboard (MDF) is a popular choice because of

its low cost, light weight, and machinability. MDF costs over \$10 per square meter (\$1 per square foot) at local home improvement stores for a 12.7 mm (0.5 in) thick board.

The equipment needed for RTM would increase the cost of manufacturing. RTM requires pumps, hoses, and vats along with the typical equipment required for a vacuumed lay-up. VARTM is not as complicated and utilizes the same equipment as a vacuumed lay-up, but it is difficult to obtain a perfect part without some amount of experience with the process, so more material will be used in trying to optimize the technique.

#### 4.3 Preimpregnated Composites (Prepreg)

Prepreg consists of fiber strands infused with partially cured epoxy resin or other matrix. The temperature-sensitive matrix requires the material to be stored at a low temperature prior to use and has a limited shelf life. Prepreg also demands special consideration with respect to mold material since it requires elevated temperatures for curing.

The material is laid out on the mold similar to dry fabric. The prepreg is carefully pressed onto the mold and any bubbles between the layers are worked out. The part is placed in an autoclave or oven where heat and pressure are applied. The absence of a pressurized autoclave for cure necessitates the use of a vacuum – the part is vacuum-bagged and a vacuum is pulled on it prior to applying heat. This process is shown in Figure 4.6 in the creation of a flat panel. A more detailed description of the lay-up procedure is provided in Chapter 5.

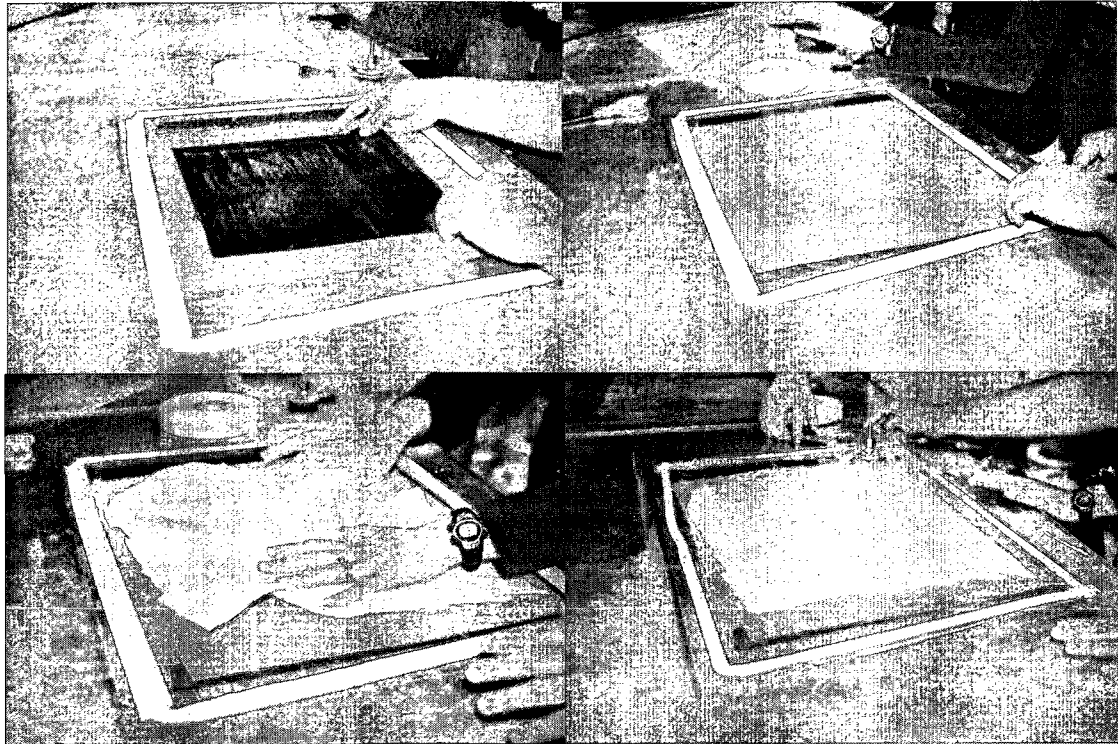


Figure 4.6 Lay-Up of a Flat Carbon Prepreg Panel

Prepreg is advantageous if weight reduction is a concern. However, the prepreg and the tooling materials are more expensive than standard wet lay-up materials and necessitate the use of special equipment, such as an autoclave and high-temperature tooling, for curing. The prepreg used for this project is NCT-301 34-700 tape manufactured by Newport Adhesives and Composites, Inc., and sells for around \$121 per kilogram (\$55 per pound) ([www.newportad.com](http://www.newportad.com)). The prepreg uses 34-700 unidirectional carbon fiber ([www.grafil.com](http://www.grafil.com)). Aluminum is a popular option for tooling material since it is lighter and easier to machine than steel; 6061 aluminum stock runs \$11.50 per kg (about \$5 per lb) from McMaster-Carr ([www.mcmaster.com](http://www.mcmaster.com)). Another tooling material option is high-density, high-temperature foam manufactured by Coastal Enterprises, which costs about \$13.50 per kg (about \$6 per lb) for their PBHT-30

Precision Board ([www.precisionboard.com](http://www.precisionboard.com)). The foam requires a temperature-resistant coating due to its porosity; this project utilized Duratec Vinylester Primer, available from RevChem at \$19 a liter (\$73 a gallon) ([www.revchem.com](http://www.revchem.com)).

## CHAPTER 5

### MATERIAL PROPERTIES

It is important to determine the mechanical properties of the materials that are used in any structurally significant component to predict the behavior of the component under various loads. Properties such as elastic modulus and Poisson's ratio can be found by performing tensile tests. The rapid prototyping materials were not available for testing in this study, so the data were compiled from various rapid prototyping companies. The carbon composites were tested and the procedures for testing, along with the data, are outlined in Section 5.2.

#### 5.1 Rapid Prototyping Materials

The material properties for various rapid prototyping materials are displayed in Table 5.1. The materials listed are only a sampling of the many materials available. UNLV only has access to a 3D Systems three-dimensional printer that uses ABS plastic material, but printing can be outsourced to a rapid prototyping company.

#### 5.2 Carbon Fiber/Epoxy Composites

Material properties for the wet lay-up plain weave carbon fiber fabric and for the unidirectional carbon prepreg were found via tensile tests performed in accordance with

ASTM Standard D 3039. The specimen preparation and testing procedures are described in detail in the following section, followed by the results of the tests.

Table 5.1 Properties for Common Rapid Prototyping Materials [17-21]

Material	Specific Gravity	UTS (MPa)	Elastic Modulus (GPa)
<b>SLA</b>			
Accura 50	1.21	48.0	2.48
Accura SI 40	1.1	57.0	2.63
ProtoTherm 12120	1.15	77.0	3.25
ProtoTool 20L	1.6	72.0	10.10
Somos 9120	1.13	30.0	1.23
WaterClear 10110	1.12	43.0	2.04
WaterShed 11110	1.12	48.0	2.64
<b>SLS</b>			
Alumide	1.36	46.0	3.80
CastForm PS	0.46	2.8	1.60
DuraForm PA	0.59	43.0	1.59
DuraForm GF	0.84	26.0	4.07
NyTek 1100	1.04	41.0	1.39
<b>FDM</b>			
ABS	1.05	22.0	1.63
Polycarbonate	1.2	52.0	2.00
PC/ABS	1.1	35.0	1.83
Polyphenylsulfone	1.28	55.0	2.07

### 5.2.1 Carbon Fiber/Epoxy Wet Lay-Up Procedure

A 3K 0/90 plain weave carbon fiber cloth, available from US Composites as part number FG-CARB5750, was laid up using a simple wet hand lay-up procedure. The plain weave fabric had a thickness of 0.30 mm (0.010 in). Lay-up began with cutting eight pieces of cloth along the fiber directions to 56 cm by 42 cm (22 in by 16.5 in). A large sheet of acrylic was waxed prior to lay-up to ensure easy removal after cure, and then the

first piece of carbon cloth was laid out and wetted with a 635 thin epoxy resin from US Composites with a mixing ratio of 3 to 1, a pot life of 20 to 25 minutes and a cure time of 8 to 10 hours (www.uscomposites.com). After the first layer was completely saturated, the next layer was added and the process was repeated until all eight layers were stacked with the fibers laid in the same direction. Excess resin was removed from the panel using a squeegee (Figure 5.1).



Figure 5.1 Wet Lay-Up of a Flat Carbon Fiber Panel

A square of Teflon peel-ply, cut larger than the panel, was placed on top, followed by a cut of breather cloth. The peel-ply allows resin to flow from the part while keeping the part itself from adhering to the breather cloth. It also provides a finely roughened surface to the finished part. The surface needs no additional preparation (e.g. sanding) prior to bonding other components to the finished part. The breather cloth, also known as bleeder or absorber cloth, is a thick, lightly woven polyester material that allows the resin to flow easily from the part and prevents the vacuum bagging from completely collapsing against



the part when a vacuum is pulled. It holds most of the excess resin during cure, preventing it from reaching the vacuum hose. Vacuum bag tape was laid around the perimeter of the assembly and vacuum bagging was placed over the panel. The bottom piece of the vacuum pump valve was placed under the bagging and a slit was cut in the bagging above it for the top piece of the valve to twist on. The vacuum lines were attached and the vacuum pump was turned on (Figure 5.2). The bagging was examined for leaks, which were subsequently filled using more tape, prior to leaving the part to cure for 24 hours. After the cure period, the bagging, breather cloth and peel ply were removed and the panel was trimmed to about 52 cm by 38 cm (20.5 in by 14.9 in). The final plate had a thickness of about 2.5 mm (0.1 in) and a weight of 624 grams. The plate had a density of 1.26 g/cm<sup>3</sup>.

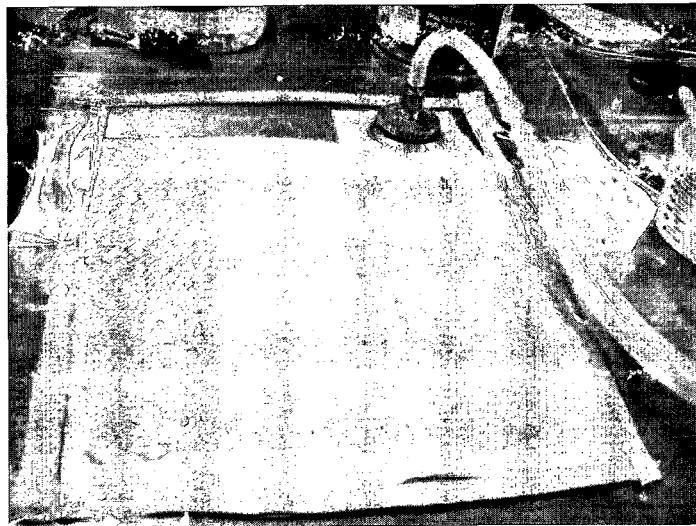


Figure 5.2 Vacuum-Bagged Carbon Fiber Panel with Vacuum Applied

### 5.2.2 Prepreg Lay-up Procedure

The prepreg available for this project was NCT 301 34-700 unidirectional carbon prepreg manufactured by Newport Adhesives and Composites, Inc., with a cure temperature of 121°C (250°F) (See Appendix 1 for the material data sheet) ([www.newportadhesives.com](http://www.newportadhesives.com)). It was stored on a roll in a freezer kept at 0°C (32°F) to prevent a slow, premature partial cure. The roll was removed from the freezer to cut eight 33 cm by 33 cm (13 in by 13 in) panels. An aluminum plate was cleaned of any surface impurities and a piece of Teflon peel-ply larger than the panel dimensions but smaller than the plate dimensions was taped down to ease removal after cure. The backing on the prepreg was carefully removed and the panels were stacked on the aluminum. As each panel was laid, air pockets were rubbed and pressed out to ensure proper alignment and adhesion. Each panel was laid with the fibers facing the same direction. The prepreg lay-up process is shown in Figure 5.3.

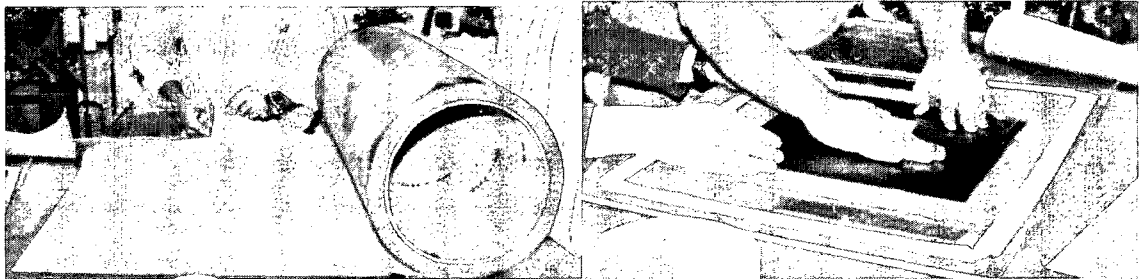


Figure 5.3 Cutting Prepreg from the Roll (Left) and Lay-Up of Flat Panels (Right)

After the final layer was pressed down, another piece of Teflon peel-ply was placed on top of the panels, followed by a cut of breather cloth trimmed to the same dimension as the peel-ply. A perimeter of vacuum bagging tape was laid on the aluminum plate and

a piece of vacuum bag was cut large enough to cover the panel. A small piece of breather cloth was placed to the side of the prepreg panel and the bottom part of the vacuum valve was set on top of it. The vacuum bag was then laid on top of the assembly, the backing from the tape was removed and the bag was pressed down onto the tape. A small slit was cut in the vacuum bag above the valve piece and the top half of the valve was inserted and twisted into place. The assembled panel and vacuum arrangement is shown in Figure 5.4.

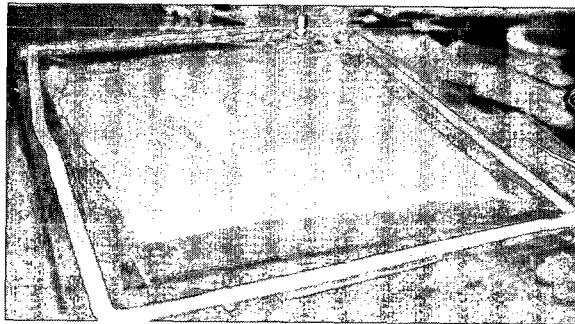


Figure 5.4 Prepreg Panel with Vacuum Bagging in Place

The autoclave (Figure 5.5) located in the Center for Materials and Structures (CAMS) at UNLV is a Laboratory Bonding Horizontal Autoclave manufactured by the American Autoclave Company. The working dimensions are a 91.4 cm (36 in) depth and a 50.8 cm (20 in) diameter. A platform sits above the heating element, reducing the maximum vertical dimension to 33 cm (13 in). It is operated by a MRC7000 controller built by The Partlow Corporation and can reach temperatures of 204.4°C (400°F) and pressures of 1.38 MPa (200 psi). The system is usually pressurized using N<sub>2</sub>, stored in two external tanks. However, the autoclave was not pressurized for the lay-ups in this project since the effectiveness of a vacuumed prepreg lay-up was analyzed. Some of the future prototyped

parts to be fabricated are too large to fit inside the autoclave, necessitating the use of an unpressurized oven with a larger internal volume. Thus, it was important to obtain lamina properties for composite panels cured under a similar arrangement. A vacuum was pulled on the parts by a Taconic TM 9140 two-stage oilless vacuum pump located below the autoclave. The maximum vacuum the pump can pull is 98.2 kPa (14.2 psi) and its flow rate is  $2.8 \times 10^{-2} \text{ m}^3/\text{min}$  (1.5 CFM). The pump pulled a vacuum of about 85.5 kPa (12.4 psi) during the cure.

The upper valve piece was connected to a vacuum line inside the autoclave, which passed through the wall and to the vacuum pump. The pump was turned on and the bag was inspected for air leaks, which were found by listening for air being sucked into the bag, which often occurs at joints in the tape and at the valve site. After the air leaks were fixed, the entire assembly was placed inside the autoclave. The autoclave pressure release valve was turned off, the water valve was turned on and the temperature control was set to 121°C (250°F). The panel was left to cure at this temperature for two hours and then was left under vacuum at room temperature for another 3 hours.

It is important to note that the autoclave would overshoot the desired temperature during heat up. It reached temperatures up to 16°C (30°F) over the target temperature before the heat was shut off and the interior cooled to around the target temperature. The heater was again turned on and a constant 121°C temperature was achieved.

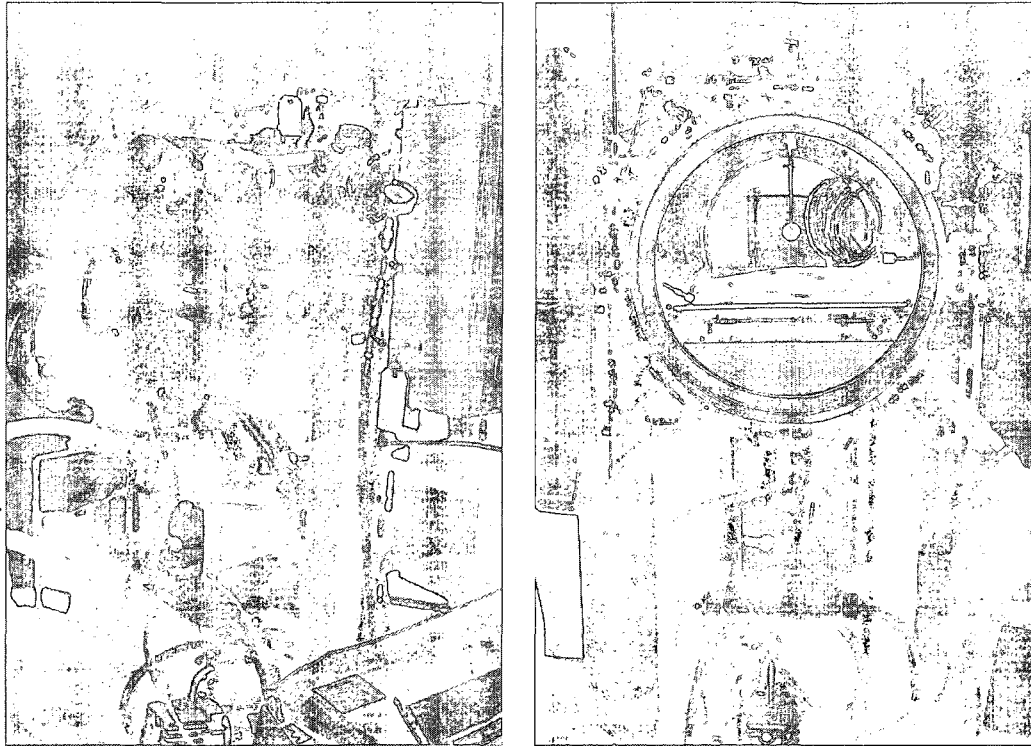


Figure 5.5 Autoclave Used to Cure the Prepreg

The assembly was removed from the autoclave after 4 hours. Removal of the bagging and peel-ply revealed a rigid carbon prepreg panel. The ends of the panel were trimmed so that the thickness was uniform on every side. One direction was trimmed down to 25.4 cm (10 in) – the intended length of the final test specimens.

### 5.2.3 Specimen Preparation

The rest of the specimen preparation was the same for both the hand lay-up and the prepreg composites. The trimmed panels were fitted with glass fiber-reinforced polymer (FRP) end tabs as recommended by ASTM Standard D 3039. The end tabs were first trimmed to the width of the panel; one edge was beveled to 30 degrees and holes were drilled into the tab material and the panels for pins to be inserted so the tabs could be

glued in the proper orientation on the panels. Since peel-ply was used during the lay-up, sanding the panels prior to gluing was not necessary. A three-to-one epoxy resin was infused with phenolic microballoons until the consistency was like that of peanut butter. The microballoons reduced the density of the epoxy while increasing the viscosity, preventing the resin from flowing out from the panels and thus providing better adhesion to the roughened surfaces. Pressure was applied to the tabs and the epoxy was left to cure for 24 hours. The specimens were cut to 2.54 cm (1 in) widths using a tile saw. The ASTM required specimen geometry is shown in Figure 5.6.

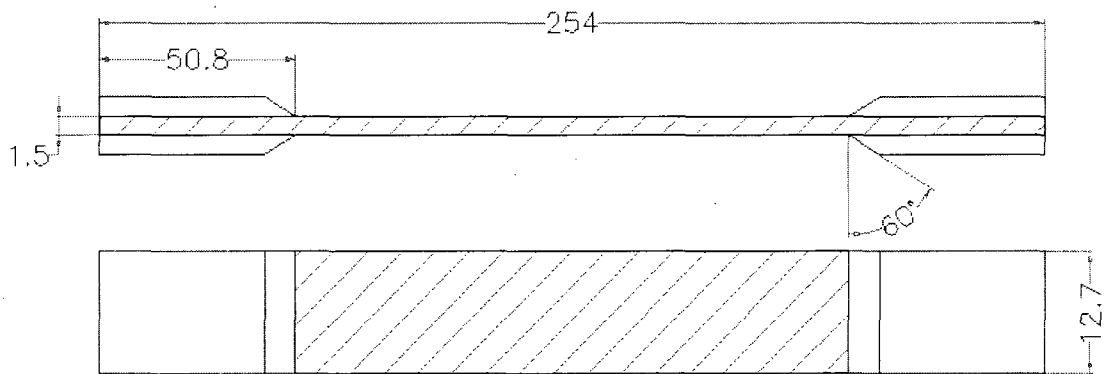


Figure 5.6 Diagram of Specimen as Required by ASTM D3037 (dimensions in mm)

The use of peel ply meant that sanding was not necessary prior to strain gage application as well. The center surface of the specimen where the strain gage was to be applied was cleaned and prepped. For these tests, Vishay CEA-06-240UZ-120 general purpose strain gages were used ([www.vishay.com](http://www.vishay.com)). The strain gages were laid out on a clean piece of plastic, one lying in the axial direction, the other in the transverse direction (some of the strain gages were combined axial/transverse rosette gages). Terminals were placed next to each specimen and a piece of tape was laid over the items. The tape was

lifted, with gages and terminals attached, and placed on the specimen. The tape was rolled back and a catalyst was applied to the gages and terminals. An adhesive was then applied and the tape was pressed down and held with pressure for approximately one minute. While the adhesive cured, wires were stripped and twisted together. The tape was removed from the specimen and a flux was applied to the terminals. The wires were soldered on to the terminals and the specimen was tested on a Vishay P-3500 strain gage box to ensure the strain gages were functioning. For consistency, the black and white wires went to one terminal while the red wire went to the other terminal. A finished specimen with strain gaging completed is shown in Figure 5.7.

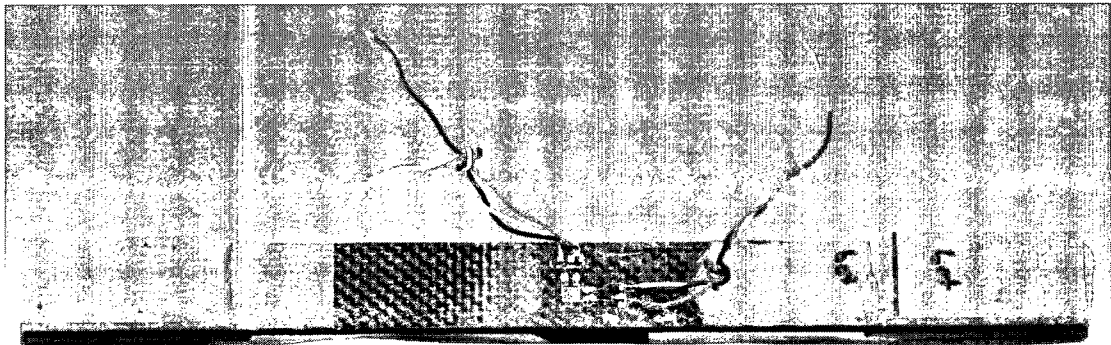


Figure 5.7 Specimen with Axial/Transverse Strain Gage in Place

#### 5.2.4 Testing Procedure

A MTS Series 319 Axial/Torsion Material Test System fitted with a 100 kN load cell (Figure 5.8) was used to perform the tensile tests on the carbon fiber specimens. The hydraulically operated test machine provides faster, smoother loading than a screw machine would have allowed, although movement in the axial direction is reduced

(compared to a screw-operated test machine). Tests were performed in accordance with ASTM Standard D 3039.

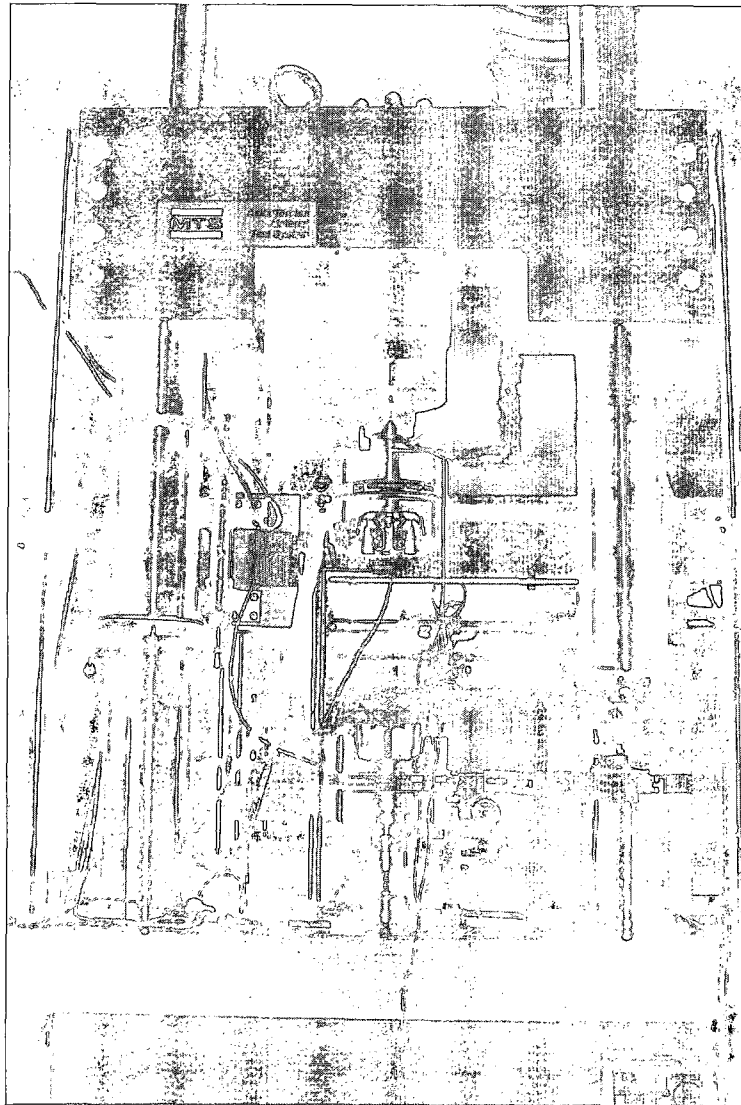


Figure 5.8 MTS Testing Machine

The specimen was held in position between the open grips, which were then closed onto the specimen at the end tabs (Figure 5.9). The hydraulic grips kept the specimen



from sliding out by applying 6.89 MPa (1,000 psi) of pressure on the end tabs normal to the loading direction.

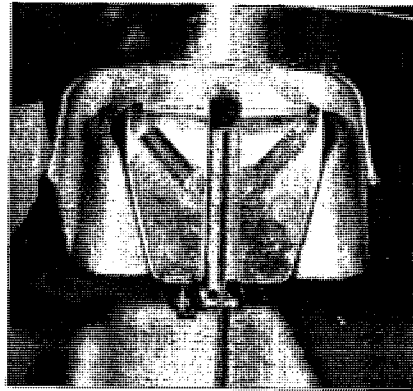


Figure 5.9 Hydraulic Grips with Specimen in Place

Some of the specimens were equipped with strain gages, while all of the specimens were outfitted with Satec E-Series clip-on axial and transverse extensometers, seen in Figure 5.10, to record the strain. The strain gages exhibit greater sensitivity to changes in dimension than the extensometers, but they are more difficult to apply and are not reusable, so half of the specimens were equipped with strain gages to validate the extensometer data. The strain gages measure microscopic strain in the material; the gages used for these tests have a gage length of 6.096 mm (0.240 in). Conversely, the extensometers measure the macroscopic strain in the specimen. With an effective gage length of 25.4 mm (1 in), they are less sensitive to minor variances in the strain. A Vishay strain gage box was used to record data from the extensometers during the test (Figure 5.11), which transferred the data to the PC where it was recorded in a Microsoft Excel spreadsheet.

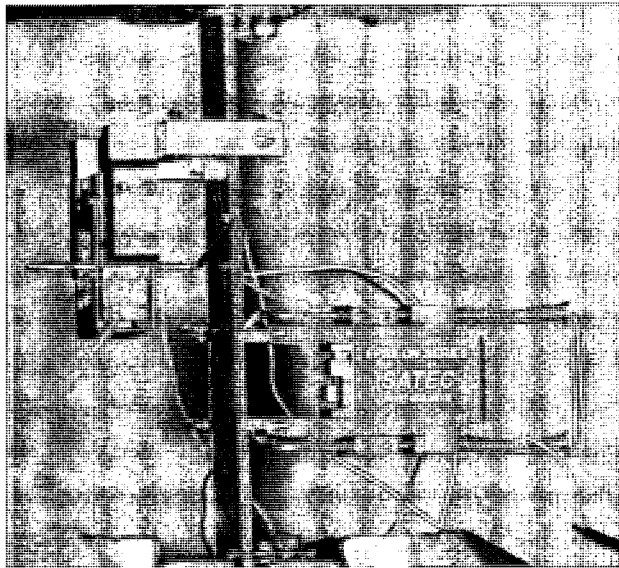


Figure 5.10 Axial and Transverse Extensometers on a Specimen

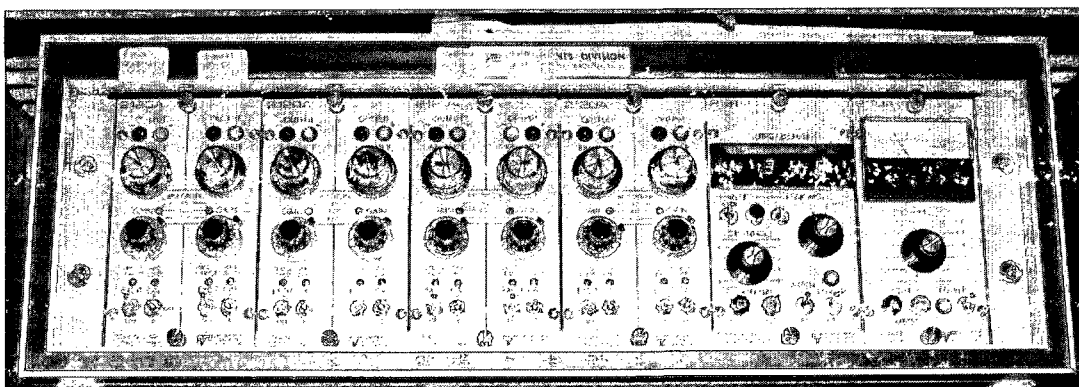


Figure 5.11 Strain Gage Box

The software for the MTS machine, TestStar and TestWare SX, was used to run the tests and collect the data. Loading on the specimen was done via displacement control, i.e., a constant strain rate of 0.75 mm per second was applied. Specimens were preloaded and then loaded until failure (Figure 5.12). A total of six 0/90 carbon fabric/epoxy specimens and six 0-degree unidirectional carbon prepreg specimens (Standard D 3039 requires a minimum of five) were tested and load and strain values were recorded.

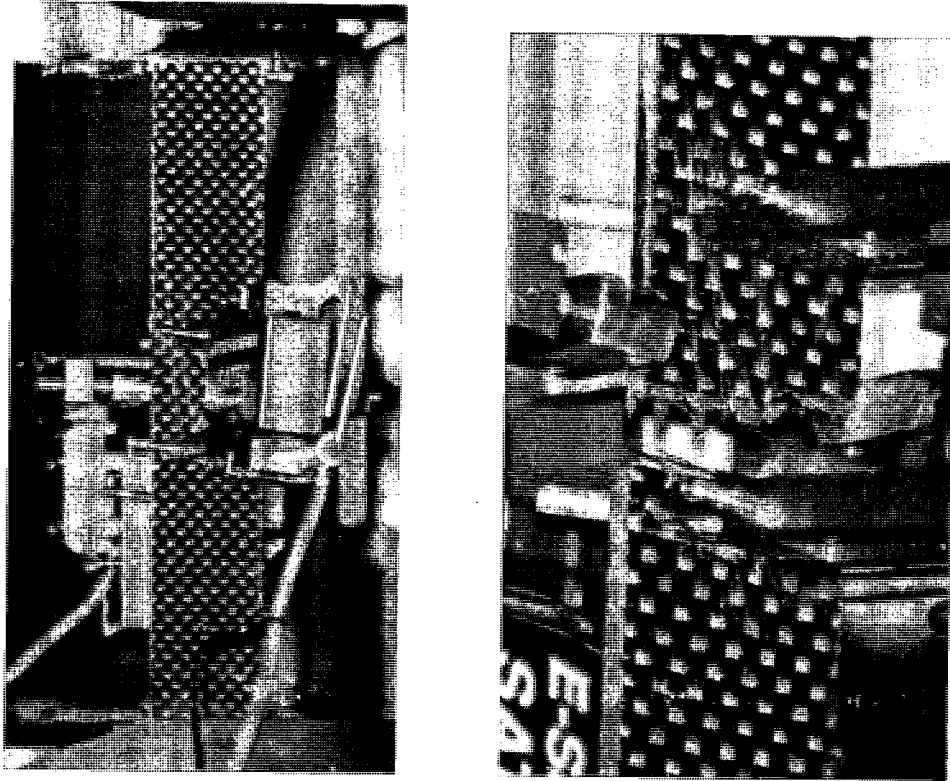


Figure 5.12 Testing and Failure of Plain Weave Carbon Fiber Specimen

### 5.2.5 Results and Analysis

Six woven and six unidirectional carbon prepreg specimens were tested until failure and time, load, displacement, and strain data were recorded. Three specimens from each material had strain gages attached so that strain values could be recorded from both the extensometers and the strain gages. The transverse extensometer provided displacement values, rather than strain, from which strain values had to be calculated. Values for tensile strength, elastic modulus, and Poisson's ratio were determined for each specimen.

The tensile stress experienced by the specimens was calculated using the instantaneous load divided by the cross-sectional area, shown in Equation 5.1, where  $P_i$

is the instantaneous load,  $w$  is the width of the specimen and  $t$  is the thickness of the specimen:

$$\sigma_t = \frac{P_i}{wt} \quad \text{Eq. 5.1}$$

From the values found for the stress range, a maximum stress, or tensile strength, of each specimen was obtained. The woven specimens had an average tensile strength of 512.73 MPa with a standard deviation of 33.46 MPa (6.53%) while the prepreg specimens had an average tensile strength of 1632.64 MPa with a standard deviation of 175.12 MPa (10.73%). The stresses for the individual specimens are shown in Table 5.1.

Table 5.1 Maximum Tensile Stress Experienced by the Specimens

	Maximum Stress (MPa) - Woven	Maximum Stress (MPa) - Prepreg
<b>Specimen 1</b>	542.09	1292.90
<b>Specimen 2</b>	495.65	1762.37
<b>Specimen 3</b>	522.92	1562.44
<b>Specimen 4</b>	518.90	1623.38
<b>Specimen 5</b>	548.46	1728.18
<b>Specimen 6</b>	448.34	1826.54
<b>Average</b>	512.73±33.46	1632.64±175.12

The elastic modulus was found for the composite specimens by plotting the tensile stress versus the axial strain as shown in Figure 5.13 (the rest of the plots can be seen in Appendix 2). A line was fitted to the data points and the line equation and the  $R^2$  value (a

determination of the quality of the fit of the line) were displayed. The slope of the line was taken as the elastic modulus of the specimen. Using data obtained from the extensometers, the average elastic modulus for the woven carbon was 45.12 GPa (6.54E+06 psi) with a standard deviation of 7.86 GPa (17.41%) and the average elastic modulus for the prepreg carbon was 129.8 GPa (1.88E+07 psi) with a standard deviation of 6.28 GPa (4.84%). The strain gages recorded an average modulus of 45.16 GPa (6.54E+06 psi) for the woven with a standard deviation of 3.94 GPa (8.72%) and a modulus of 118.26 GPa (1.72E+07 psi) for the prepreg with a standard deviation of 3.60 GPa (3.04%). The elastic modulus for each specimen is shown in Table 5.2.

A plot of the transverse strain versus the axial strain for each specimen was created to determine the Poisson's ratio of the composite materials and is shown in Figure 5.14 (the rest of the plots can be seen in Appendix 3). Similarly to the method used to find the elastic modulus, the data were plotted and trimmed to provide a linear distribution. A line was fitted to the data and the slope of the line was taken to be the Poisson's ratio for the specimen. The average Poisson's ratio using data from the extensometers was 0.07 for the woven and 0.33 for the prepreg with standard deviations of 0.01 (18.18%) and 0.02 (6.63%), respectively. The strain gage data provided an average Poisson's ratio,  $\nu_{12}$ , of 0.06 for the woven and 0.29 for the prepreg with standard deviations of 0.02 (32.44%) and 0.01 (4.27%), respectively. The Poisson's ratio for each specimen is shown in Table 5.3.

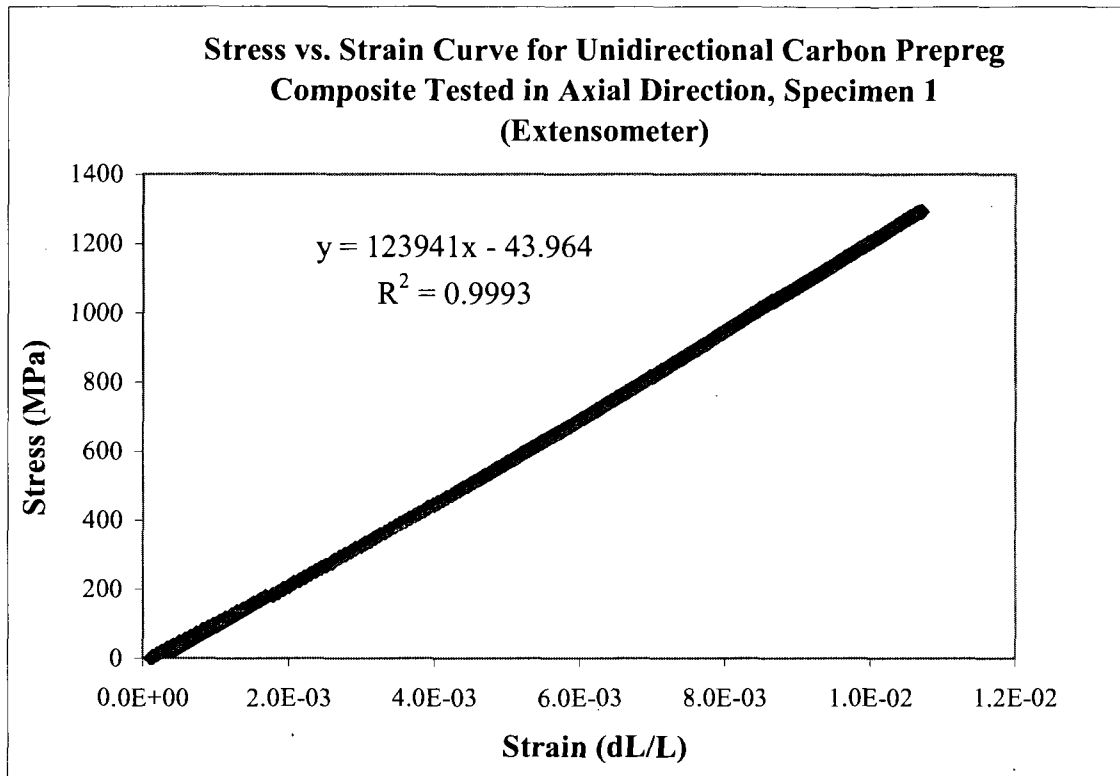


Figure 5.13 Plot of Stress versus Strain for Carbon Prepreg

Table 5.2 Tensile Modulus Values for Carbon Composite Specimens

	Elastic Modulus (GPa) (Extensometer) - Woven	Elastic Modulus (GPa) (Strain Gage) - Woven	Elastic Modulus (GPa) (Extensometer) - Prepreg	Elastic Modulus (GPa) (Strain Gage) - Prepreg
<b>Specimen 1</b>	62.54	41.78	123.94	113.87
<b>Specimen 2</b>	39.71	50.68	136.01	122.67
<b>Specimen 3</b>	41.30	no data	134.69	118.25
<b>Specimen 4</b>	42.82	43.02	129.91	no data
<b>Specimen 5</b>	41.85	no data	119.10	no data
<b>Specimen 6</b>	42.47	no data	134.87	no data
<b>Average</b>	45.12	45.16	129.75	118.26
<b>Std Dev</b>	7.86	3.94	6.28	3.60
<b>% Std Dev</b>	17.41%	8.72%	4.84%	3.04%

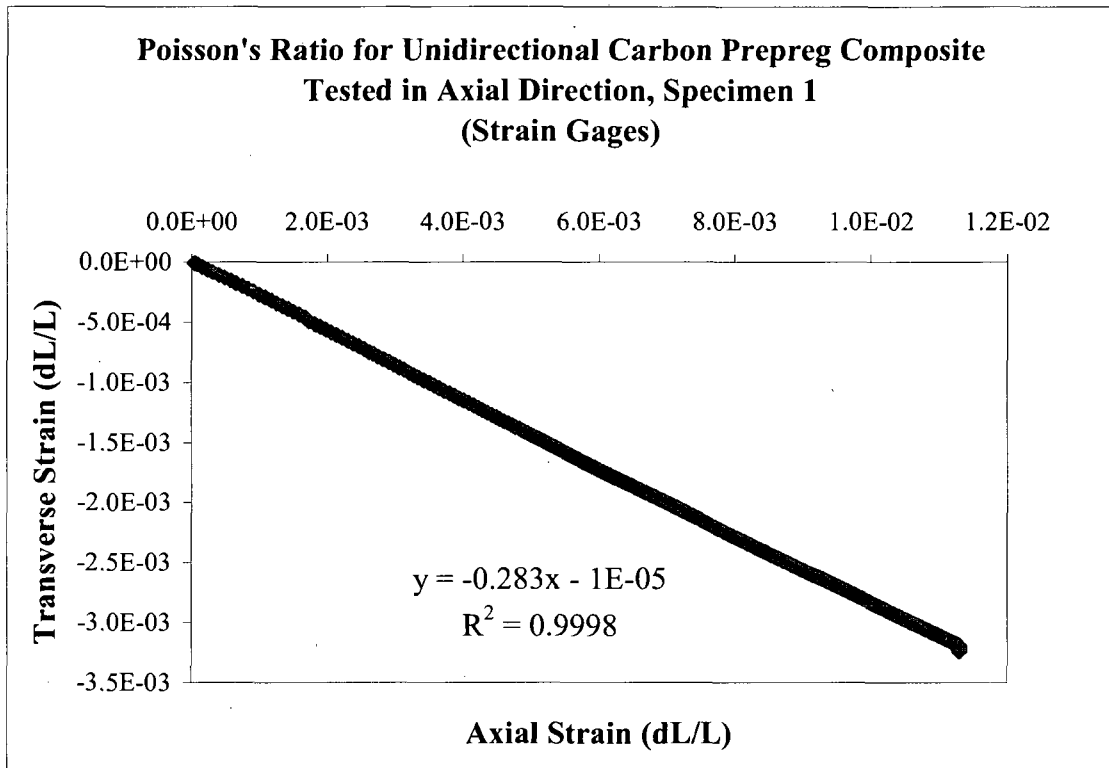


Figure 5.14 Plot of Poisson's Ratio for Carbon Prepreg

Table 5.3 Poisson's Ratio Values for Carbon Composite Specimens

	Poisson's Ratio (Extensometer) - Woven	Poisson's Ratio (Strain Gage) - Woven	Poisson's Ratio (Extensometer) - Prepreg	Poisson's Ratio (Strain Gage) - Prepreg
<b>Specimen 1</b>	0.08	0.06	0.31	0.28
<b>Specimen 2</b>	no data	0.09	0.31	0.31
<b>Specimen 3</b>	0.06	no data	0.37	0.28
<b>Specimen 4</b>	0.05	0.04	0.33	no data
<b>Specimen 5</b>	0.06	no data	0.31	no data
<b>Specimen 6</b>	0.08	no data	0.35	no data
<b>Average</b>	0.07±0.01	0.06±0.02	0.33±0.02	0.29±0.01

It is important to note that the values for the maximum tensile stress ( $S_2$ ), the elastic modulus ( $E_{21}$ ), and Poisson's ratio ( $\nu_{21}$ ) in the transverse direction will be much lower

than those in the axial direction for the unidirectional material. These values will be equivalent for the woven material since fibers run in both the axial and transverse directions.

#### 5.2.6 Wet Lay-Up Unidirectional Carbon Tape

The wet lay-up nacelles will be reinforced with 12K unidirectional carbon fabric along with the 0/90 satin weave cloth. Therefore it is important to include the measured properties from samples tested at the University. The unidirectional carbon fiber tape is available from US Composites under part number FG-CFU13 ([www.uscomposites.com](http://www.uscomposites.com)). This material was previously characterized by Nelson, et al. and values for the ultimate tensile strength, the tensile modulus, and the major Poisson's ratio were found and are shown in Table 5.4 [22].

Table 5.4 Material Properties for Wet Lay-Up Unidirectional Carbon Tape

Maximum Stress (MPa)	Elastic Modulus (GPa)	Poisson's ratio
1159±1.7%	16.39±7.2%	0.16±13%

#### 5.2.7 Conclusion

The unidirectional carbon prepreg clearly shows an advantage over the plain weave carbon fiber. It is both stronger and lighter. However, since the prepreg has limited strength in the transverse direction, similar to that of the epoxy, it will require two layers of prepreg, one placed in the axial direction and one in the transverse direction, to achieve strength in the transverse direction and the same directional stiffness as one layer



of plain weave carbon fiber. It can thus be deduced that a part will require up to twice as many layers of prepreg, but since the fiber directions can be optimized, not as many layers may be needed in a particular direction, so less layers may be used. One drawback to prepreg is its tendency to fail catastrophically, which can be seen in Figure 5.15. Applying layers in the transverse or other directions will help to alleviate this issue. The wet lay-up unidirectional carbon fiber exhibited a very low elastic modulus.

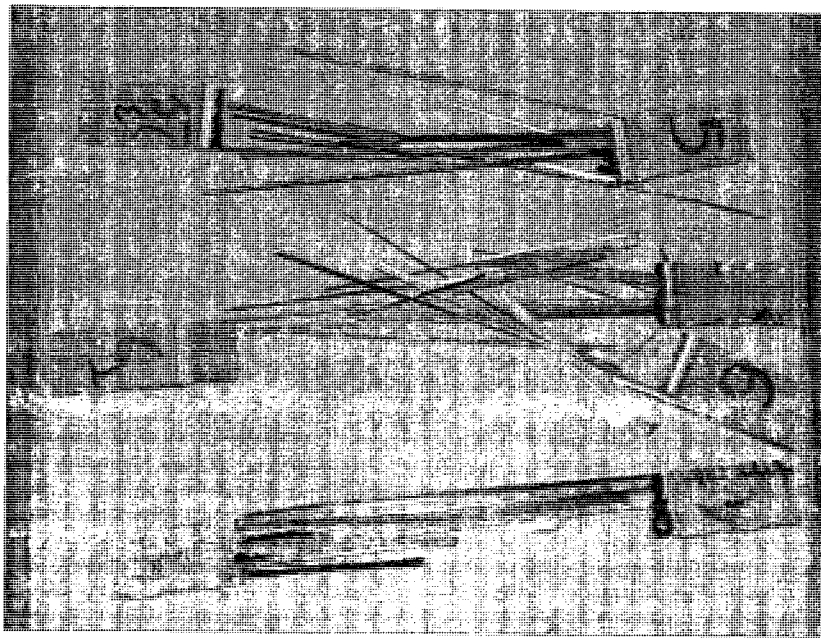


Figure 5.15 Carbon Prepreg Specimens After Tensile Testing

## CHAPTER 6

### PROTOTYPE DESIGN AND FABRICATION

To test manufacturing techniques and verify design, a simple fuselage mock-up, a functional wing, and several nacelles were constructed. Aesthetic designs for the aircraft were provided by an artist involved with the main project committee and were not to be drastically changed, but functional aspects were left to be designed by the engineers. No aerodynamic analysis or design optimization was performed on the first prototype airframe since it was based off a proven design. The original artist's rendering is shown in Figure 6.1.

The general shape of the aircraft was redrawn using SolidWorks solid modeling software, Version 2007. Attempts at importing the original renderings from AutoDesk 3DSMax, a three-dimensional modeling program, into SolidWorks proved futile as they imported into SolidWorks as unmodifiable surfaces.

#### 6.1 Wing Design and Fabrication

The wing design for the aircraft includes an outer wing structure attached to a wing stub. The wing is connected to the wing stub via a hinge joint to allow the wings to fold for different flight missions. Fabrication of the outer wing structure, shown in Figure 6.2, is described in this section. While the first wing was not designed for translational flight,

a National Advisory Committee for Aeronautics (NACA) four-digit airfoil shape was still included in the design for aesthetics and simplicity. On the prototype, wing section 1 transitions from a NACA 2418 to a 2415; section 2 goes from a 2415 to a 2412, and sections 3 and 4 are a 2412 [23].

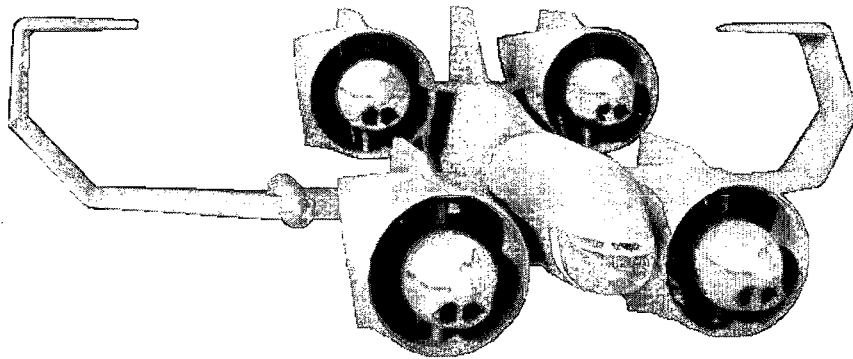


Figure 6.1 Artist's Rendering of VTOL UAV Prototype

The final solid model did not differ much from the original artist's concept, aside from slight changes in the airfoil shape and the joints. The sweep angles for the wing are  $24^\circ$ ,  $32.5^\circ$ ,  $27^\circ$ , and  $10^\circ$  for sections 1, 2, 3, and 4, respectively. The wing model is shown in Figure 6.2 with the sections labeled by number.

The wing prototype was created in part to test manufacturing skills for difficult geometries. The complex shape of the wing required much forethought into the order of construction; the final decision was to create a foam core and perform a single wet lay-up of satin weave carbon fiber over the entire preassembled core as opposed to laying up each section individually prior to mating the sections. It was determined at the time that the latter would result in more complicated construction and a weaker structure requiring

extra reinforcement in the joints, making the wing heavier. Other options for wing construction included ribbing and laying up the skins in female molds; while potentially producing a lighter-weight wing, those options proved too complicated and time-consuming for this stage of the project with its limited schedule.

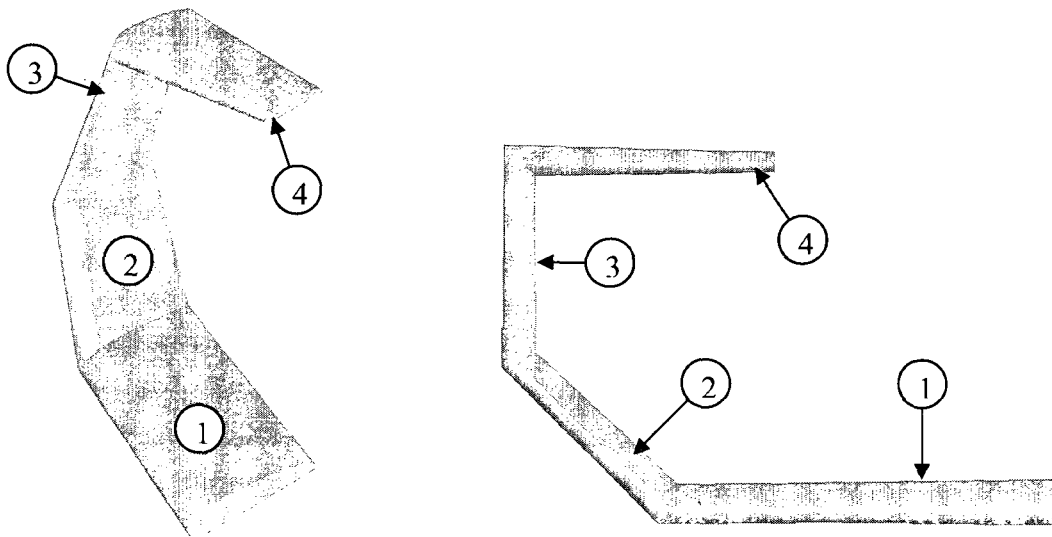


Figure 6.2 Model of Wing Structure: Isometric View (Left) and Front View (Right)

The cutting of the foam core was performed using a hotwire as recommended by Rutan Aircraft Factory Inc. [24]. Templates were cut from 6.3 mm (0.25 in) thick particle board stock and marked in increments to match the cutting rate for both sides of the foam piece. A small, thin metal rod was glued into the leading edge of the template for the hotwire to rest upon. Inset areas were cut into the top and the bottom of the template so that reinforcing carbon strips could be included on the foam cut-outs without any surface irregularity (Figure 6.3).

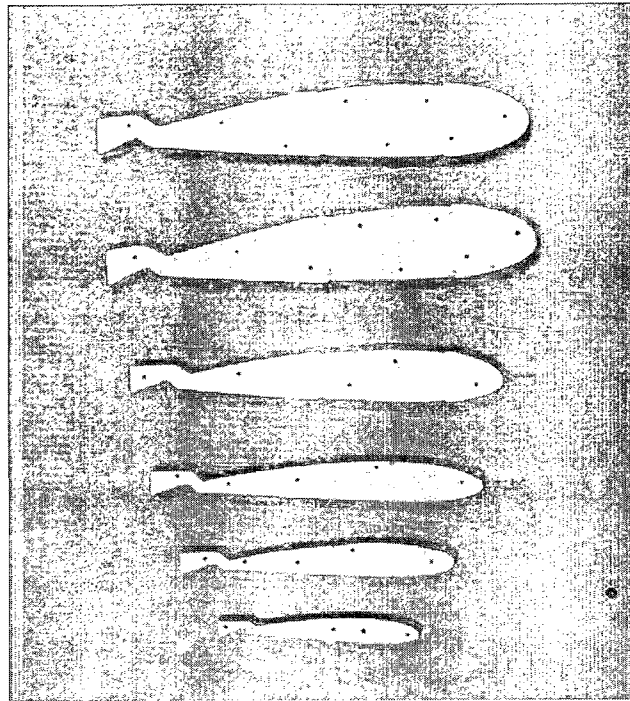


Figure 6.3 Wing Profile Patterns

The foam used for the core material was Dow Styrofoam Square Edge brand polystyrene with a density of  $32 \text{ kg/m}^3$  ( $2 \text{ lb/ft}^3$ ), available from Wick's Aircraft Supply ([www.wicksaircraft.com](http://www.wicksaircraft.com)). Styrofoam can be dissolved using acetone or other solvents, thinners, and fuels, making it a good choice if any material removal is necessary. Its closed-cell properties and ease of cutting, along with its low cost, made it a good choice for a core. Blocks of foam were trimmed to the intended length of the wing part and one wing part could be cut from each 10 cm (4 in) thick block. The templates were fixed to opposite ends of the block and offset at the correct sweep angle prior to commencing cutting. A large hotwire was used to trim away the excess foam and leave a core in the shape of the wing, as shown in Figure 6.4. Any rough-cut areas were trimmed and sanded. The sides where the wing parts would be bonded together were cut at the appropriate angles.

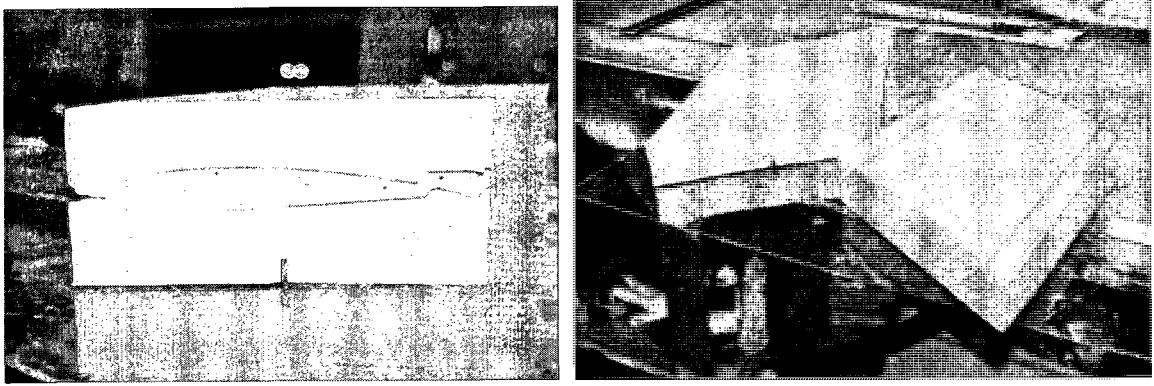


Figure 6.4 Wing Cores Cut from Closed-Cell Foam

The wing cores were glued together using epoxy resin and a three inch wide strip of unidirectional carbon fiber cloth was laid on either side of the bottom two pieces within the groove for reinforcement as shown in Figure 6.5.

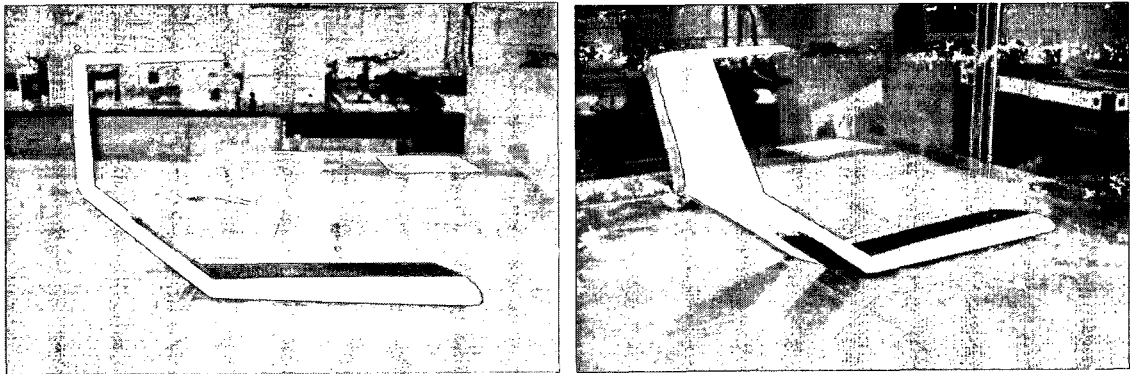


Figure 6.5 Assembled Wing Cores with Unidirectional Fiber Reinforcement

Satin weave carbon fiber fabric was draped over the wing assembly and cut to size. Using epoxy resin to wet the fibers, the cloth was pressed and worked onto the foam to try to produce an even surface. This process is shown in the images in Figure 6.6. After it was worked into the curvature and remained in place, the assembly was covered in peel

ply to try to produce a decent finish and reduce air pockets. The wing was suspended and allowed to cure for 24 hours (Figure 6.7).



Figure 6.6 Lay-Up of Wing Structure

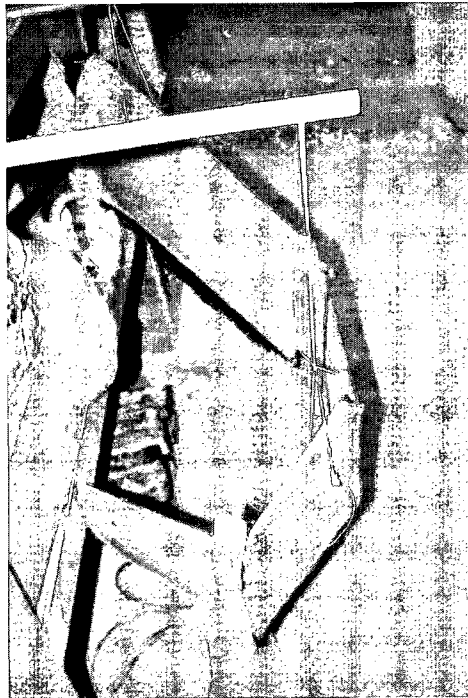


Figure 6.7 Laid Up Wing Hung to Cure

The final product contained some voids where the peel ply and the resin did not meet. These voids were filled in with automotive body filler and sanded smooth to provide a nice airflow surface. The surface was then prepped and painted to provide an aesthetically pleasing final product. The wing prior to final prep work is shown in Figure 6.8.

This process for constructing the wing, while maintaining strength by using a continuous piece of composite material, caused the wing to weigh more than desired due to the large amounts of body filler required to fix the poor surface finish. The final weight after filler and paint was 604 grams. This method is not recommended unless the manufacturer has better technology for vacuum-bagging the wing without acquiring voids.

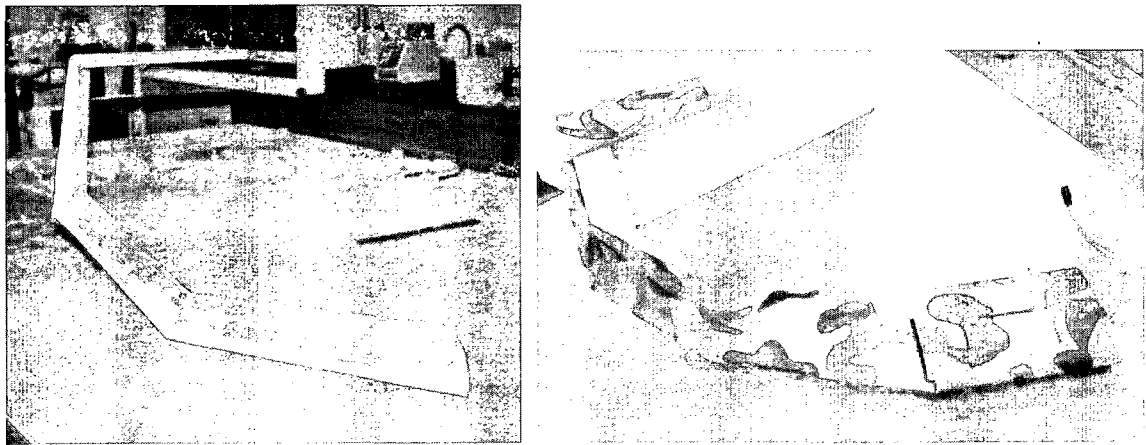


Figure 6.8 Finished Wing Structure

## 6.2 Fuselage Design and Fabrication

Like the wing, the overall shape of the fuselage experienced very little modification from the original artist's design; the design is shown in Figure 6.9 as a SolidWorks



model. However, the original requirements for the first prototype only necessitated a simple platform with nacelle mounting points to demonstrate the hovering capabilities of the aircraft. This meant that manufacturing the entire fuselage body was not necessary, greatly reducing design and manufacturing time. The first mock-up of the fuselage was not modeled in SolidWorks since it was only a simplified version of the true fuselage. The basic structure was discussed and decided upon through rough sketches and notes.

Thoughts on manufacturing methods and material choices went through multiple iterations until a simple flat panel with support rings covered by a skin was chosen as the easiest and most cost-effective design to produce. The nacelle mount stubs were swapped out for simple “hats” with aluminum tubing supporting the nacelles, and the nose cone and tail were not included.

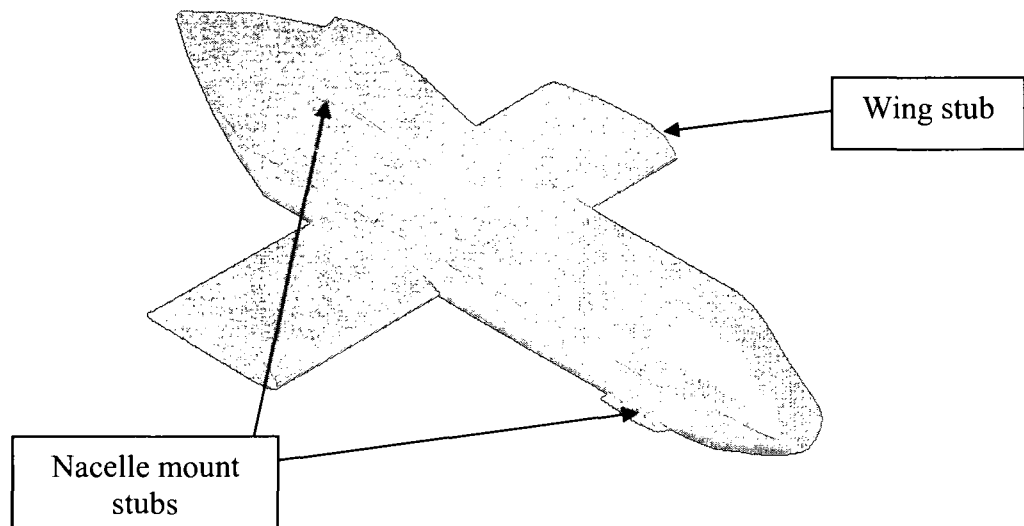


Figure 6.9 SolidWorks Model of Fuselage

A sandwich panel 80.9 cm (31.9 in) by 20.6 cm (8.1 in) was constructed from 6.4 mm thick Divinycell F polymer foam and plain weave carbon fiber. The foam was first cut to the correct size, then four slightly oversized pieces of carbon cloth were cut. The first layer of carbon on each side of the foam was wetted with 3M glass microballoon-impregnated epoxy resin for better adhesion to the rough open-cell surface of the foam. The second layers were placed on using epoxy resin without microballoons. The panel was then sandwiched between two pieces of plexiglass and pressure was applied to squeeze out excess resin and hold the panel together during the curing process. After 8 to 10 hours of cure time, the panel was removed and the excess carbon was trimmed off around the edges of the foam. While the panel was left to cure, the side skins for the fuselage were laid up. These skins were constructed from unidirectional carbon prepreg. Using a flat aluminum plate as a mold, three layers of prepreg were laid, two in the zero degree direction and one sandwiched between them in the 90 degree direction, and pressed down and the bubbles were worked out. The skins were vacuum-bagged and placed in the oven to cure at 127°C (260°F) for 4 hours.

The support rings were made from foam molds cut using templates printed from the SolidWorks drawing. The templates were used to trace the cross-section of the fuselage onto the foam, after which the excess foam was trimmed away. The edges of the foam where the carbon cloth would be laid up on were covered in vacuum bag for easy removal of the part after cure. Two layers of two inch wide strips of plain weave carbon fiber were cut and wetted with epoxy resin and laid on the mold. The rings were wrapped in more vacuum bag to ensure a nice surface finish and were left to cure. Once dry, the rings were trimmed and sanded where bonding would occur.

The rings were bonded to the panel with microballoon-infused epoxy resin. Once the epoxy had set, the skins were glued on to the rings and clamped in place until the epoxy cured.

Foam cores for nacelle mount supports and a wing support were cut and shaped. A single layer of plain weave carbon fiber was laid on the nacelle mount supports to add rigidity and strength. After curing, the excess carbon was trimmed and one-inch diameter holes were drilled through the nacelle mount supports for the aluminum tubes. The supports were then glued to the panel in their respective locations. The in-progress nacelle mount supports and the final assembly are shown in Figures 6.10 and 6.11, respectively.

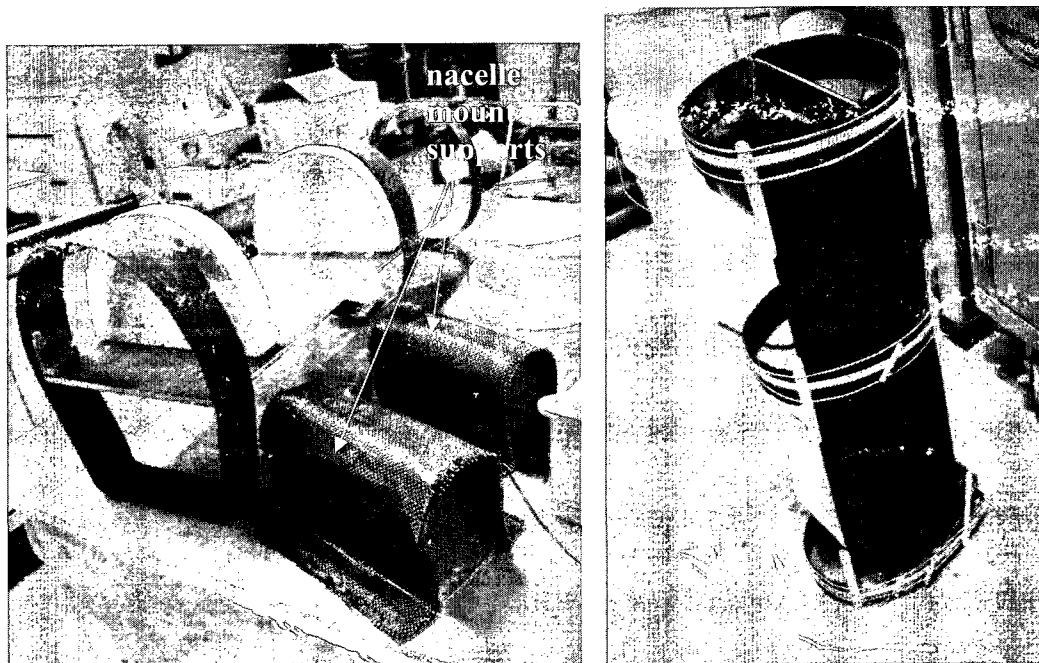


Figure 6.10 Fuselage Frame Mock-Up Construction

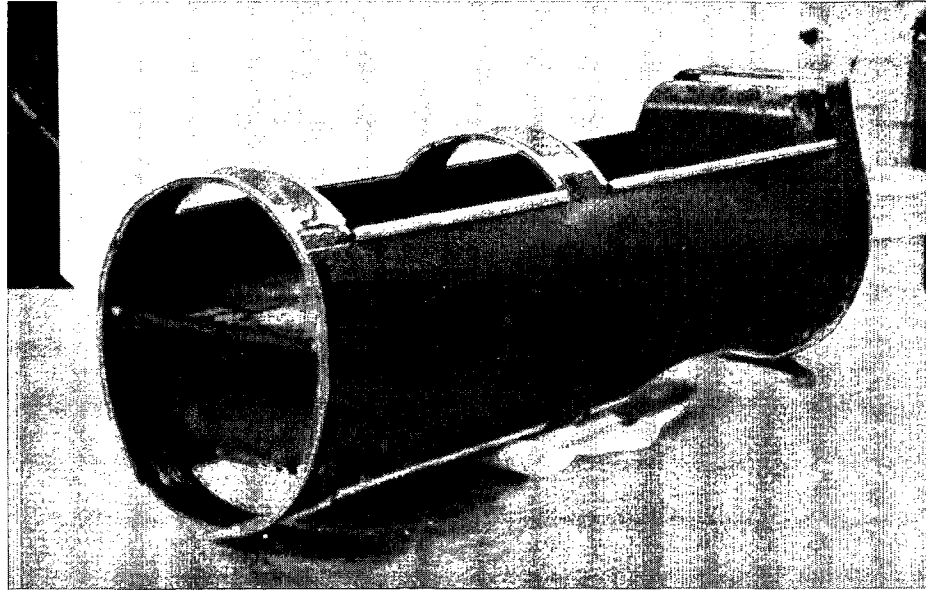


Figure 6.11 Complete Fuselage Frame Mock-Up

The final structure, which was suitable for mild vertical flight as required for the first prototype, weighed 1.1 kg (2.4 lbs).

### 6.3 Nacelle Design

The overall design has remained relatively unchanged from the original concept. The design, shown in Figure 6.12, included an inner and outer skin with an average of 1.27 cm (0.5 in) of separation for internal components such as fuel lines and wiring. However, for the first prototype, only hovering would be demonstrated and it was determined that the internal components could be exposed; therefore, only the inner nacelle surface, shown in Figure 6.13, would be needed, eliminating long design times and difficult manufacturing.

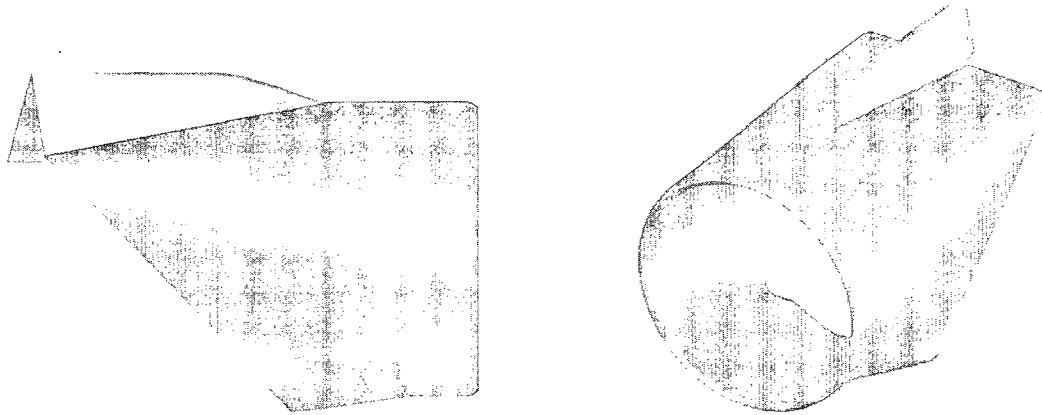


Figure 6.12 SolidWorks Model of Original Nacelle Design

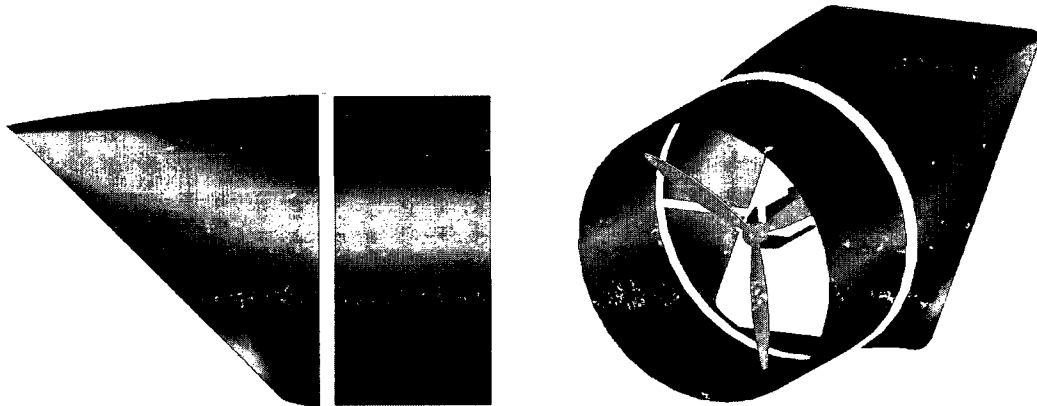


Figure 6.13 SolidWorks Model of Inner Skin of Nacelle with Engine Mount

#### 6.4 Finite Element Analysis of Nacelle Structure

Prior to construction, the nacelle geometry was analyzed using the finite element modeling software Altair HyperWorks V 7.0. The software was run on a PC with a 3.20 GHz Pentium 4 processor and 2 GB of RAM. The properties determined through the material characterization tests described in Chapter 5, along with data from previous characterization tests and from manufacturers, were used to define the materials. The material values used in the analysis are listed in Tables 6.1, 6.2 and 6.3 for the prepreg,

woven cloth and unidirectional carbon/epoxy composites, respectively. The models were defined by individual laminas of a specified thickness, stacked in varying orientations, and modeled using the MAT8 composite model. The model was oriented so that the axial direction of the nacelle followed the z axis and the hoop direction followed the x (horizontal) and y (vertical) axes of the global coordinates. The ply stacking sequence began with the innermost layer. Figures 6.14 through 6.16 show the element orientation, ply stacking direction, and an example of the individual fiber orientations by ply, respectively.

Property	Value
Ply thickness	0.10 mm
Young's modulus (E1)	130 GPa
Transverse modulus (E2)	8.96 GPa*
Poisson's ratio (NU12)	0.33
Shear modulus (G12)	48.87 GPa
Density (RHO)	8.4E-07 kg/mm <sup>3</sup>
Tensile strength in axial direction (Xt)	1632.64 MPa
Compressive strength in axial direction (Xc)	1241.1 MPa*
Tensile strength in transverse direction (Yt)	59.98 MPa*
Compressive strength in transverse direction (Yc)	198.57 MPa*
Shear strength (S)	91.01 MPa*

Table 6.1 Carbon Fiber/Epoxy Prepreg Properties per Lamina used in FE Analysis.

\* - Data obtained from [www.newportad.com](http://www.newportad.com)

Property	Value
Ply thickness	0.30 mm
Young's modulus (E1)	45 GPa
Transverse modulus (E2)	45 GPa
Poisson's ratio (NU12)	0.07
Shear modulus (G12)	21.03 GPa
Density (RHO)	1.6E-06 kg/mm <sup>3</sup>
Tensile strength in axial direction (Xt)	512.73 MPa
Compressive strength in axial direction (Xc)	123.9 MPa*
Tensile strength in transverse direction (Yt)	512.73 MPa
Compressive strength in transverse direction (Yc)	123.9 MPa*
Shear strength (S)	60 MPa*

Table 6.2 Plain Weave Carbon Fiber/Epoxy Properties per Lamina used in FE Analysis.

\* - Data obtained from previous material characterization tests [25]

Property	Value
Ply thickness	0.40 mm
Young's modulus (E1)	138 GPa*
Transverse modulus (E2)	10 GPa*
Poisson's ratio (NU12)	0.16
Shear modulus (G12)	6.5 GPa*
Density (RHO)	1.3E-6 kg/mm <sup>3</sup>
Tensile strength in axial direction (Xt)	1159 MPa
Compressive strength in axial direction (Xc)	1159 MPa
Tensile strength in transverse direction (Yt)	44.8 MPa*
Compressive strength in transverse direction (Yc)	44.8 MPa*
Shear strength (S)	62 MPa*

Table 6.3 Unidirectional Carbon Fiber/Epoxy Properties per Lamina used in FE

Analysis. \* - Data obtained from *Fiber-Reinforced Composites* [13]

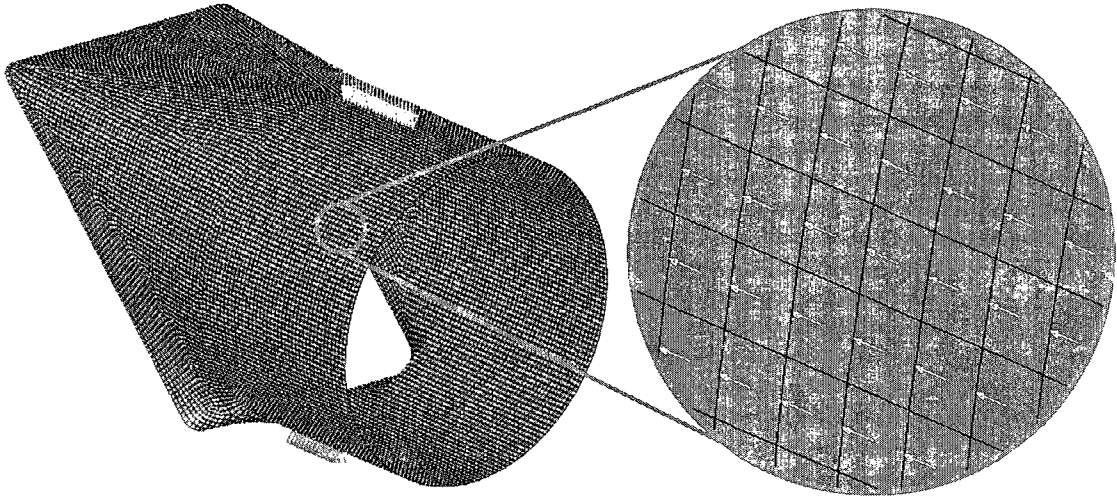


Figure 6.14 Element Orientation in FEA Model (arrows represent 0 degree direction)

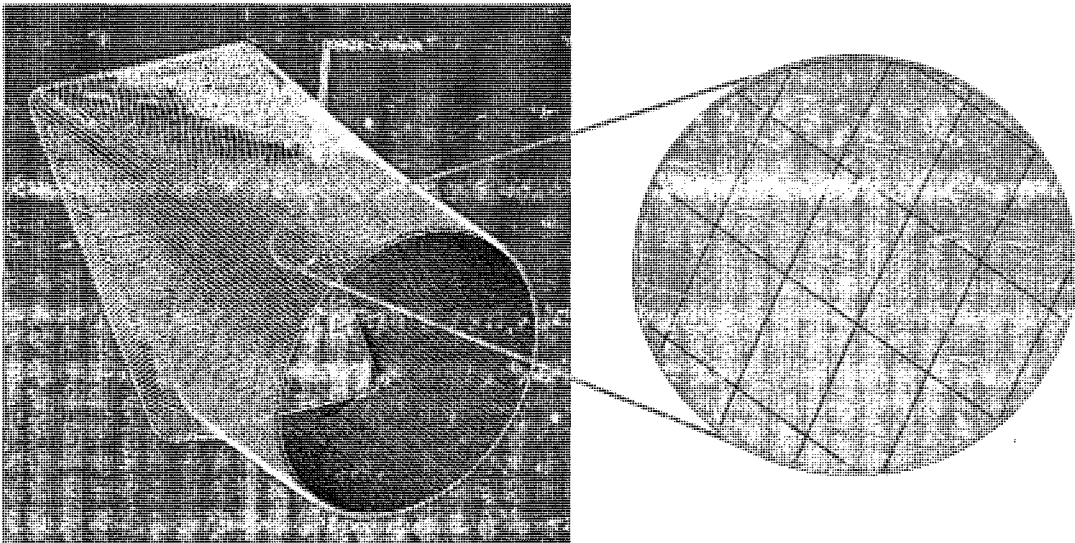


Figure 6.15 Ply Stacking Orientation in FEA Model



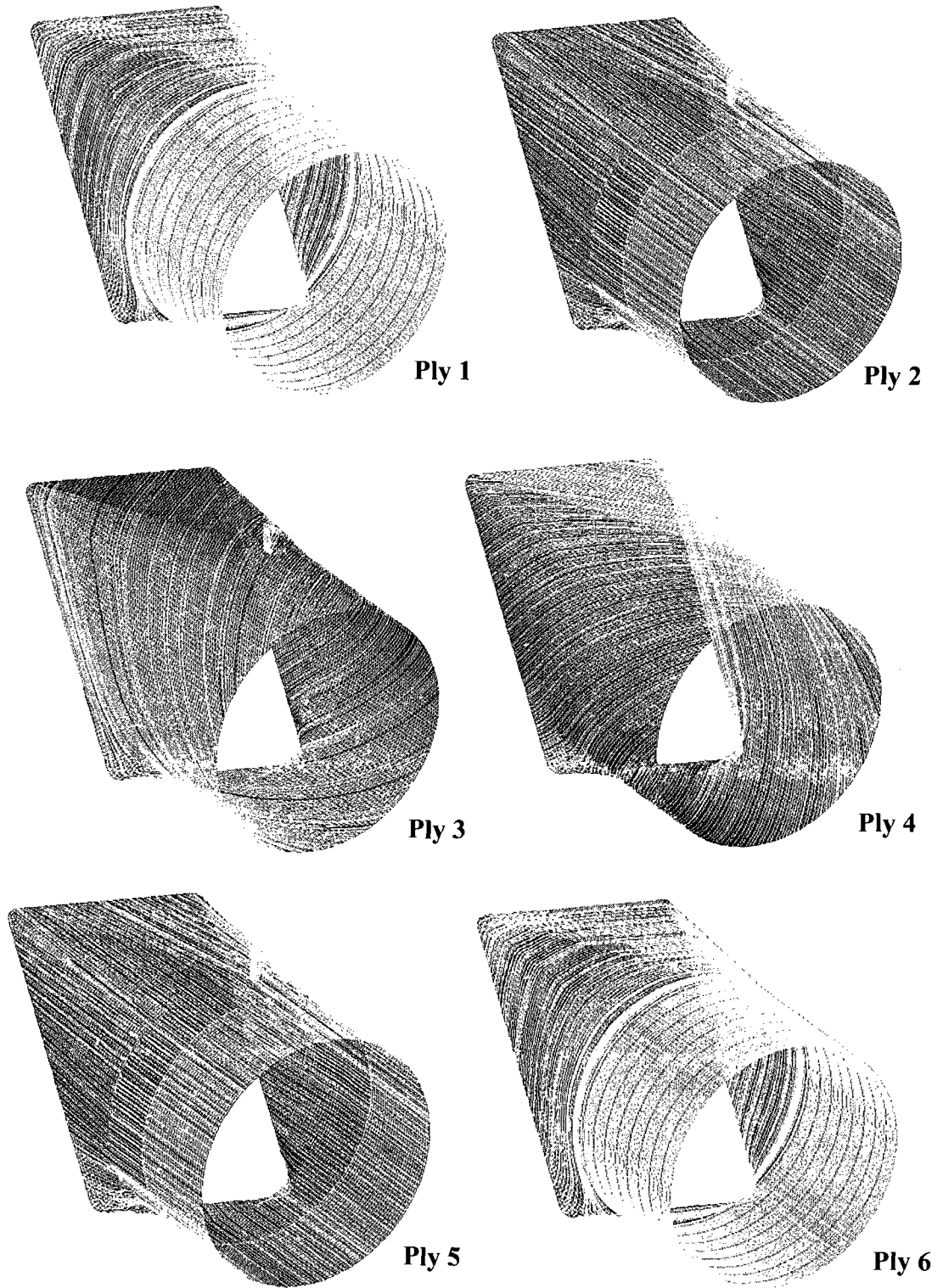


Figure 6.16 Fiber Orientation by Ply ([90/0/+45/-45/0/90] Prepreg Model)

Using the solver OptiStruct, several fiber orientations for the nacelle were simulated under a simple compressive load of 445 N (100 lbs) along the length of the nacelle to obtain the most efficient fiber layout. The first models contained six and eight layers of carbon fiber and epoxy resin applied uniformly over the nacelle without any additional reinforcement. The other models had additional reinforcement in the hoop (transverse) direction on both ends of the cylindrical portion of the nacelle. The reinforcing strips were 2.54 cm (1 inch) wide and models contained two layers of equivalent (prepreg and woven cloth) material. (A list of the different nacelle compositions along with the maximum stress and deflection results are provided in Tables 6.1 and 6.2 for prepreg and wet lay-up, respectively. From the results, the six-layer  $[90/0/+45/-45/0/90]$  orientation for the prepreg and the four-layer  $[0_w/+45_u/-45_u/0_w]$  for the wet lay-up nacelles were chosen for construction (W is woven and U is unidirectional for the wet lay-up nacelle notation). The FEA model is shown in Figure 6.17 and the displacement contours for the prepreg and the wet lay-up nacelles are provided in Figures 6.18 and 6.19, respectively.

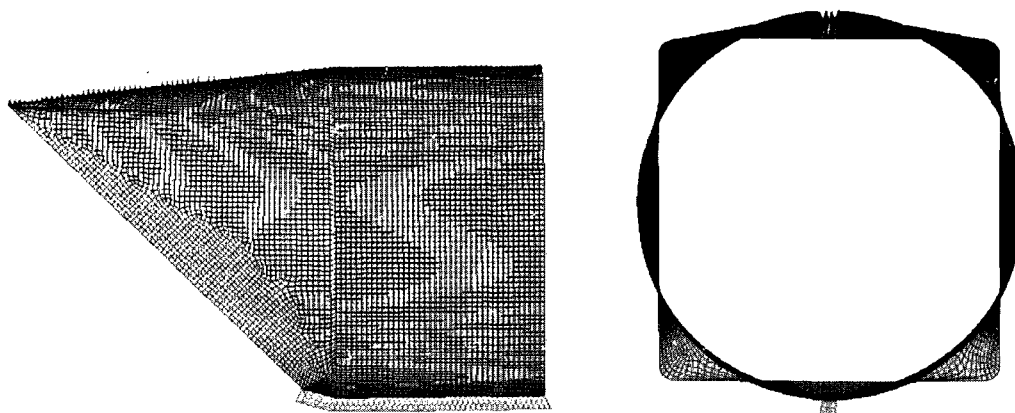


Figure 6.17 FEA Model of Nacelle Showing Loading (green) and Constrains (red).

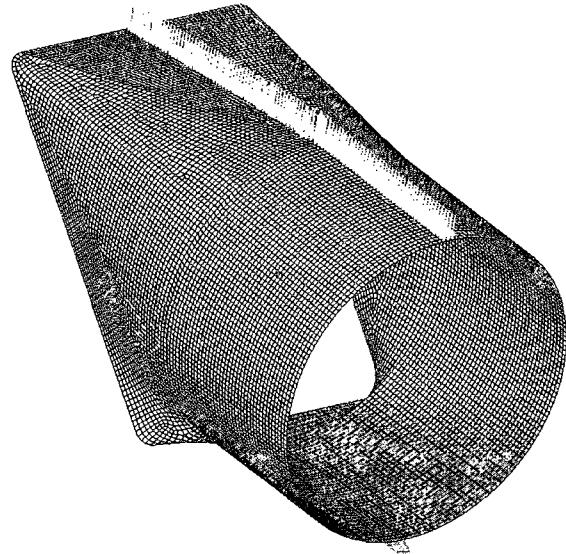
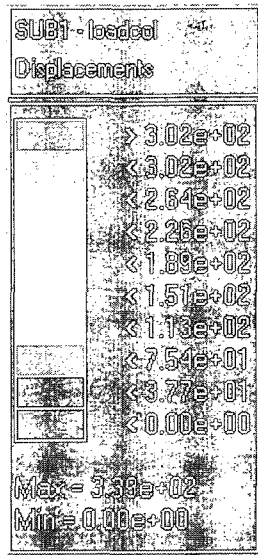


Figure 6.18 Displacement Contours for [90/0/+45/-45/0/90] Prepreg Nacelle

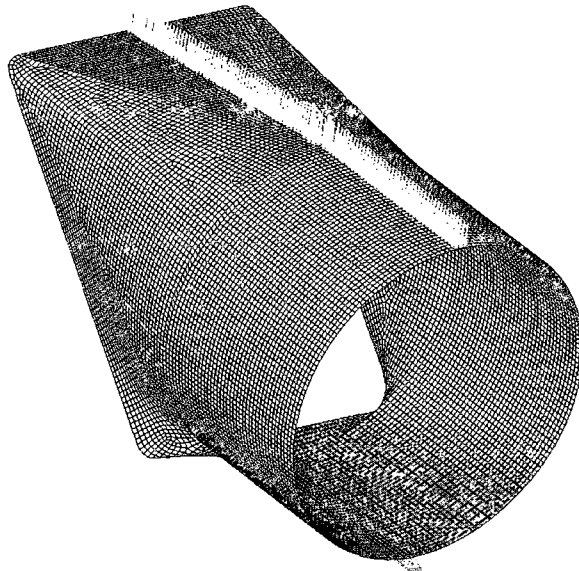
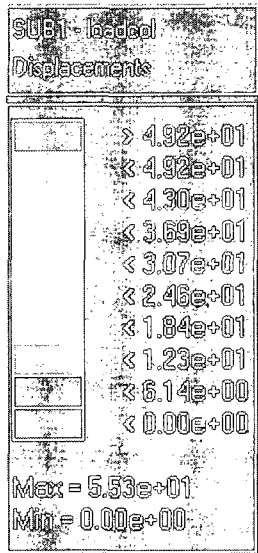


Figure 6.19 Displacement Contours for [0/+45/-45/0] Wet Lay-Up Nacelle

Table 6.1 Maximum Stress and Deformation in a Nacelle Loaded Along its Centerline  
for Various Laminates made from Prepreg Carbon/Epoxy

Orientation	Max Stress (MPa)	Max Def (mm)
<b>Prepreg</b>		
<i>Unreinforced - 6 Layers</i>		
0/90/45/-45/90/0	2.98E+03	472
90/0/45/-45/0/90	2.44E+03	345
90/45/0/90/-45/90	3.01E+03	371
90/45/90/90/-45/90	3.15E+03	397
90/45/-45/90/45/-45	2.66E+03	467
90/90/45/-45/90/90	3.53E+03	360
90/90/90/90/90/90	3.67E+03	487
<i>Reinforced - 6 Layers</i>		
0/90/45/-45/90/0	2.96E+03	466
90/0/45/-45/0/90	2.45E+03	343
90/45/0/90/-45/90	3.00E+03	370
90/45/90/90/-45/90	3.15E+03	397
90/45/-45/90/45/-45	2.59E+03	460
90/90/45/-45/90/90	3.53E+03	359
90/90/90/90/90/90	3.67E+03	487
<i>Unreinforced - 8 Layers</i>		
90/0/45/0/90/-45/0/90	1.48E+03	184
90/45/0/0/0/0/-45/90	1.34E+03	198
90/45/90/0/0/90/-45/90	1.53E+03	183
90/45/90/90/90/90/-45/90	1.68E+03	198
90/45/90/-45/90/45/90/-45	1.30E+03	193
90/45/-45/90/90/-45/45/90	1.23E+03	176
90/90/90/90/90/90/90/90	1.96E+03	233
<i>Reinforced - 8 Layers</i>		
90/0/45/0/90/-45/0/90	1.47E+03	182
90/45/0/0/0/0/-45/90	1.33E+03	194
90/45/90/0/0/90/-45/90	1.53E+03	182
90/45/90/90/90/90/-45/90	1.67E+03	197
90/45/90/-45/90/45/90/-45	1.28E+03	190
90/45/-45/90/90/-45/45/90	1.22E+03	174
90/90/90/90/90/90/90/90	1.95E+03	232

Table 6.2 Maximum Stress and Deformation in a Nacelle Loaded along its Centerline  
for Various Laminates made from Wet Lay-Up Carbon/Epoxy

Orientation	Max Stress (MPa)	Max Def (mm)
<b>Woven</b>		
<i>Unreinforced - 6 Layers</i>		
0/90/45/-45/90/0	1.30E+03	447
90/0/45/-45/0/90	1.09E+03	341
90/0/90/0/90/0	1.16E+03	466
<i>Reinforced - 6 Layers</i>		
0/90/45/-45/90/0	1.23E+03	428
90/0/45/-45/0/90	1.06E+03	329
90/0/90/0/90/0	1.10E+03	448
<i>Unreinforced - 8 Layers</i>		
0/90/0/90/0/90/0/90	638	233
0/90/90/0/0/90/90/0	647	246
45/-45/0/90/90/0/-45/45	519	237
45/-45/45/-45/45/-45/45/-45	550	353
45/-45/45/-45/-45/45/-45/45	653	359
90/0/45/-45/45/-45/0/90	588	179
90/0/45/-45/-45/45/0/90	570	178
90/0/90/0/45/-45/0/90	618	179
<i>Reinforced</i>		
90/0/45/-45/45/-45/0/90 2R	566	170
90/0/45/-45/45/-45/0/90 4R	558	168

## 6.5 Nacelle Fabrication

Several nacelle skins were constructed from unidirectional carbon prepreg and satin weave carbon cloth for weight conservation. The prepreg material choice required tooling considerations since typical materials such as low-temperature foam or medium-density fiberboard (MDF) cannot be used at elevated temperatures. Several tooling materials were considered, including aluminum, high-temperature MDF, and high-temperature foam. For cost and ease of machining, Precision Board PBHT high temperature foam was used. This foam is good up to 149°C (300°F) and has a low coefficient of thermal

expansion. The 480 kg/m<sup>3</sup> (30 lb/ft<sup>3</sup>) density foam was used, being the lowest density usable without noticeable movement at elevated temperatures. Properties for the PBHT are shown in Table 6.3 [26].

Table 6.3 Properties of PBHT-30 Foam

<b>Density</b>	480.55 kg/m <sup>3</sup>
<b>Compressive Strength</b>	10.49 MPa
<b>Tensile Strength</b>	9.65 MPa
<b>Dimensional Stability</b>	1.2% max.
<b>Maximum Service Temperature</b>	148.9°C
<b>CTE</b>	57.6E-06 m/m/°C

The geometry of the nacelle was such that a solid male mold could not be used. To combat this issue, the foam mandrel was split into 7 pieces so that the center piece could be slid out and the other pieces could collapse inward and be easily removed from the skin after curing. Initially, the center piece of the mandrel was tapered to ease removal after the part had cured; however, it was determined that the mandrel pieces would be very difficult to machine in the current geometry. Thus the model was modified so that the center piece had a constant cross section and the other pieces required machining on only two or three sides. The initial and final geometries of the center piece of the mold are shown in Figure 6.20, and the final mold assembly is pictured in Figure 6.21. Excess material was left on either end of the nacelle mold so that the mold pieces could be clamped together during lay-up and cure. Any sharp internal edges were filleted to make machining easier. Figure 6.22 shows the CNC mill used to machine the foam.

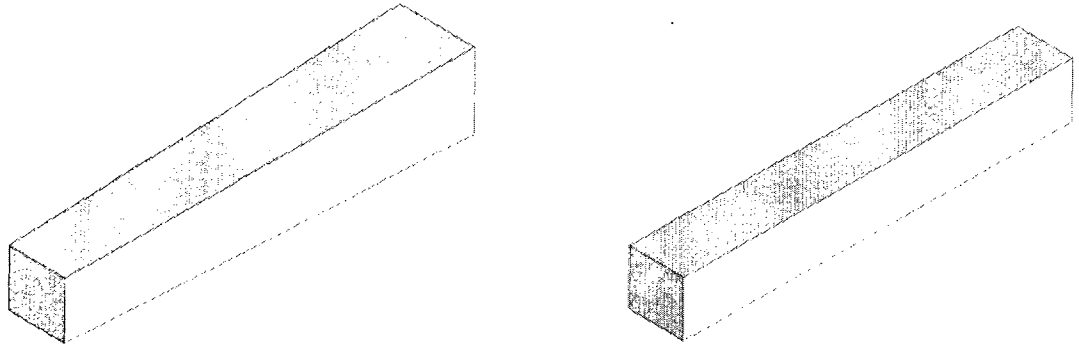


Figure 6.20 SolidWorks Model of Central Mold Piece. Final Design Shown on Right

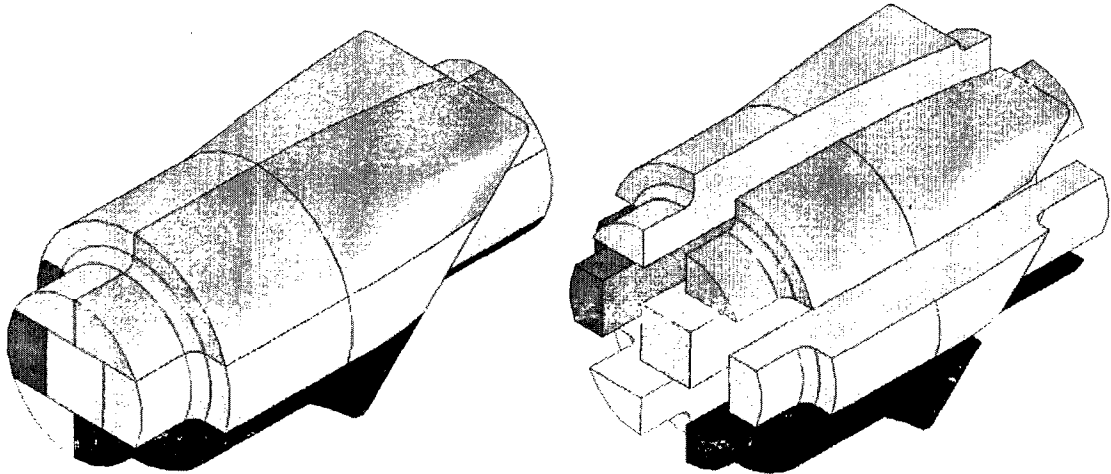


Figure 6.21 SolidWorks Model of Mandrel: Assembled (Left) and Exploded View

After the parts were machined and sanded, they were coated in Duratec 1799-005 vinyl ester, a primer capable of withstanding temperatures up to 149°C (300°F) ([www.revchem.com](http://www.revchem.com)). After the initial coat dried, another coat was applied. The surface was then sanded smooth. The coating provided a smooth, finished surface that would allow the pieces to slide easily against one another and, since the foam was porous, it would prevent the composite part from adhering to the mold. Another purpose for using

the coating was to be able to re-use the mold. This mold, shown in Figure 6.23, was used for both the prepreg and wet hand lay-ups. It weighed 10.3 kg (22.5 lbs) and was easily moved by one person. An equivalent aluminum mold would have weighed 58 kg (127 lbs).

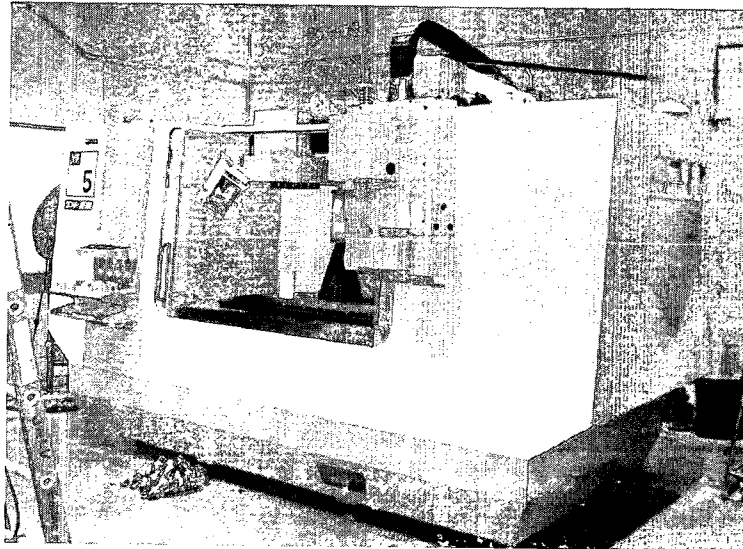


Figure 6.22 In-House CNC Mill

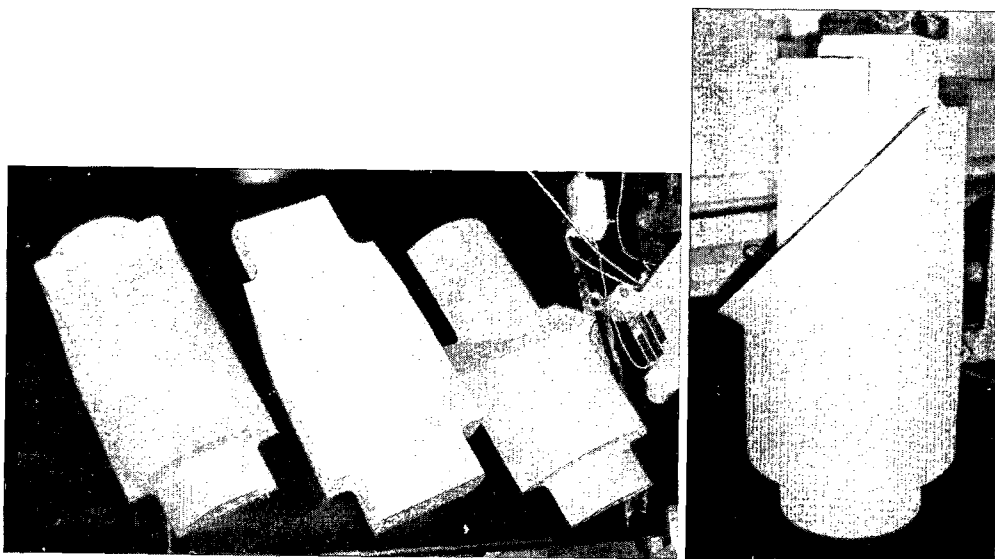


Figure 6.23 Nacelle Mold



### 6.5.1 Prepreg Nacelle Construction

For the first lay-up, the mold was prepped with two coats of PTM&W Industries PA0801 paste wax mold release on all surfaces (the inner surfaces were coated for ease of removal after the part cured) [18]. The mold pieces were assembled and hose clamps were placed on each end to hold the pieces together during the lay-up. The prepreg was then cut from the roll in 84 cm by 43 cm (17 in by 33 in) panels: two panels of 0 degree fibers and two panels of 90 degree fibers were cut. The two  $\pm 45$  degree layers were assembled from strips of prepreg ranging from 1.3 cm to about 13 cm ( $\frac{1}{2}$  in to 5 in). Similar to laying up a simple panel, the prepreg was laid onto the mold with the fibers laid in the 90 degree or hoop direction and pressed down. Bubbles and voids were removed by pressing and rubbing on the fibers until the desired surface was achieved. The sharp curves at the rear of the nacelle required extra attention since the fibers needed some coaxing to conform to the sudden direction changes. Another layer was then placed on the mold with the fibers set 0 degrees from the longitudinal axis. A total of six layers were laid up in the order of [90/0/-45/+45/0/90] relative to the x-axis (Figure 6.24).

The entire assembly was wrapped in Teflon peel-ply, breather cloth, and vacuum bag, in order, as shown in Figure 6.25. The vacuum pump valve was placed along the cylindrical part of the mold, away from the prepreg material, to avoid deformity in the fibers. The pump was turned on and the bagging was inspected for leaks by listening for the characteristic “hissing” sound of air intake through the plastic bagging. The part was then placed in the autoclave (Figure 6.26) and cured at 127°C (260° F) under vacuum for about 4 hours (the autoclave reached 135°C (275°F) after 40 minutes before it was

brought down to 127°C after an additional 10 minutes). The pressure exerted on the part was 84.7 kPa (12.3 psi).

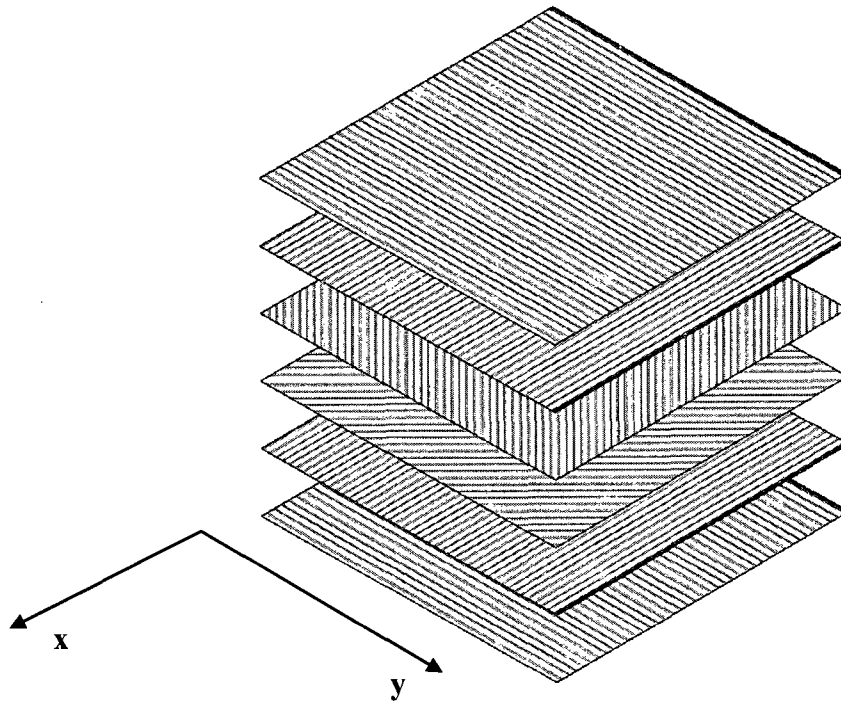


Figure 6.24 Fiber Orientation for Prepreg Lay-Up

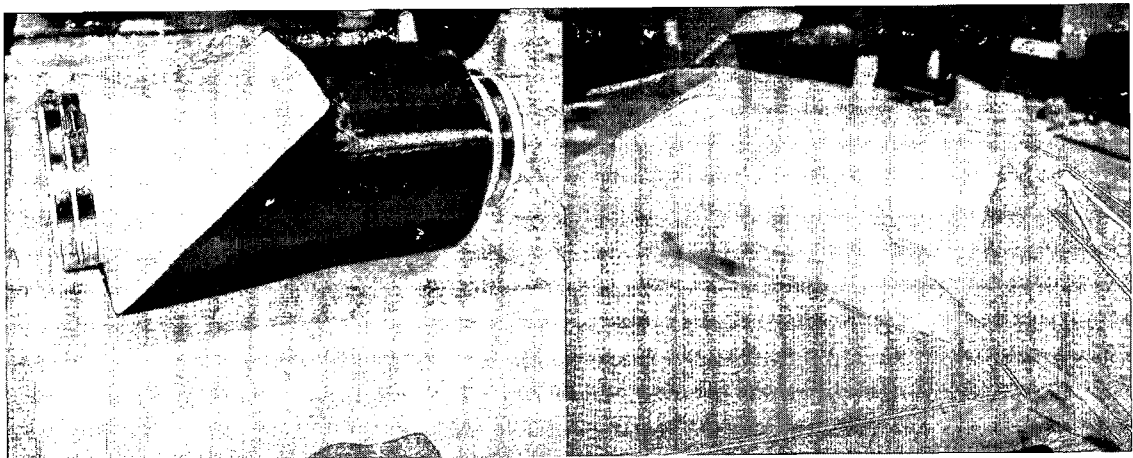


Figure 6.25 Prepreg Nacelle Lay-Up (Left) and Preparation for Cure

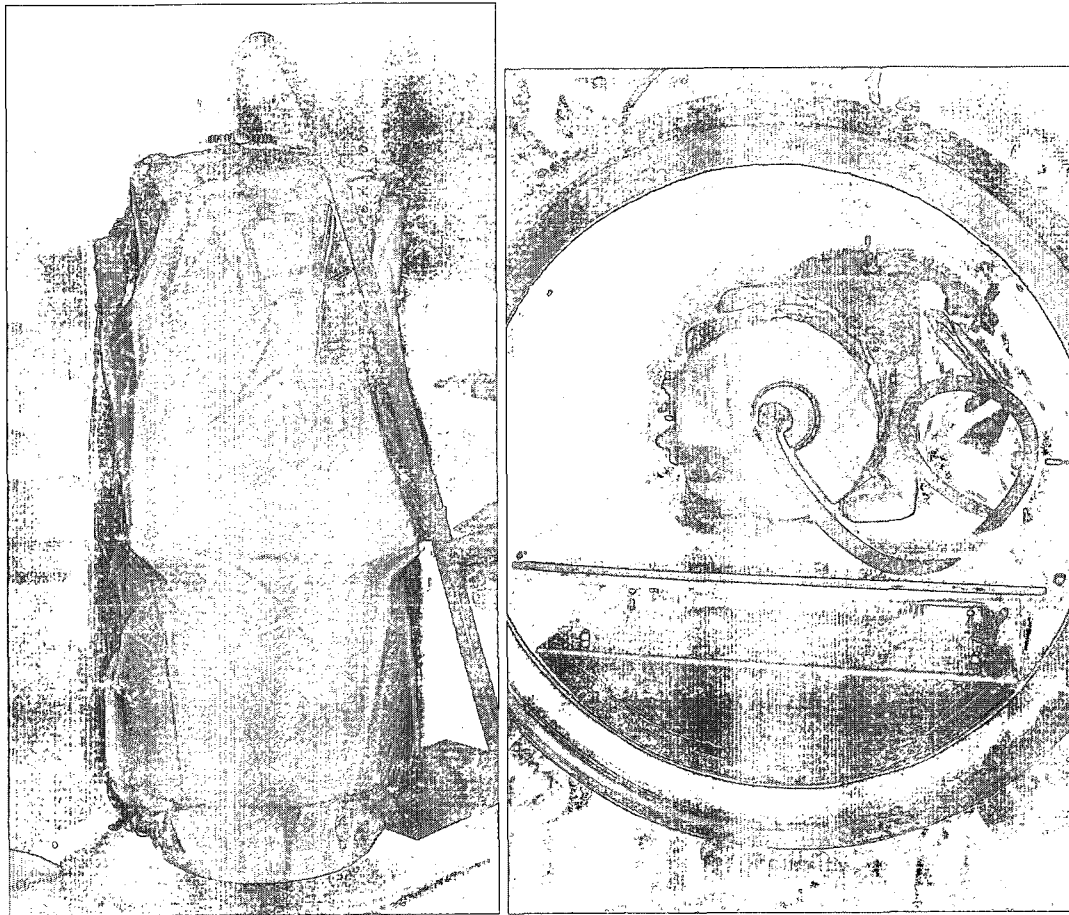


Figure 6.26 Prepreg Nacelle Under Vacuum (Left) and Ready for Cure in Autoclave

The assembly was removed from the autoclave after 4 hours. After removing the vacuum bag, breather cloth and peel-ply, the center mold piece was tapped out with a rubber mallet as shown in Figure 6.27. The other pieces were then able to individually break away from the carbon fiber and slide out from the part. Some of the mold edges broke off upon removal, showing signs that the mold release was ineffective in those areas. An example of the mold damage is shown in Figure 6.28.

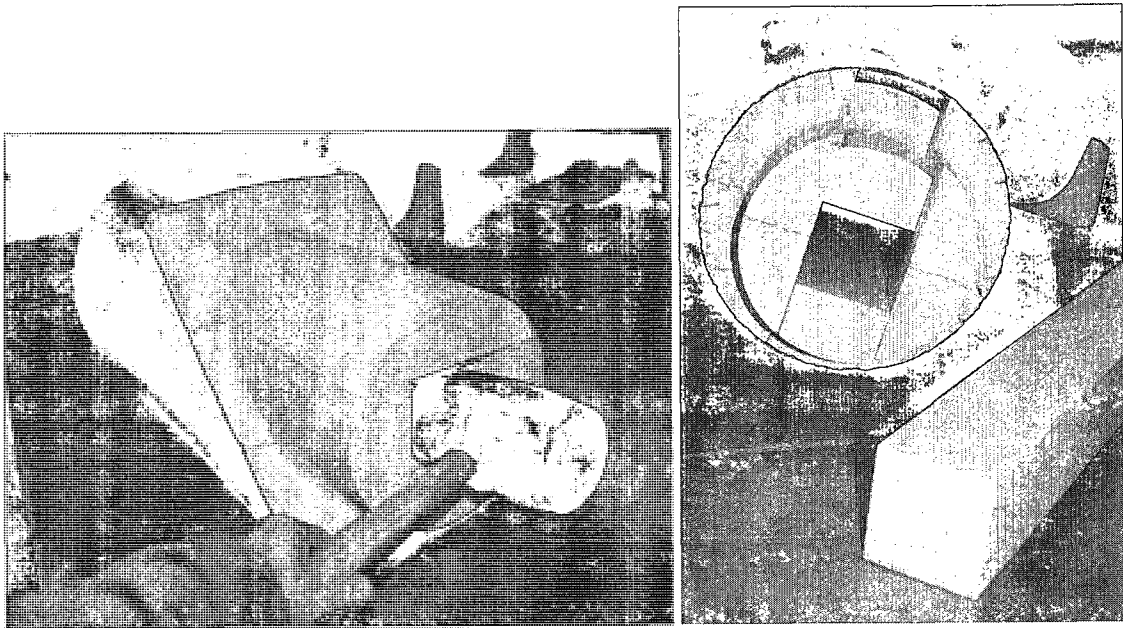


Figure 6.27 Removal of Mold from Cured Nacelle

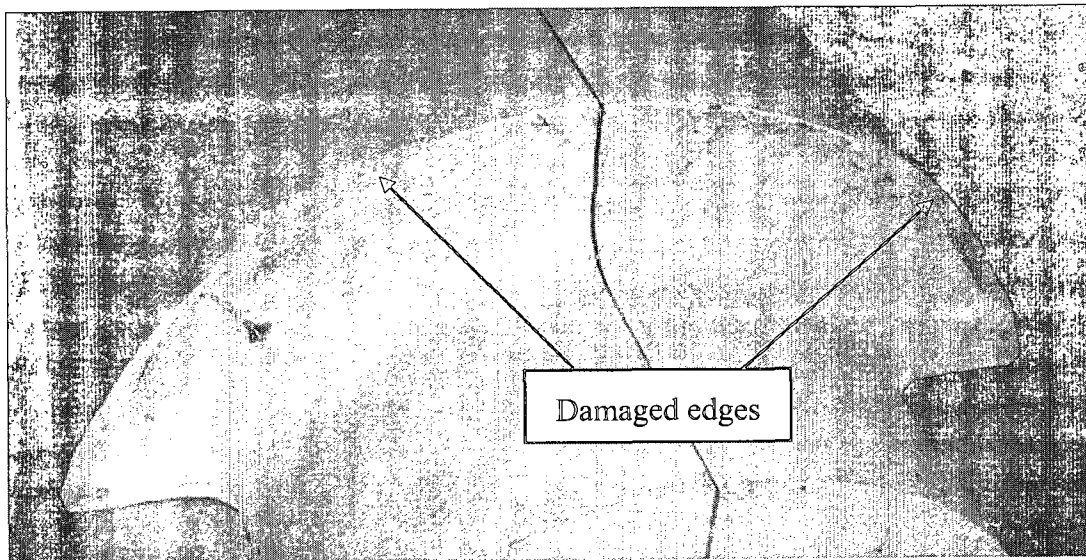


Figure 6.28 Damage Caused by Nacelle Removal

The damaged edges of the molds were rebuilt using several layers of the vinyl ester coating and the rest of the mold surface was recoated. Once the edges were built up, they were sanded down to the proper shape.

A different mold release was used for the second lay-up to attempt to ease the breakaway issues encountered with the first lay-up. Seven layers of TR 104 high temperature mold release were applied to the mold where the composite material would contact it; the other surfaces received three coats. The carnuba wax-based mold release was applied in a thin layer and allowed to set in the recommended 10 to 15 minutes before the part was buffed. The parts were left to dry for thirty minutes before the next layer of mold release was applied.

The second nacelle was laid up and cured in the same way as the first nacelle. Upon removal of the mold, however, damage again occurred, albeit in a different form. The coating peeled off the mold and adhered to the part surface (Figure 6.29). The cause of the damage was determined to be poor surface prepping prior to recoating the mold surfaces after the first lay-up. The mold was sanded and recoated.

Two more prepreg nacelles were laid up. The molds were prepped with Partall Paste #2 mold release, and although mold damage still occurred, it was not as significant and was easily repairable in the same manner as described for the first repair. An example of the finished prepreg nacelle is shown in Figure 6.30.

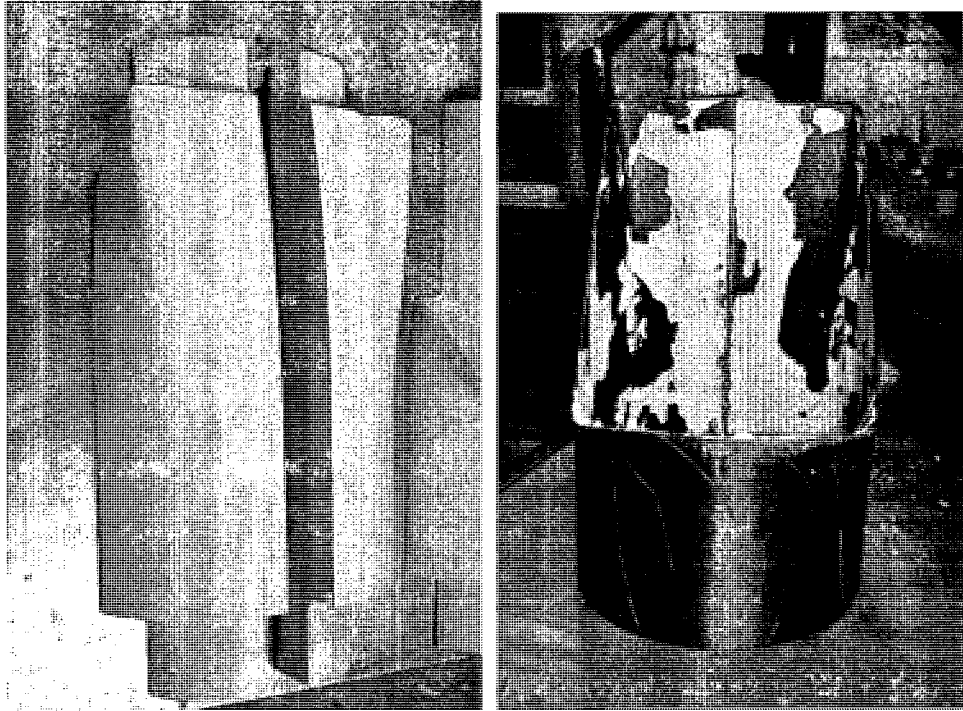


Figure 6.29 Surface Damage from Second Prepreg Lay-up

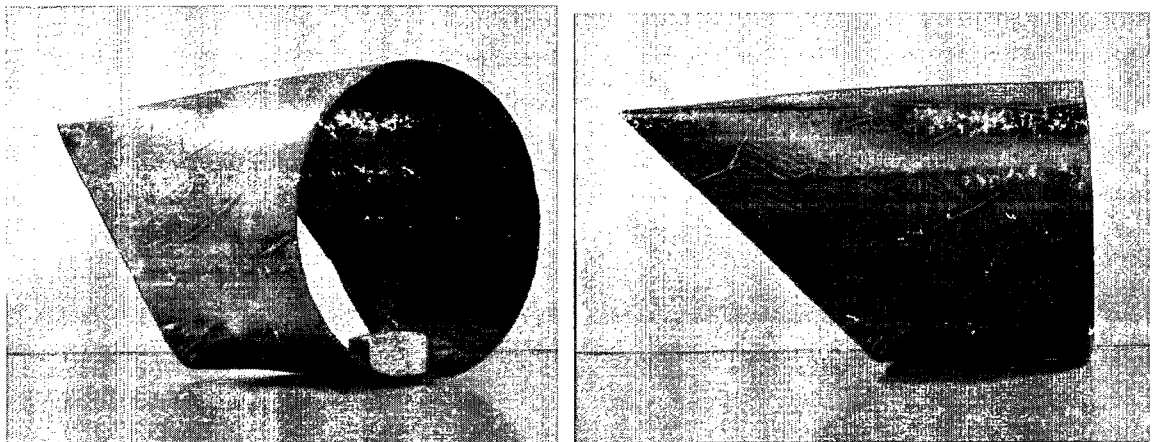


Figure 6.30 Finished Prepreg Nacelle

### 6.5.2 Wet Lay-up Nacelle Construction

The mold was coated with Partall Paste #2 prior to the lay-up. The satin weave fabric was cut to two 81 cm by 43 cm (32 in by 17 in) panels and the unidirectional cloth was trimmed into 8 cm to 10 cm (3 in to 4 in) wide strips of varying lengths with a maximum around 69 cm (27 in). The mold was wetted with a 3 to 1 epoxy resin prior to fiber placement. The wet lay-up prototypes were made with a combination of satin weave fabric and unidirectional cloth. Four layers of fabric were laid in a  $[0/+45/-45/0]$  orientation relative to the x-axis: the outer 0 degree layers contained the satin weave fabric with fibers in both the 0 and the 90 degree directions; the two opposing layers of unidirectional were placed in the  $\pm 45$  directions as shown in Figure 6.31. The ends were trimmed to remove large amounts of excess material, but some overhang was left on the part due to the noticeable movement of the woven fibers when the excess was trimmed close to the mold edge (as compared to the prepreg fibers). The part was then wrapped with Teflon peel-ply, breather cloth, and vacuum bag identical to the wrapping for the prepreg parts. The part was connected to the vacuum pump and a vacuum was pulled on it for about 16 hours (overnight) while the epoxy cured. The wet lay-up procedure is shown in Figure 6.32.

Once cured, the excess material was trimmed from the nacelle with a rotary cutter. The mold was then removed and the edges of the part were sanded. An example of the finished part is shown in Figure 6.33. The removal of the wet lay-up parts caused very little to no damage to the mold, except in one instance. The lack of high-temperature curing probably contributed to the successful removal of the mold.

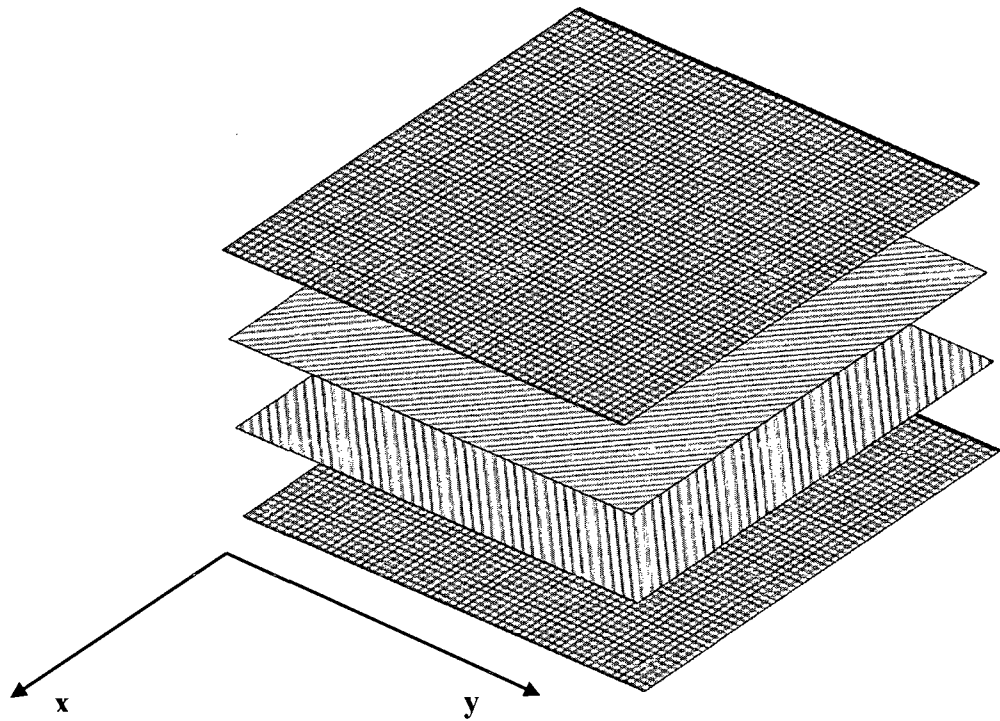


Figure 6.31 Fiber Orientation for Wet Lay-Up



Figure 6.32 Wet Lay-Up of Nacelle (Left) and Preparation for Cure



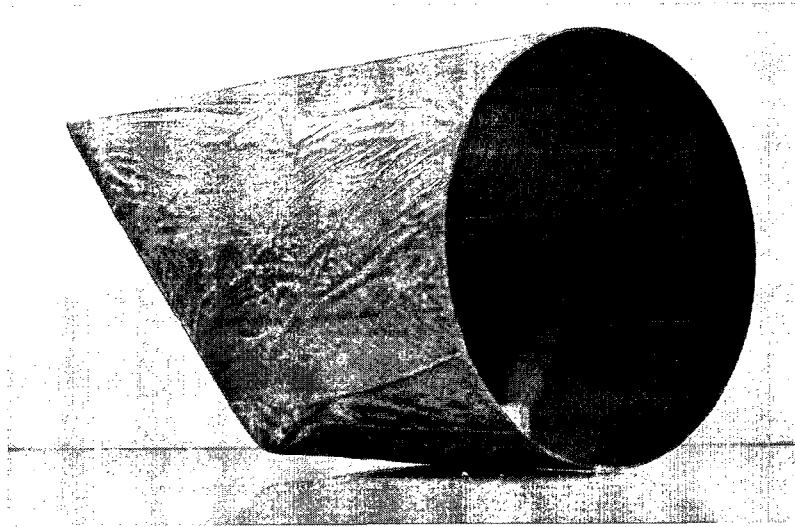


Figure 6.33 Finished Wet Lay-Up Nacelle

One wet lay-up caused extensive damage to the mold. It was thought to be due to insufficient trimming prior to mold removal in combination with the overall degradation of the mold itself. The degradation in the mold material most likely was a result of the heating and cooling cycles from the autoclave cure for the prepreg. The damage was more severe than, but similar in nature to, the damage caused by the prepreg lay-up shown in Figure 6.28. The mold was rebuilt by using epoxy resin to reattach the broken segments to the mold and then building up the rest with vinyl ester coating.

#### 6.6 Nacelle Compression Testing

To verify the design of the nacelles, they were tested in compression. The material properties and fabrication processes of each composite material are vastly different, particularly with complex shapes like the nacelle. Design verification via testing is necessary since the consistency of the parts made from each material should be known and the repeatability of the manufacturing processes should be compared. This test was

designed to check the deformation response within the elastic range of the materials. The consistency of the load-displacement response of the four nacelles of each material are compared and the results are compared to a finite element analysis prediction of the response.

The nacelles were tested on a United model SSTM-1 testing machine fitted with a 45 kg (100 lb) load cell utilizing a three-point bend fixture with a span of 10 cm (4 in). The choice in the fixture type was dependent on the unusual geometry of the nacelle; support at two points provided greater stability and smaller contact points provided better uniformity in loading. An ASTM testing standard was not referenced for these tests, aside from being used as a basis for the testing template (explained below). The test set-up is shown in Figure 6.34.

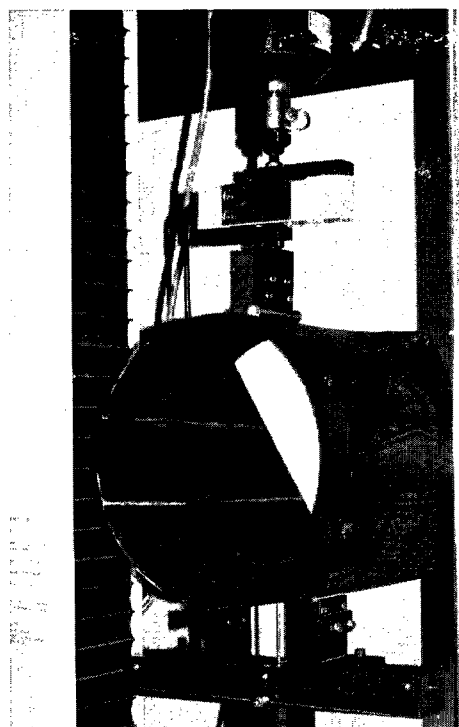


Figure 6.34 Compression Test Set-Up with Three-Point Bend Fixture

Loading was only applied to the cylindrical portion of the nacelles for ease of repeatability; since the results were compared only to the FEA of the nacelles under identical load and not to any data outside of the project, only uniformity among the tests was required. The software for the United machine, DATUM 4.0, was used to run the tests and collect the load and displacement data. A testing template was created, referenced from ASTM Standard D-790 (a Standard reference is necessary) due to the fixture choice, and a strain rate of 0.5 cm (0.2 in) per minute and a maximum displacement of 2.5 cm (1 in) were applied. Specimens were preloaded to 2.2 N (0.5 lb) and then loaded until the maximum displacement was achieved (Figure 6.35). The data were saved and transferred to a Microsoft Excel spreadsheet.

It was noticed that during loading, the deformation of the nacelle caused the load roller to lose contact with the nacelle in the front region. This resulted in a point load, which must be accounted for in the FEA.

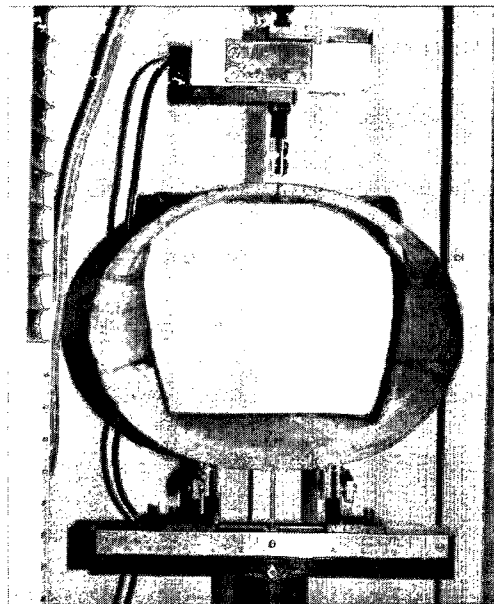


Figure 6.35 Compression Test of Woven Nacelle

From the data, a load versus deflection curve was plotted for each specimen. Figure 6.36 compares the plots of a woven nacelle (specimen 2) and a prepreg nacelle (specimen 1). The remaining plots are shown in Appendix V.

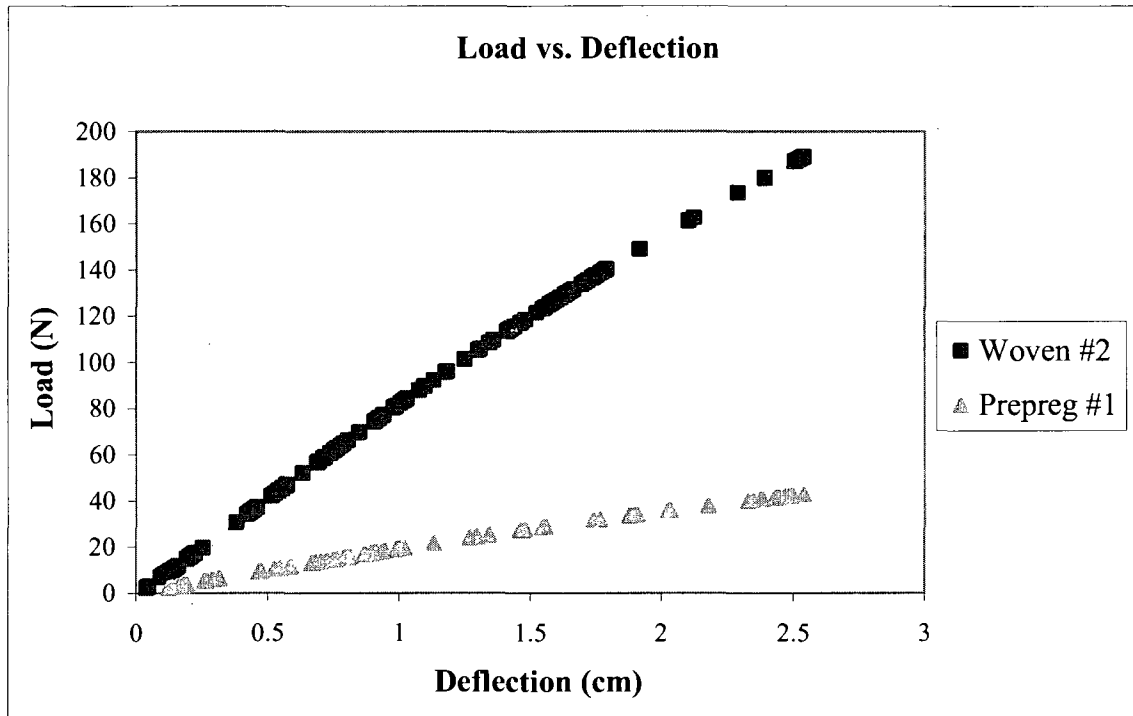


Figure 6.36 Plot of Load Versus Deflection for Sample Specimens

The maximum load experienced at a 2.54 cm deflection was divided by the weight to get the load to weight ratio for each specimen. The results are shown in Table 6.4.

Table 6.4 Maximum Load, Weight, and Load to Weight Ratios of Nacelles

Specimen	Max Load (N)	Weight (kg)	L/W Ratio
Prepreg 1	42.85	0.221	193.90
Prepreg 2	34.11	0.221	154.32
Prepreg 3	42.78	0.220	194.45
Prepreg 4	41.44	0.225	184.18
Woven 1	189.00	0.452	418.14
Woven 2	216.21	0.473	457.10
Woven 3	220.27	0.486	453.23
Woven 4	253.89	0.492	516.04

The FEA models were modified to reflect the physical test set-up, including the point loading experienced by the specimens. They were then run to determine the load necessary to deflect the model 25.4 mm (1 in). This was achieved by running two simulations of each model under a different load and then, since a linear static analysis is being performed, determining a line equation from which the load could be calculated. For verification, a final simulation was run under the calculated load. The results showed that the load required to deflect the prepreg nacelle 25.4 mm at the loading location was 93.1 N (20.9 lb) while the load required to deflect the hand lay-up nacelle the same distance was 500.4 N (112.5 lb). The FEA models are shown in Figure 6.37 and the OptiStruct reports for the 2.5 cm deflection are shown in Appendix VII. Contour plots of the displacement of the prepreg and wet lay-up nacelles are shown in Figures 6.38 and 6.39, respectively.

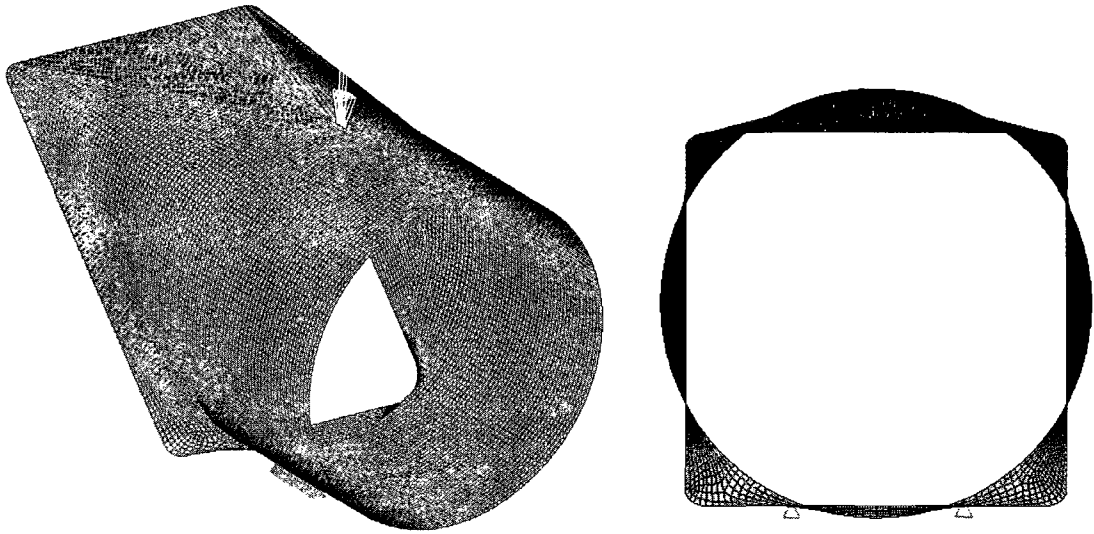


Figure 6.37 Load and Constraint Locations for FEA: Isometric (left) and Front Views

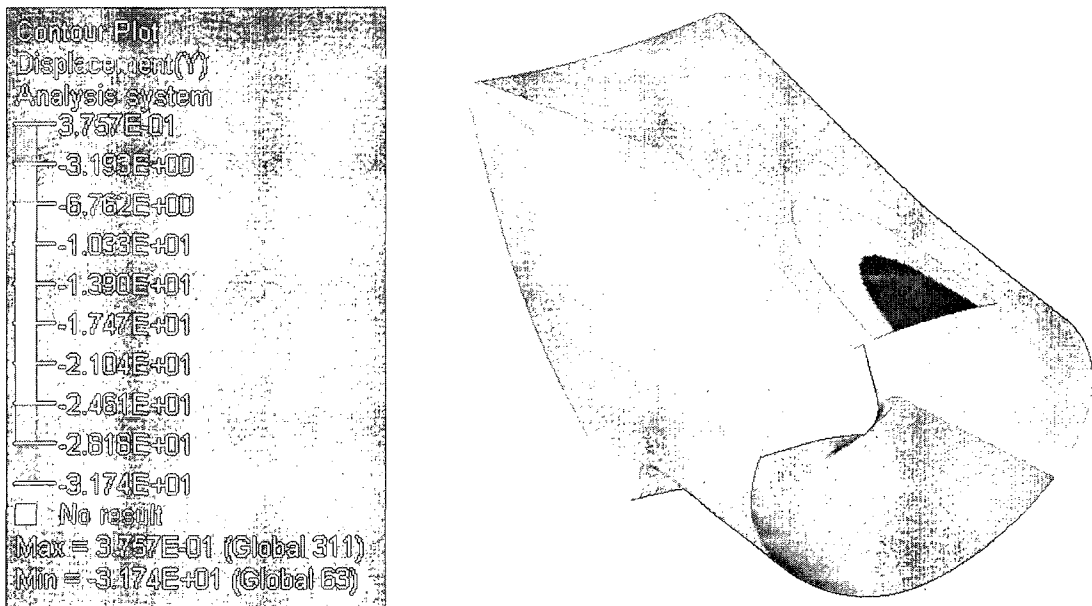


Figure 6.38 Contour Plot of Displacement for Prepreg Nacelle

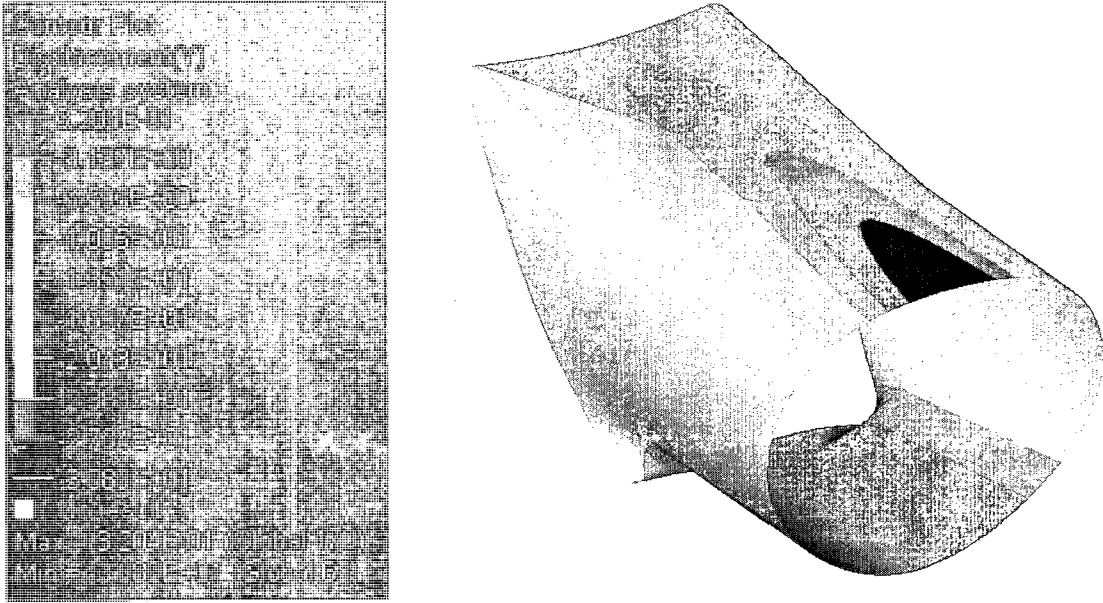


Figure 6.39 Contour Plot of Displacement for Wet Lay-Up Nacelle

The results for both analysis methods are shown in Table 6.5. Comparing the FEA results to the tests, the FEA models are optimistic by a factor of over two with respect to the required load. This is due in part to the idealized models in FEA – it is difficult to account for irregularities in the manufacturing process, such as variances in the amount of resin removed during the vacuum process, excess material in the regions of complicated geometry, and the difficulty of lining up the fibers exactly in the specified orientations (if the fiber orientation is off even a couple degrees, the strength of the part can be greatly affected). FEA should not replace physical testing especially for composite materials, but it is a good indicator of the behavior of the part.

Table 6.5 Load Results from FEA and Experimental Analysis

<b>Load Required for 25.4 mm Deflection (N)</b>		
<b>Nacelle Type</b>	<b>FEA</b>	<b>Exp</b>
Prepreg	93.1	40.29
Hand Lay-Up	500.4	219.84

The results of the experiments show that the wet lay-up nacelles are stiffer than the prepreg nacelles. The highest load to weight ratio under a 25.4 mm (1 in) displacement for a wet lay-up specimen was 516 while the highest ratio experienced by a prepreg specimen was 194. However, these results do not mean that equivalent weight nacelles will result in equivalent strength nacelles. The fiber orientation has been optimized for each material type and changing the orientation will change the strength of the part.



## CHAPTER 7

### CONCLUSIONS AND RECOMMENDATIONS

Based on the research conducted for this project, a mixed material airframe is recommended for research institutes with similar resources. A wet lay-up is easier to perform for the wings; prepreg is a better choice for the nacelles because of weight constraints. The woven nacelles would be a good choice based on strength and rigidity if the maximum airframe weight limit was greater.

The cost of materials has been broken down for each component. Tables 7.1 and 7.2 show the cost breakdown for the wings and the fuselage, respectively.

Table 7.1 Estimated Material Cost for Wings

	<b>Part</b>	<b>Quantity</b>	<b>Unit Cost</b>	<b>Total Cost</b>
<b>Wings</b>	satin weave	1.28 m	\$42.65/m	\$54.59
	unidirectional	1.19 m	\$11.26/m	\$13.40
	peel-ply	1.28 m	\$6.01/m	\$7.69
	epoxy resin	0.47 L	\$16.11/L	\$7.57
	Dow 2# blue foam	0.65 m <sup>2</sup>	\$43.06/m <sup>2</sup>	\$27.99
<b>Total cost</b>				<b>\$111.24</b>

Table 7.2 Estimated Material Cost for Fuselage

	Part	Quantity	Unit Cost	Total Cost
<b>Fuselage</b>	prepreg	1.28 m	\$18.73/m	\$23.97
	plain weave	0.77 m	\$47.57/m	\$36.63
	divinycell	0.051 m <sup>3</sup>	\$152.21/m <sup>3</sup>	\$7.76
	peel-ply	1.10 m	\$6.01/m	\$6.61
	epoxy resin	0.47 L	\$16.11/L	\$7.57
	Dow 2# blue foam	0.316m <sup>2</sup>	\$43.06/m <sup>2</sup>	\$13.61
	vacuum bag	0.08 m	\$4.65/m	\$0.37
<b>Total cost</b>				<b>\$96.53</b>

Tables 7.3 and 7.4 show the total cost for the four prepreg nacelles and four wet lay-up nacelles, respectively. Each quantity consists of all the material required for the fabrication of four nacelles.

Table 7.3 Estimated Material Cost for Prepreg Nacelles

	Part	Quantity	Unit Cost	Total Cost
<b>Prepreg nacelles</b>	prepreg	11 m	\$18.73/m	\$206.03
	peel-ply	1.94 m	\$6.01/m	\$11.66
	breather	1.94 m	\$4.37/m	\$8.48
	vacuum bag	2.56 m	\$4.65/m	\$11.90
	vacuum tape	6.22 m	\$.91/m	\$5.66
	PBHT 30lb foam	7.93E-2 m <sup>3</sup>	\$6356.70/m <sup>3</sup>	\$508.00
	Duratec 1799-005	3.8 L	\$19.30/L	\$73.00
<b>Total cost</b>				<b>\$824.73</b>

Table 7.4 Estimated Material Cost for Wet Lay-Up Nacelles. \* - MDF was not actually used in this project

	<b>Part</b>	<b>Quantity</b>	<b>Unit Cost</b>	<b>Total Cost</b>
<b>Woven nacelles</b>	satin weave	3.47 m	\$42.65/m	\$148.00
	unidirectional	15.27 m	\$11.26/m	\$171.94
	epoxy resin	1.89 L	\$16.11/L	\$30.45
	peel-ply	1.94 m	\$6.01/m	\$11.66
	breather	1.94 m	\$4.37/m	\$8.48
	vacuum bag	2.56 m	\$4.65/m	\$11.90
	vacuum tape	6.22 m	\$.91/m	\$5.66
	MDF*	7.93E-2 m3	\$847.55/m3	\$67.20
<b>Total cost</b>				<b>\$455.28</b>

These costs do not include supplies such as mixing cups and squeegees, or time on equipment such as vacuum pumps and autoclaves. Equipment costs would need to be considered for a research organization that does not already possess them.

Table 7.5 lists the timeframe and associated costs for design and fabrication for each component of the airframe. The time estimates have been broken down into the time required for design and for fabrication and the costs have been broken down into material and labor costs.

Table 7.5 Estimated Cost and Time of Completion for Airframe Components

<b>Part</b>	<b>Time - Design</b>	<b>Time - Build</b>	<b>Cost - Materials</b>	<b>Cost - Labor</b>
<b>Fuselage</b>	2 weeks	1 week	\$97	\$2,400
<b>Wing</b>	2 weeks	2 weeks	\$112	\$3,200
<b>Nacelle</b>	2 weeks	4 weeks	\$1,213	\$4,800
<b>Total</b>	<b>6 weeks</b>	<b>7 weeks</b>	<b>\$1,422</b>	<b>\$10,400</b>

The recommendations provided are based on the materials and technologies available to the University. The time and cost estimates will vary depending on the budget, materials and technologies, and number of people involved in the design and fabrication of the prototype. This estimate should be typical for a college or university with limited resources. The labor costs were based on an hourly rate of \$20, the typical rate for a graduate research assistant. Work days typically lasted eight hours and weeks consisted of five days. Most of the work on the airframe was performed by graduate students. One student was involved in the solid modeling and two to three students performed the fabrication.

A comparison all of the possible fabrication methods for the nacelles is shown in Table 7.6. The labor cost includes the design time for the nacelles from Table 7.4. The prepreg nacelles required the longest fabrication time because of the necessary mold repair after every lay-up. The wet lay-up nacelle demonstrated superior stiffness during testing, but the prepreg proved to be the lightest. The behavior of neither method can be accurately predicted using the FEA utilized in this paper. The rapid prototyped parts were too heavy to consider at this point. Rapid prototyping the nacelles would have cost between \$5,400 and \$19,980 for one set (the average cost is shown in the Table).

Table 7.6 Comparison of Cost and Time for Nacelle Fabrication Methods

	RP	Prepreg	Wet Lay-Up
<b>Material Cost</b>	\$9,400.00	\$824.73	\$455.28
<b>Labor Cost</b>	\$1,600.00	\$3,680.00	\$3,040.00
<b>Time for Fabrication</b>	4 days	13 days	9 days

Further research should be pursued on the structural integrity of the airframe for more advanced prototypes. Impact testing would be very beneficial to the project since the nature of the aircraft lends itself to minor and possibly major impacts with stationary and moving objects. More efficient methods for manufacturing are already being studied for this project. Aerodynamic analysis should also be performed on the current design before testing the aircraft in translational flight.

Studies in the rapid prototyping of airframe components should also be done should funding continue. While the current budget for this project could not allow such research to be done, RP is still a very feasible prototyping method, especially for limited timeframes.

More work should also be done with respect to mold materials. The primary concern is the integrity of the mold when used for multiple high temperature cure lay-ups. Proper temperature ramp-up procedures for the PBHT 30 foam should be applied to determine if the foam was heated too quickly during this study and if rapid heating leads to rapid material degradation.

## APPENDIX I

### MATERIAL DATA SHEET FOR CARBON PREPREG

This data sheet was taken from <http://www.newportad.com/pdf/PL.NB-301.pdf>

#### **34-700 Standard Modulus Uni-directional Carbon Fiber tape reinforcement**

The mechanical property data supplied in the following table are average values obtained from NCT-301 with 34-700 carbon fiber at 35% RC. All values are based using a press cure at 275° F for 60 minutes using 25 psi. All data are normalized to 60% fiber volume, except for SBS.

<b>NCT-301 34-700</b>	<b>Test Method</b>	<b>RT*</b>
0° Tensile strength, ksi	ASTM D- 3039	295
0° Tensile modulus, Msi		19.0
Strain, $\mu\text{in/in}$		14,700
Poisson's ratio		0.304
0° Compression strength, ksi	SACMA SRM 1R-94	180
0° Compression modulus, Msi		18.6
0° Flexural strength, ksi	ASTM D-790	280
0° Flexural modulus, Msi		18.2
0° Short Beam Shear str., ksi	ASTM D-2344	13.2

<b>NCT-301 34-700</b>	<b>Test Method</b>	<b>RT*</b>
90° Tensile strength, ksi	ASTM D- 3039	8.7
90° Tensile modulus, Msi		1.3
Strain, $\mu\text{in/in}$		6,100
Poisson's ratio		0.017
90° Compression strength, ksi	SACMA SRM 1R-94	28.8
90° Compression modulus, Msi		1.2
90° Flexural strength, ksi	ASTM D-790	16.7
90° Flexural modulus, Msi		1.2
90° Short Beam Shear str., ksi	ASTM D-2344	1.3

\* Values are average and do not constitute a specification



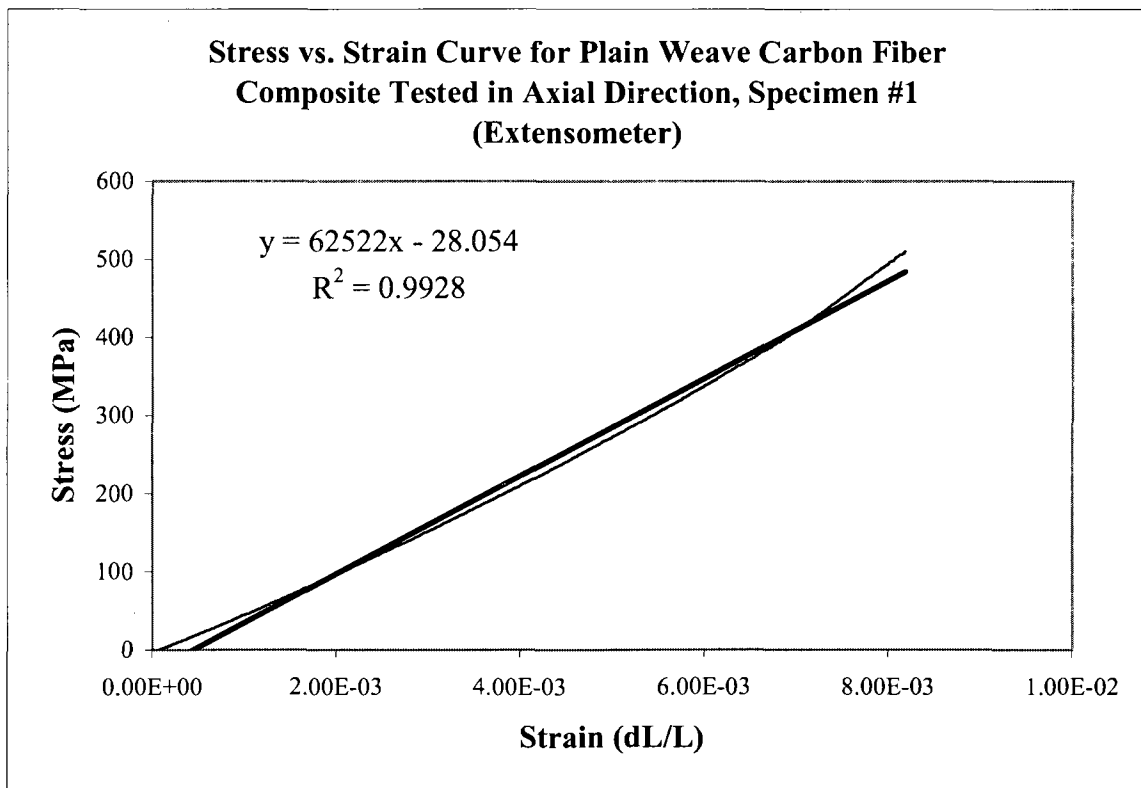
Newport 301 Product Data Sheet  
PL.NB-301.042307.doc

©2006 Newport Adhesive and Composites, Inc  
All rights reserved.

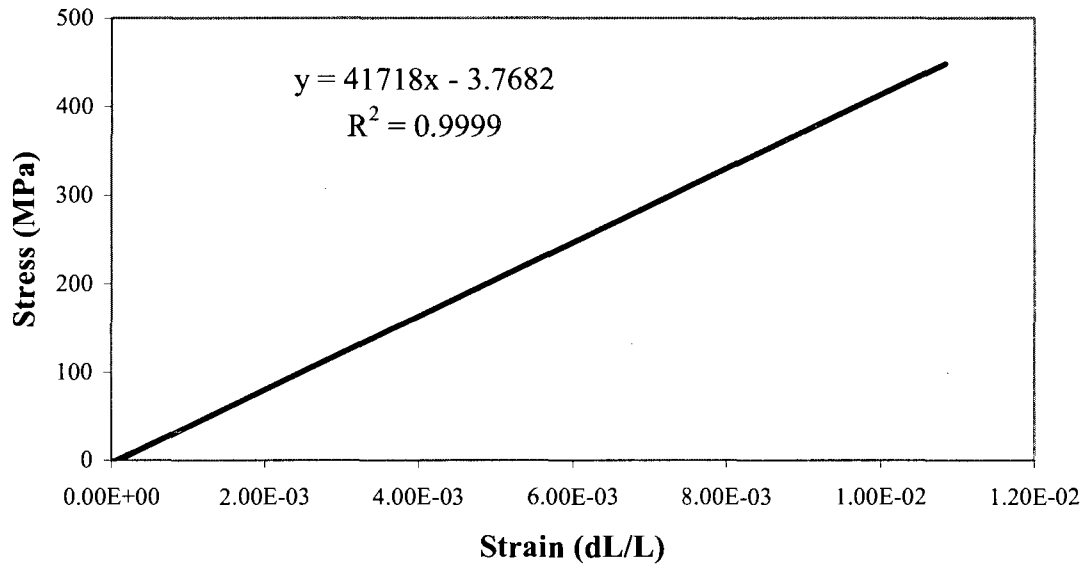
## APPENDIX II

### STRESS VS. STRAIN PLOTS FOR PLAIN WEAVE CARBON FIBER

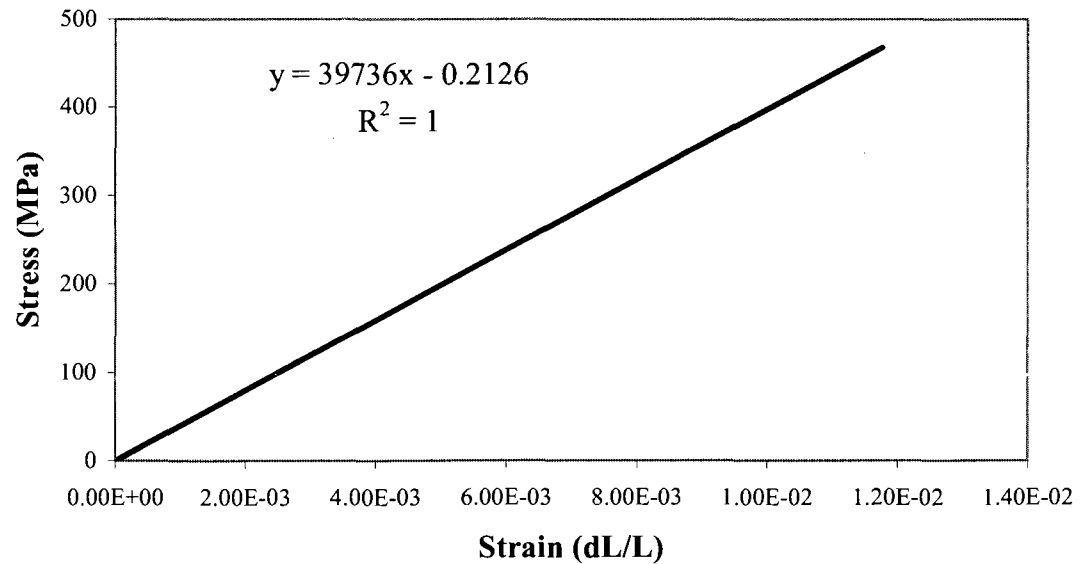
Shown in this appendix are the rest of the stress versus strain plots for the carbon plain weave material.



**Stress vs. Strain Curve for Plain Weave Carbon Fiber Composite Tested in Axial Direction, Specimen #1 (Strain Gages)**

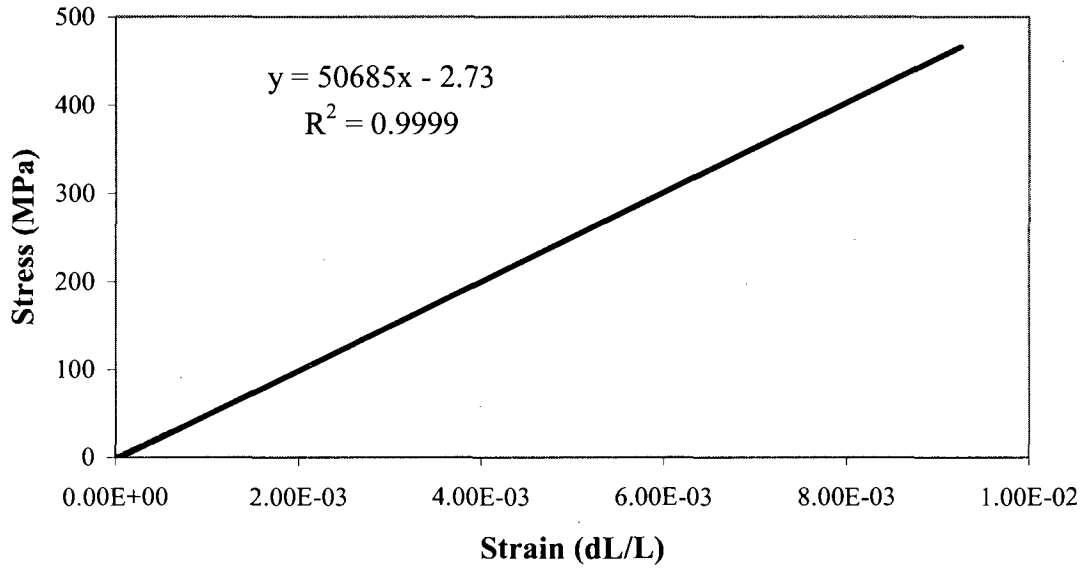


**Stress vs. Strain Curve for Plain Weave Carbon Fiber Composite Tested in Axial Direction, Specimen #2 (Extensometer)**

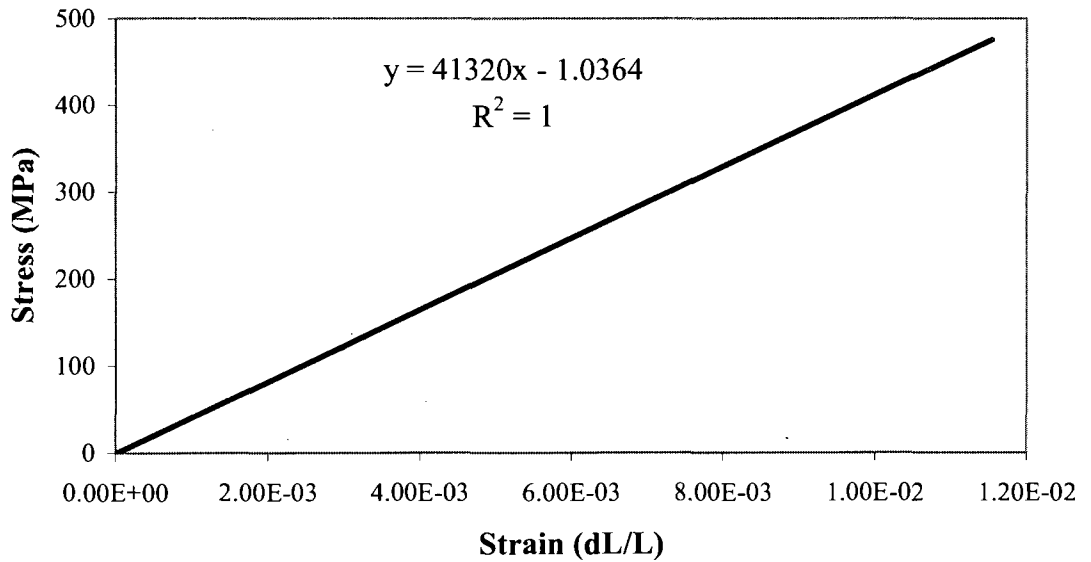




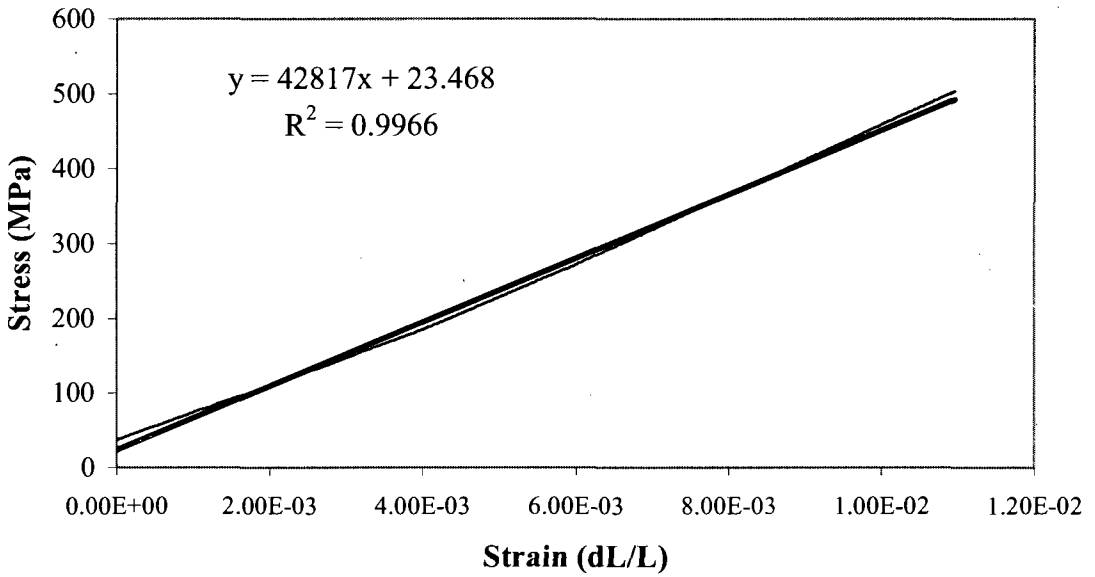
**Stress vs. Strain Curve for Plain Weave Carbon Fiber Composite Tested in Axial Direction, Specimen #2 (Strain Gage)**



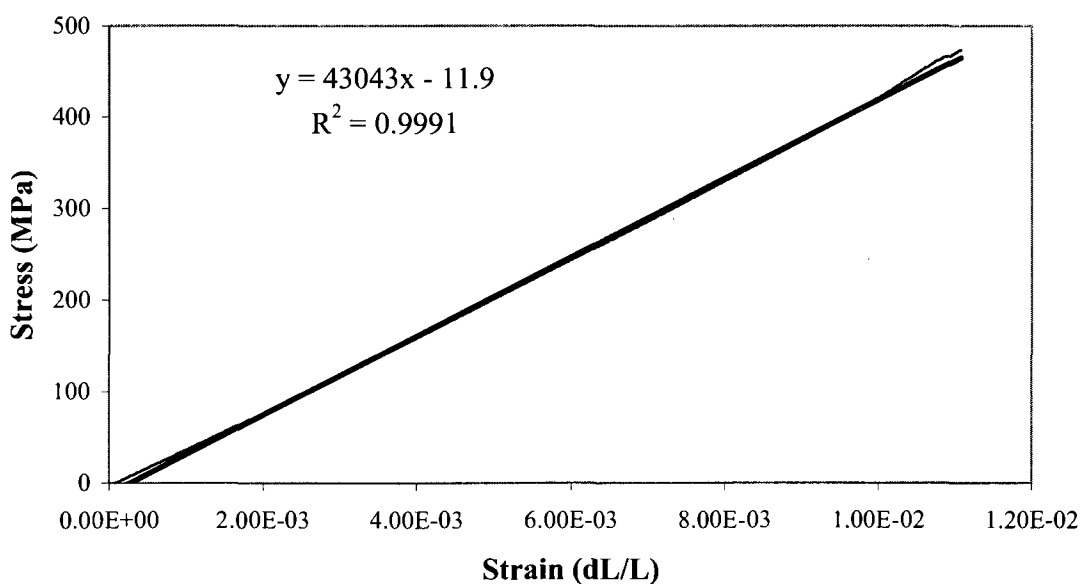
**Stress vs. Strain Curve for Plain Weave Carbon Fiber Composite Tested in Axial Direction, Specimen #3 (Extensometer)**



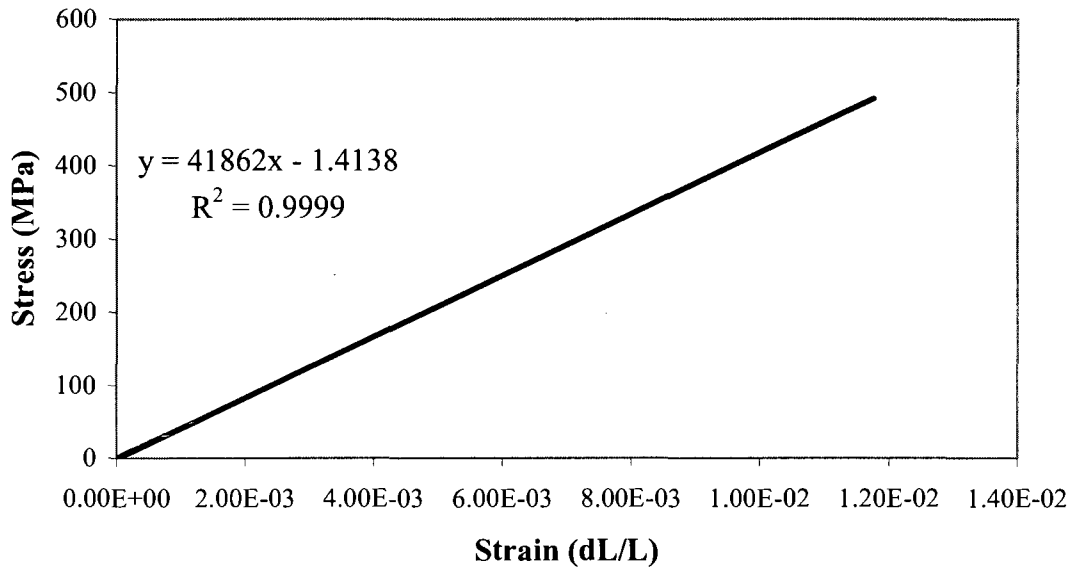
**Stress vs. Strain Curve for Plain Weave Carbon Fiber Composite Tested in Axial Direction, Specimen #4 (Extensometer)**



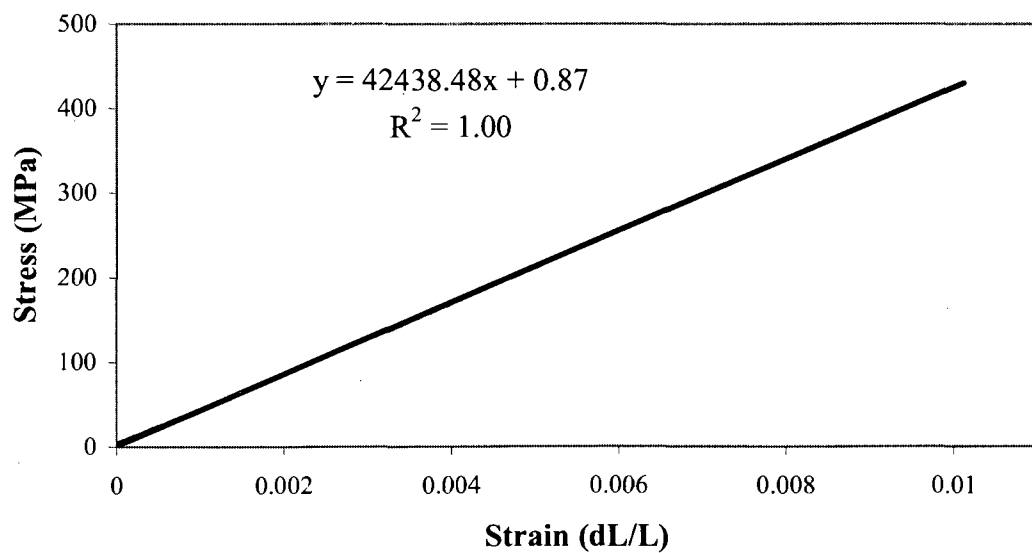
**Stress vs. Strain Curve for Plain Weave Carbon Fiber Composite Tested in Axial Direction, Specimen #4 (Strain Gage)**



**Stress vs. Strain Curve for Plain Weave Carbon Fiber Composite Tested in Axial Direction, Specimen #5 (Extensometer)**



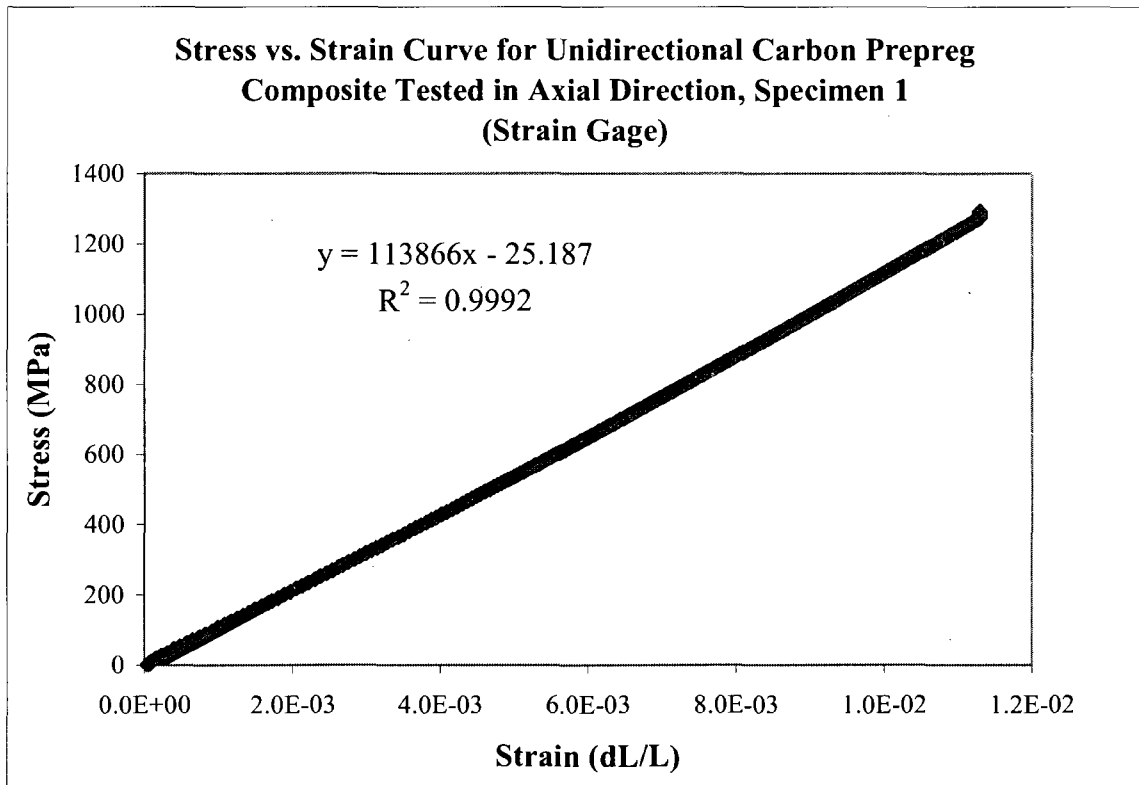
**Stress vs. Strain Curve for Plain Weave Carbon Fiber Composite Tested in Axial Direction, Specimen #6 (Extensometer)**



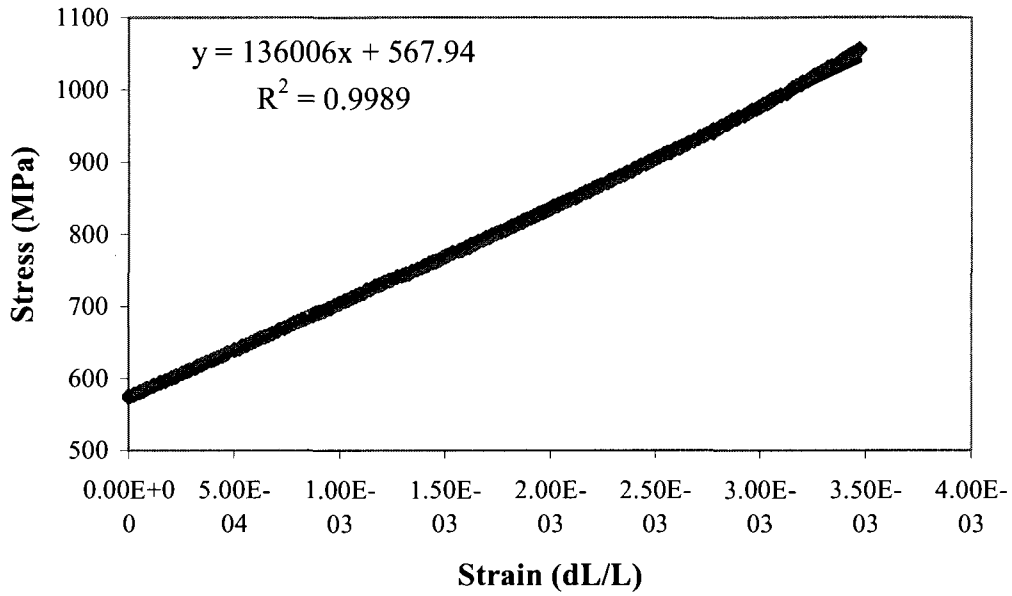
### APPENDIX III

#### STRESS VS. STRAIN PLOTS FOR PREPREG CARBON FIBER

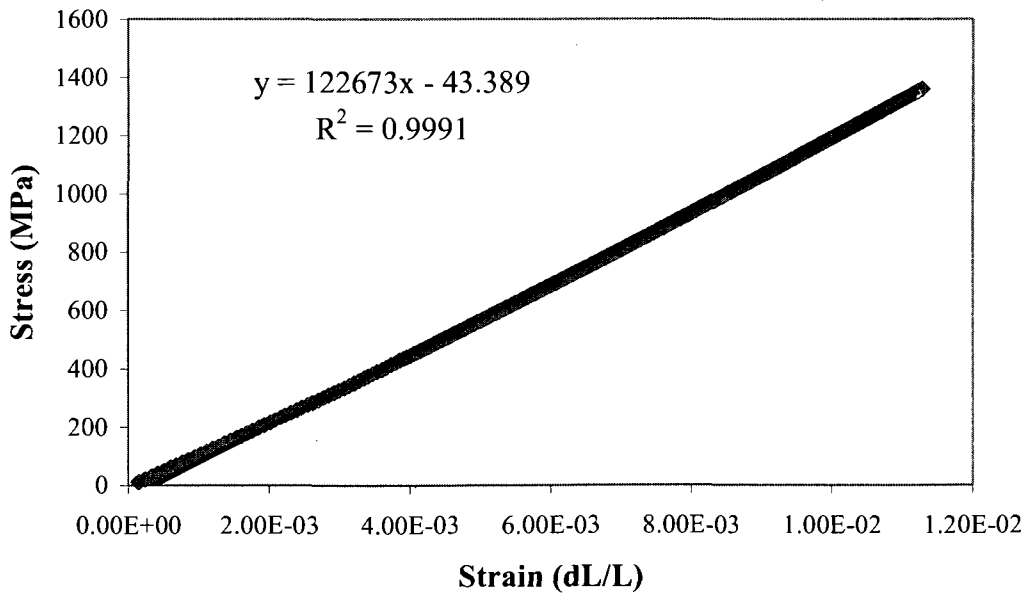
Shown in this appendix are the rest of the stress versus strain plots for unidirectional carbon fiber prepreg material.



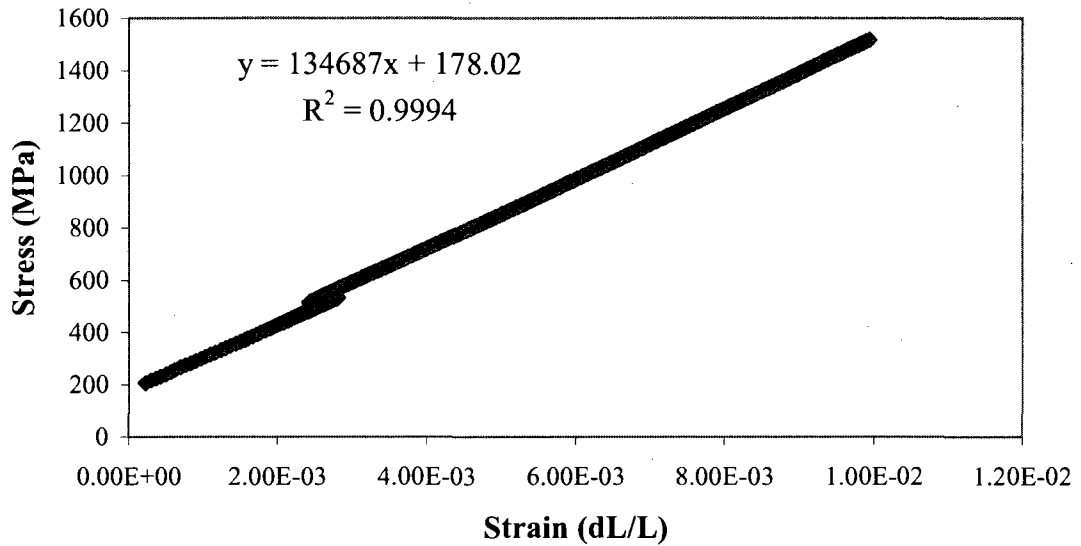
**Stress vs. Strain Curve for Unidirectional Carbon Prepreg  
Composite Tested in Axial Direction, Specimen 2  
(Extensometer)**



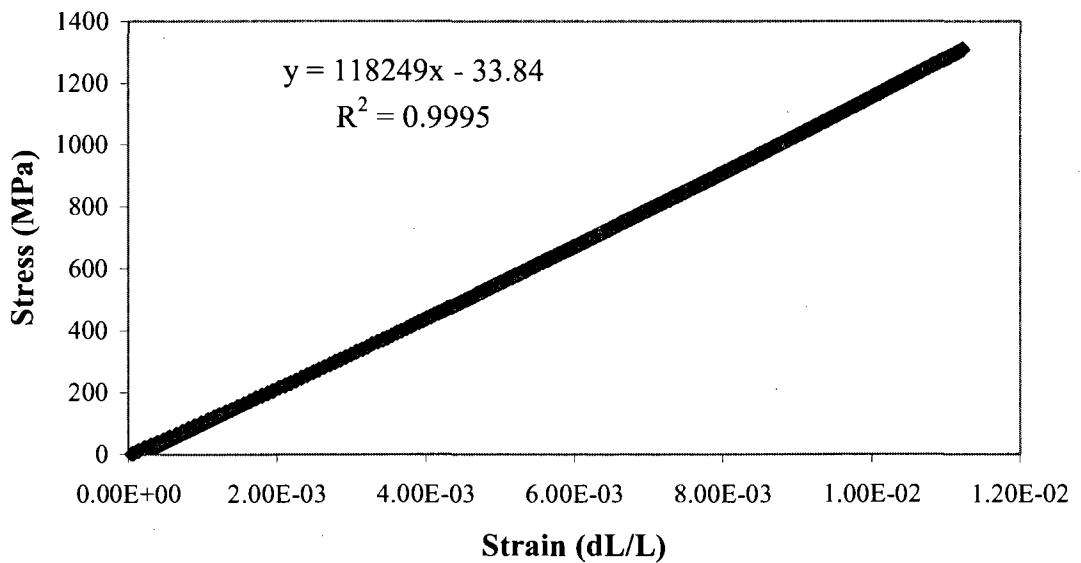
**Stress vs. Strain Curve for Unidirectional Carbon Prepreg  
Composite Tested in Axial Direction, Specimen 2  
(Strain Gage)**



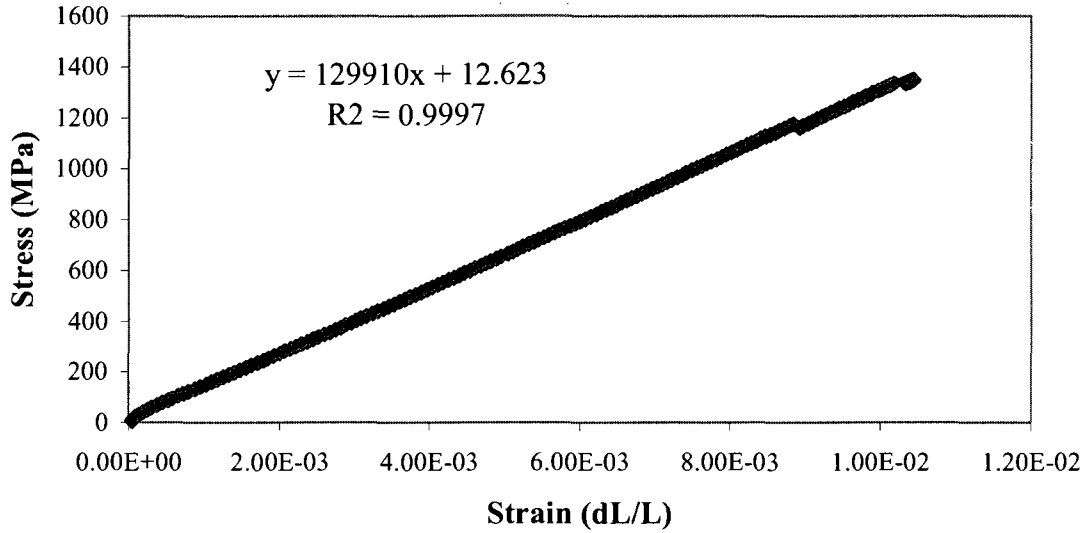
**Stress vs. Strain Curve for Unidirectional Carbon Prepreg Composite Tested in Axial Direction, Specimen 3 (Extensometer)**



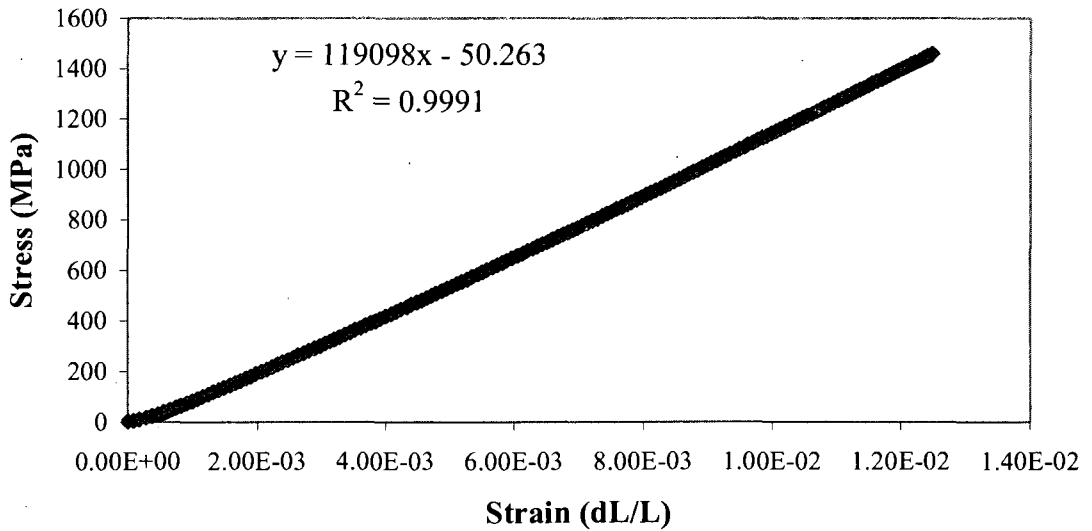
**Stress vs. Strain Curve for Unidirectional Carbon Prepreg Composite Tested in Axial Direction, Specimen 3 (Strain Gage)**



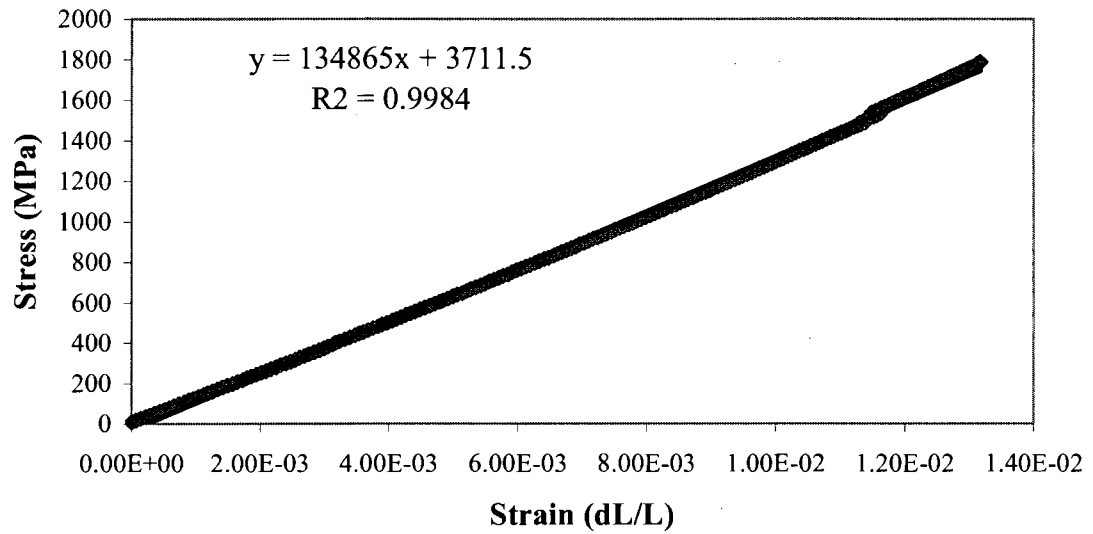
**Stress vs. Strain Curve for Unidirectional Carbon Prepreg  
Composite Tested in Axial Direction, Specimen 4  
(Extensometer)**



**Stress vs. Strain Curve for Unidirectional Carbon Prepreg  
Composite Tested in Axial Direction, Specimen 5  
(Extensometer)**



**Stress vs. Strain Curve for Unidirectional Carbon Prepreg  
Composite Tested in Axial Direction, Specimen 6  
(Extensometer)**

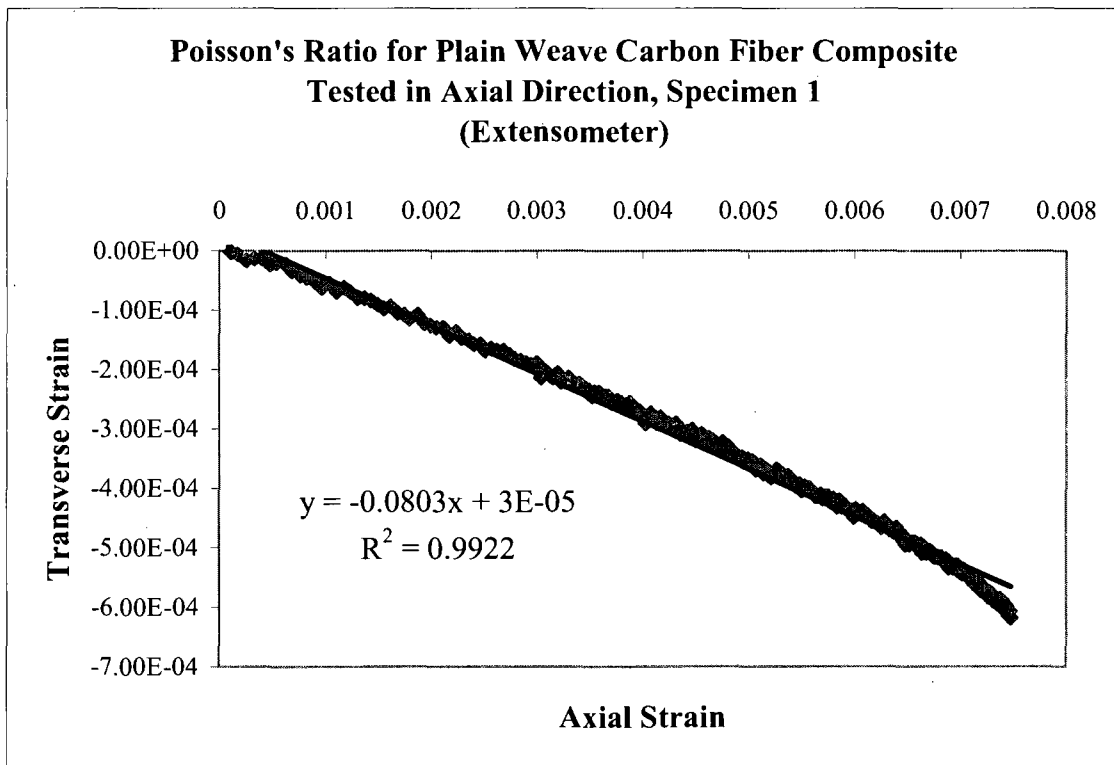




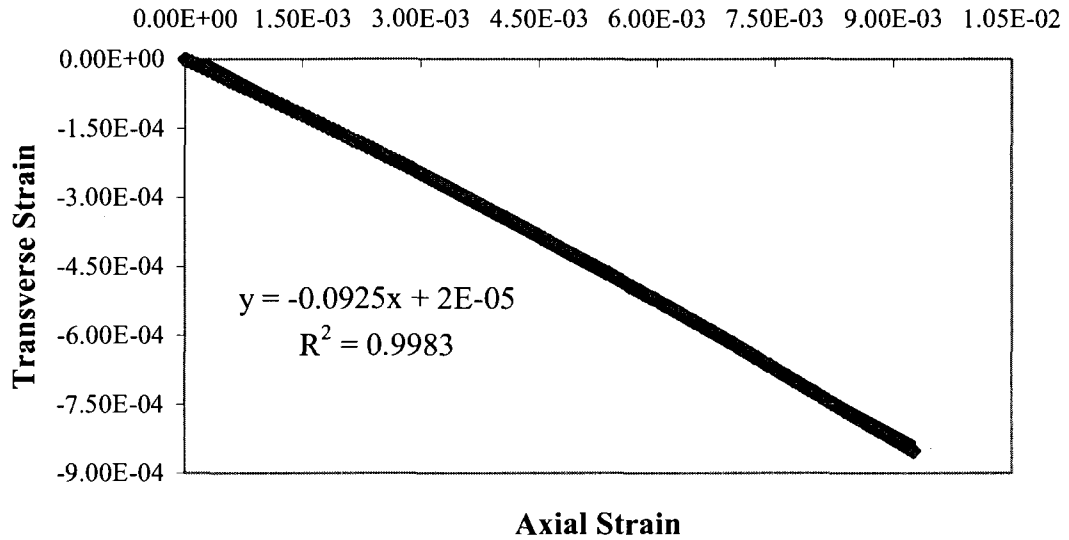
APPENDIX IV

AXIAL VS. TRANSVERSE STRAIN PLOTS FOR PLAIN WEAVE CARBON FIBER

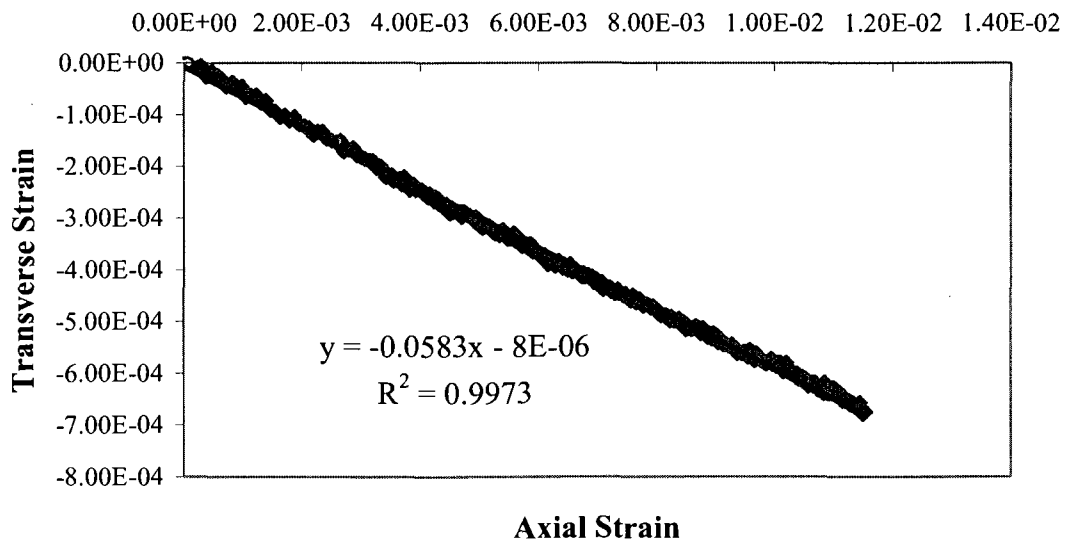
The remaining axial strain versus transverse strain plots for the carbon plain weave material are included in this appendix.



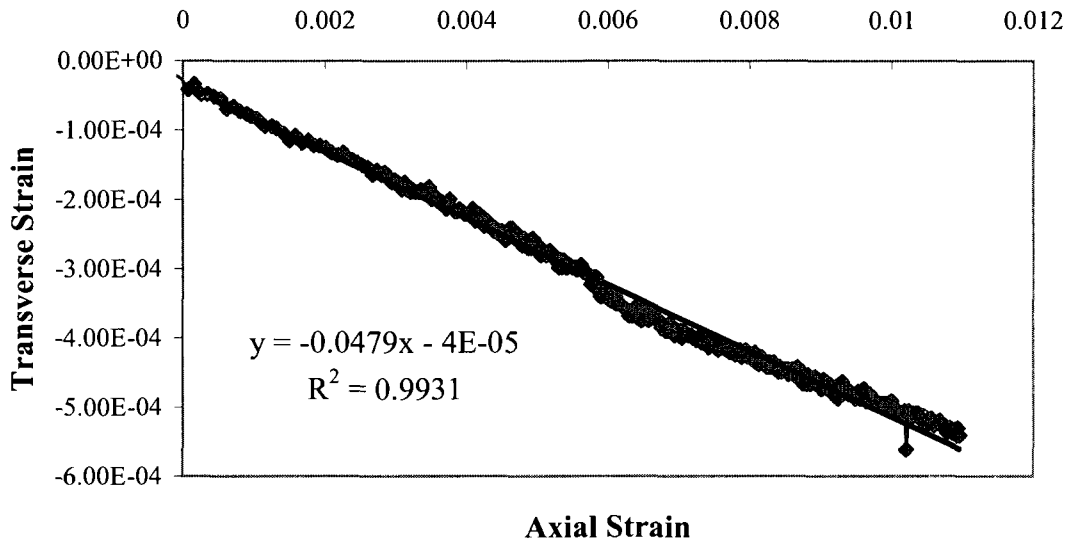
**Poisson's Ratio for Plain Weave Carbon Fiber Composite  
Tested in Axial Direction, Specimen 2  
(Strain Gages)**



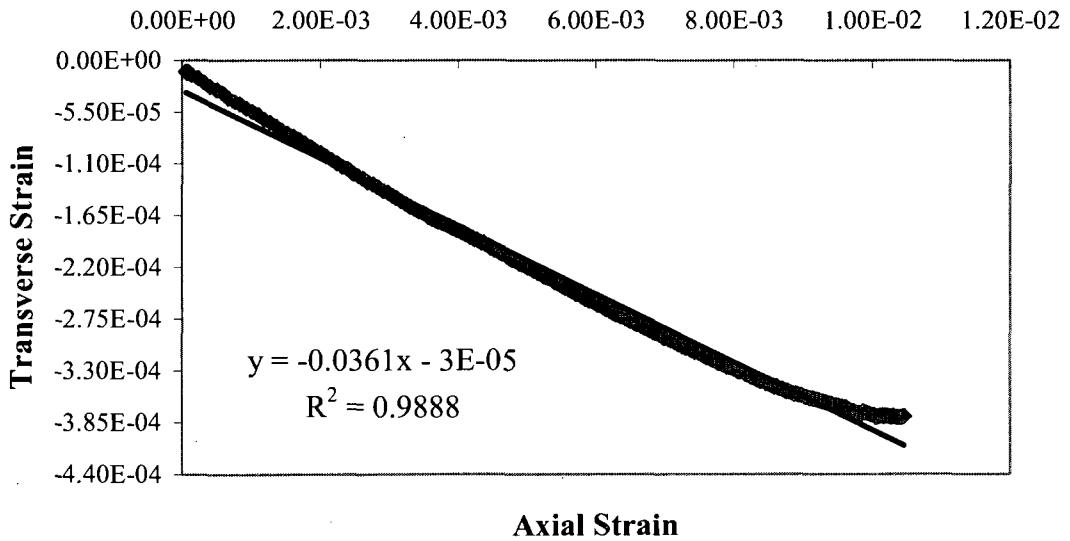
**Poisson's Ratio for Plain Weave Carbon Fiber Composite  
Tested in Axial Direction, Specimen 3  
(Extensometer)**



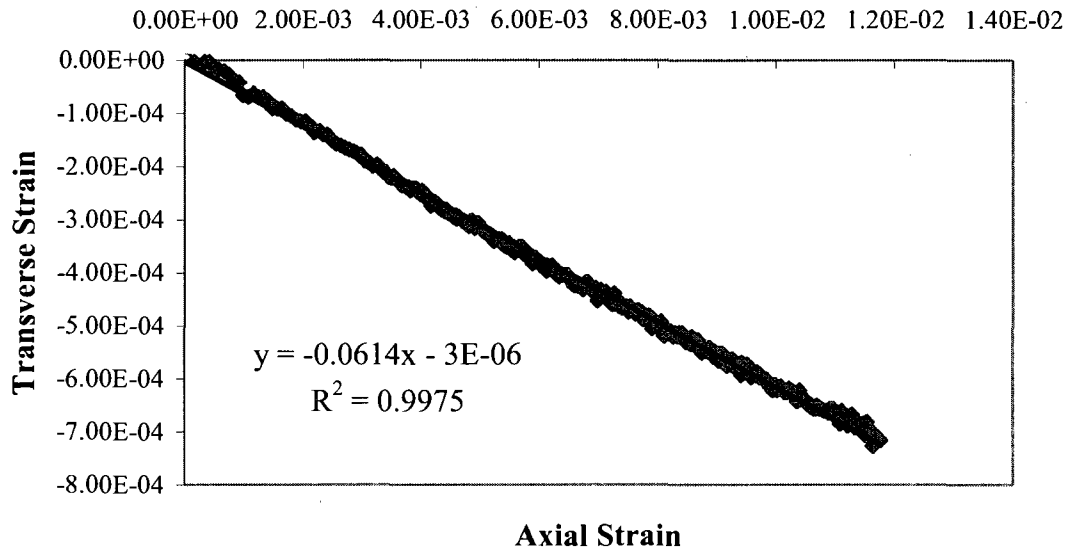
**Poisson's Ratio for Plain Weave Carbon Fiber Composite  
Tested in Axial Direction, Specimen 4  
(Extensometer)**



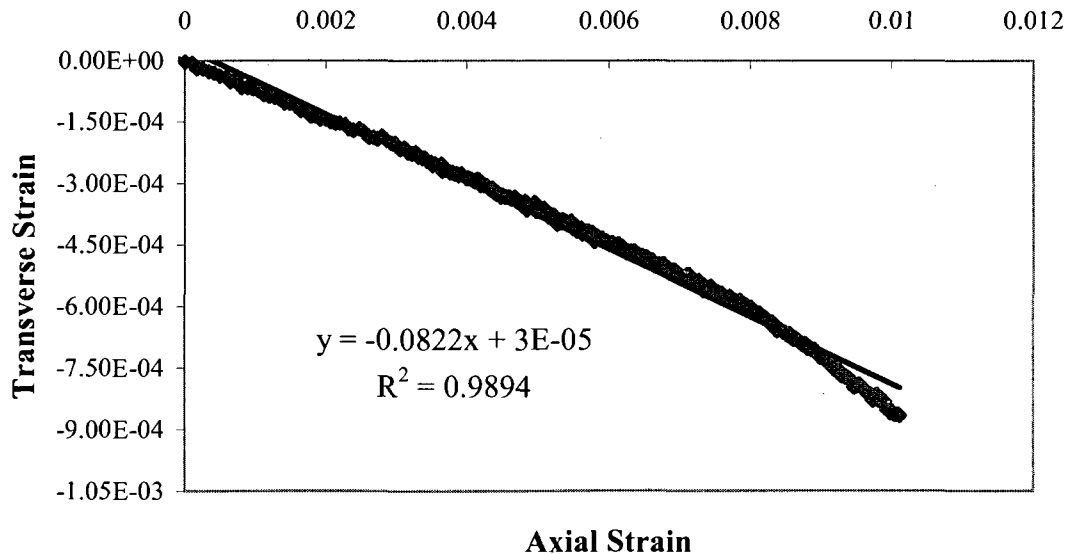
**Poisson's Ratio for Plain Weave Carbon Fiber Composite  
Tested in Axial Direction, Specimen 4  
(Strain Gages)**



**Poisson's Ratio for Plain Weave Carbon Fiber Composite  
Tested in Axial Direction, Specimen 5  
(Extensometer)**



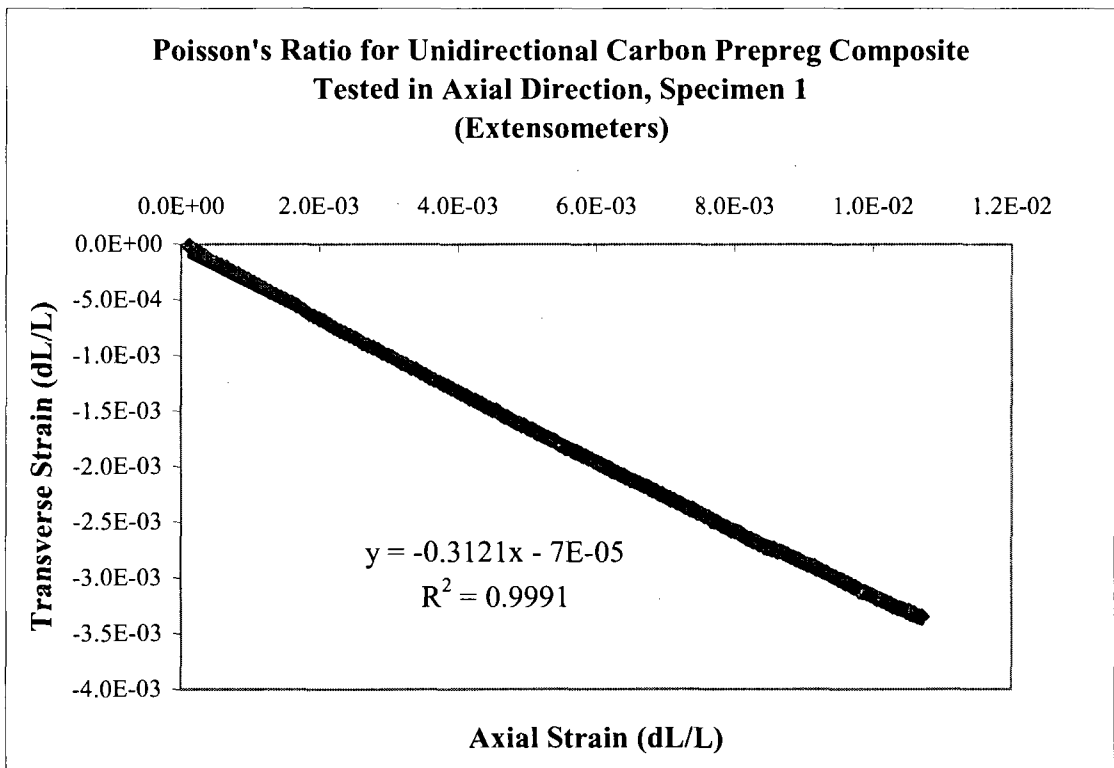
**Poisson's Ratio for Plain Weave Carbon Fiber Composite  
Tested in Axial Direction, Specimen 6  
(Extensometer)**



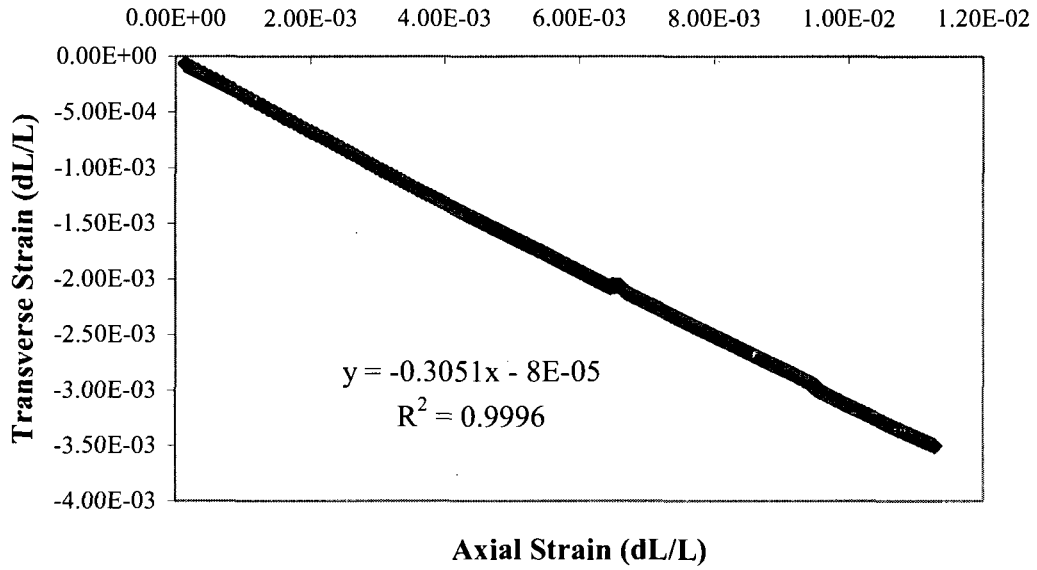
## APPENDIX V

### AXIAL VS. TRANSVERSE STRAIN PLOTS FOR PPREPREG CARBON FIBER

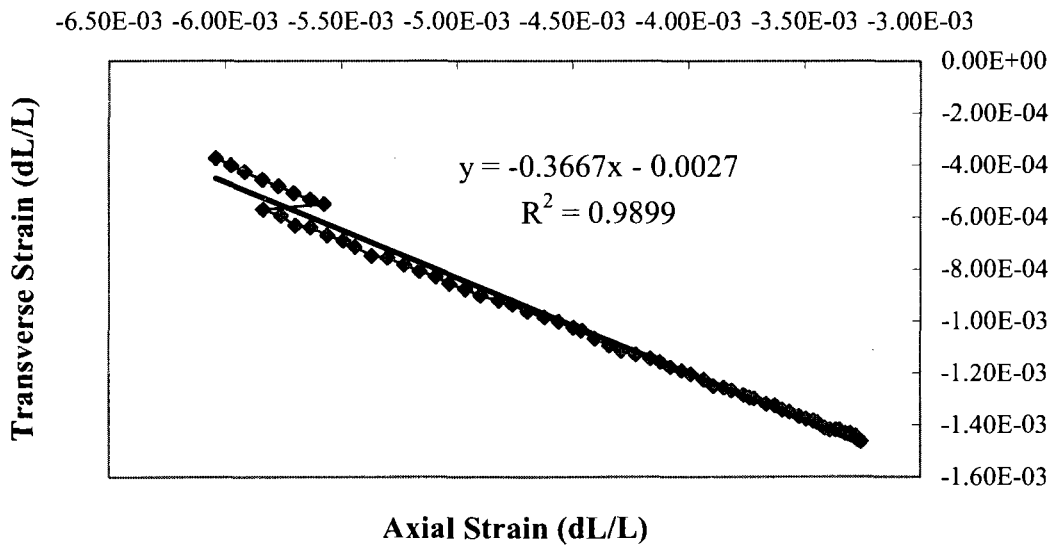
The remaining axial strain versus transverse strain plots for the carbon prepreg materials are included in this appendix.



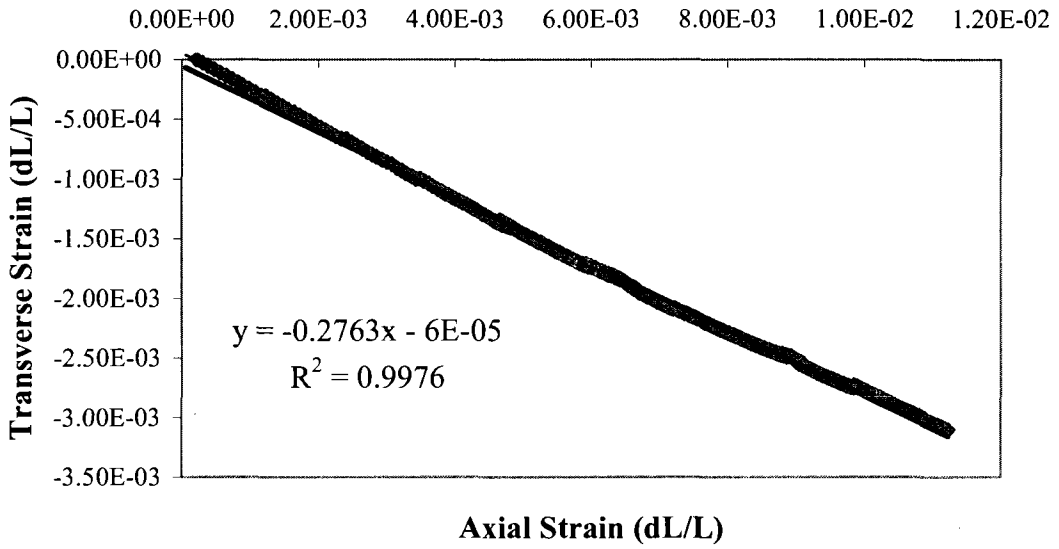
**Poisson's Ratio for Unidirectional Carbon Prepreg Composite  
Tested in Axial Direction, Specimen 2  
(Strain Gage)**



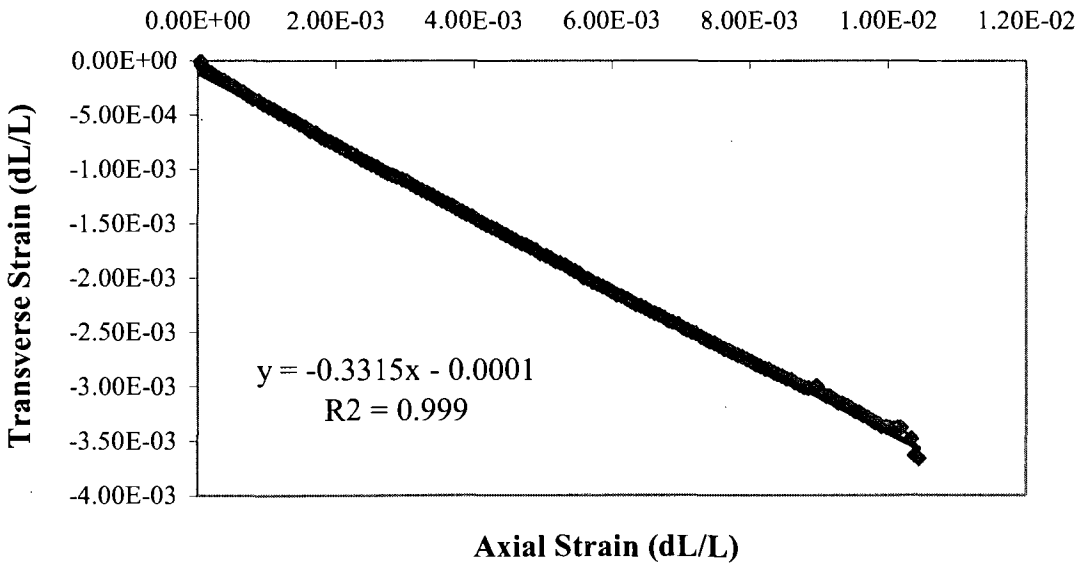
**Poisson's Ratio for Unidirectional Carbon Prepreg  
Composite Tested in Axial Direction, Specimen 3  
(Extensometer)**



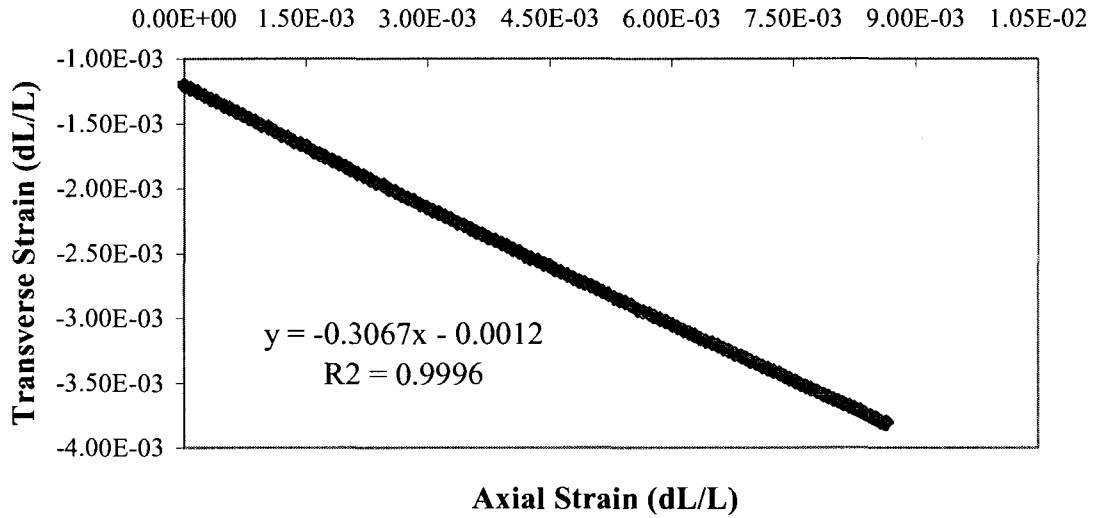
**Poisson's Ratio for Unidirectional Carbon Prepreg  
Composite Tested in Axial Direction, Specimen 3  
(Strain Gages)**



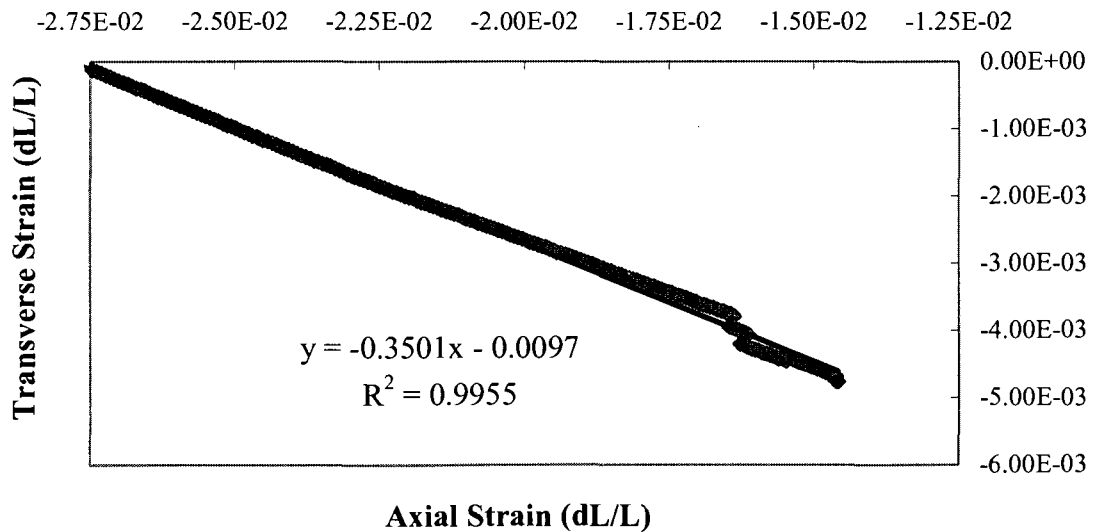
**Poisson's Ratio for Unidirectional Carbon Prepreg  
Composite Tested in Axial Direction, Specimen 4  
(Extensometer)**



**Poisson's Ratio for Unidirectional Carbon Prepreg  
Composite Tested in Axial Direction, Specimen 5  
(Extensometer)**



**Poisson's Ratio for Unidirectional Carbon Prepreg  
Composite Tested in Axial Direction, Specimen 6  
(Extensometer)**





## APPENDIX VI

### SAMPLE OPTISTRUCT REPORT FOR NACELLES

Sample OptiStruct report for the nacelle FEA analysis is shown here. The maximum displacement is in millimeters and the maximum 2-D element stress is in MPa.

# OptiStruct 7.0 Report

---

Problem submitted Tue Nov 18 12:28:57 2008

Input file C:/Documents and Settings/mstang96/Desktop/Thesis/FEA/Nacelle Skin.fem

## Problem summary

---

- Problem parameters: *C:/Documents and Settings/mstang96/Desktop/Thesis/FEA/Nacelle Skin.fem*
- Finite element model: *C:/Documents and Settings/mstang96/Desktop/Thesis/FEA/Nacelle Skin.fem*
- Output files prefix: *Nacelle Skin*

### ■ Finite element model information

Number of nodes: 15813  
Number of elements: 15586  
Number of degrees of freedom: 94632  
Number of non-zero stiffness terms: 2572824

- **Elements**

Number of QUAD4 elements: 15576  
Number of TRIA3 elements: 10

- **Loads and boundaries**

Number of FORCE sets: 1  
Number of SPC sets: 1

- **Materials and properties**

Number of PCOMP cards: 1  
Number of MAT8 cards: 1

### ■ Subcases & loadcases information

- **Static subcases**

Subcase ID	SPC ID	Force ID	Weight
1	1	2	1.00

## Results summary

---

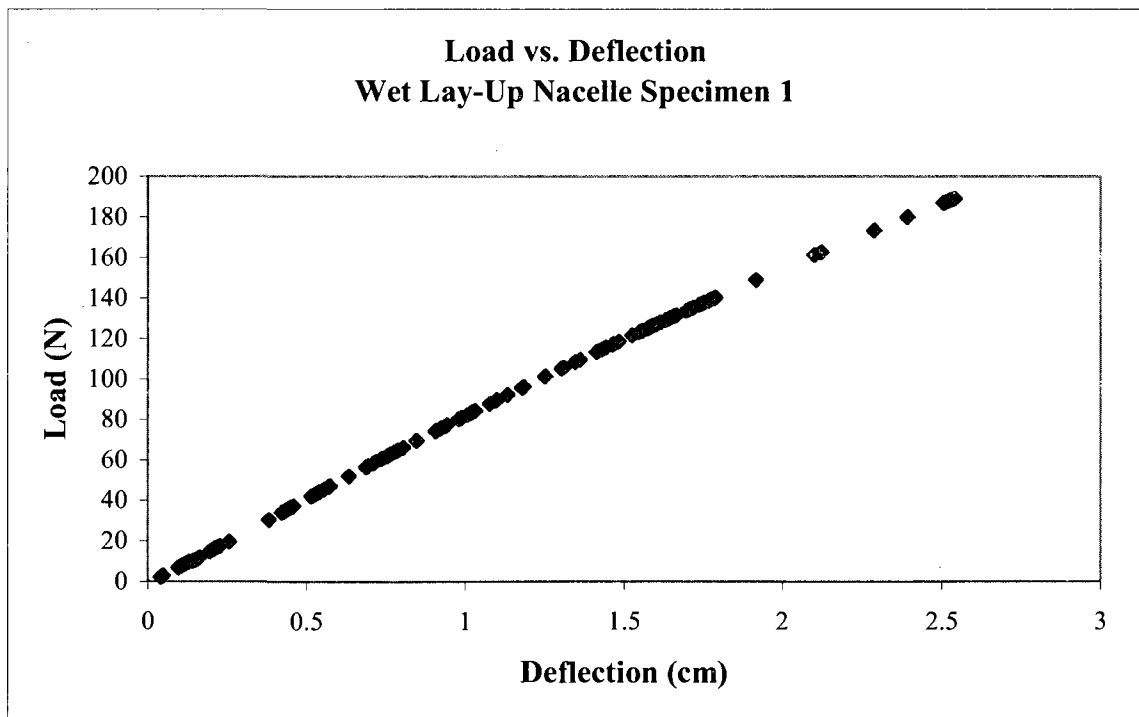
### ■ Subcase 1 - loadcol

- Maximum displacement is 99.3 at grid 10019.
- Maximum 2-D element stress is 236. in element 12181.

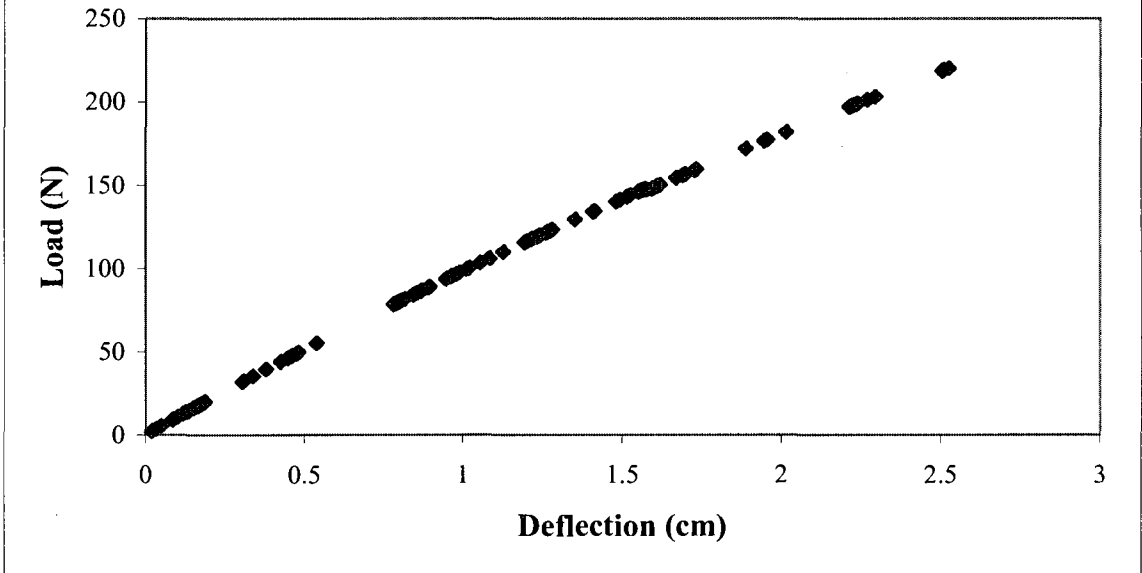
## APPENDIX VII

### LOAD VERSUS DEFLECTION PLOTS FOR NACELLES

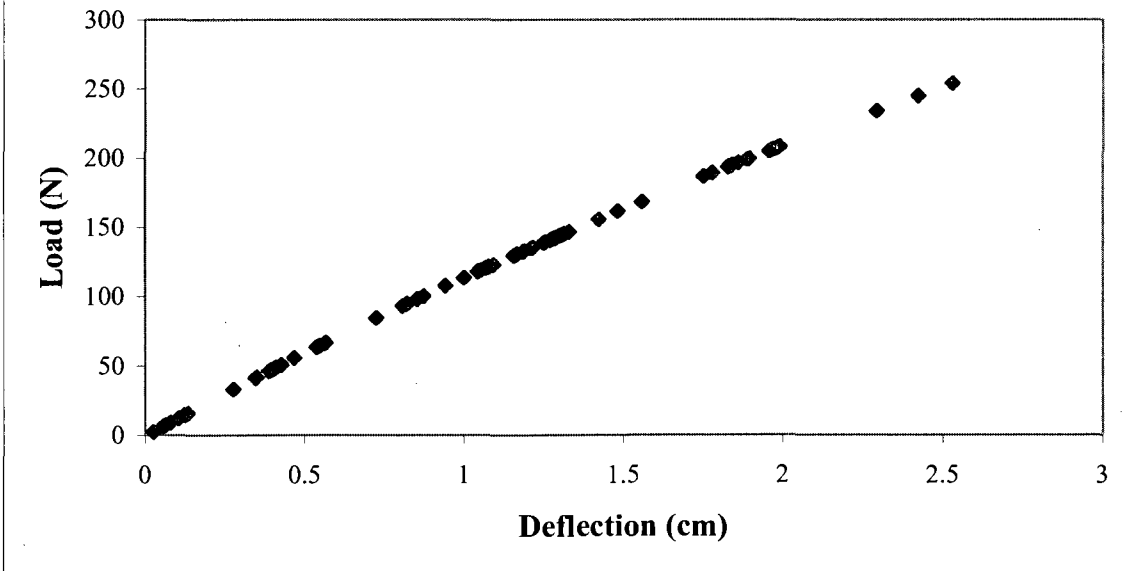
The remaining plots of load versus deflection for the nacelle compression tests are shown here.



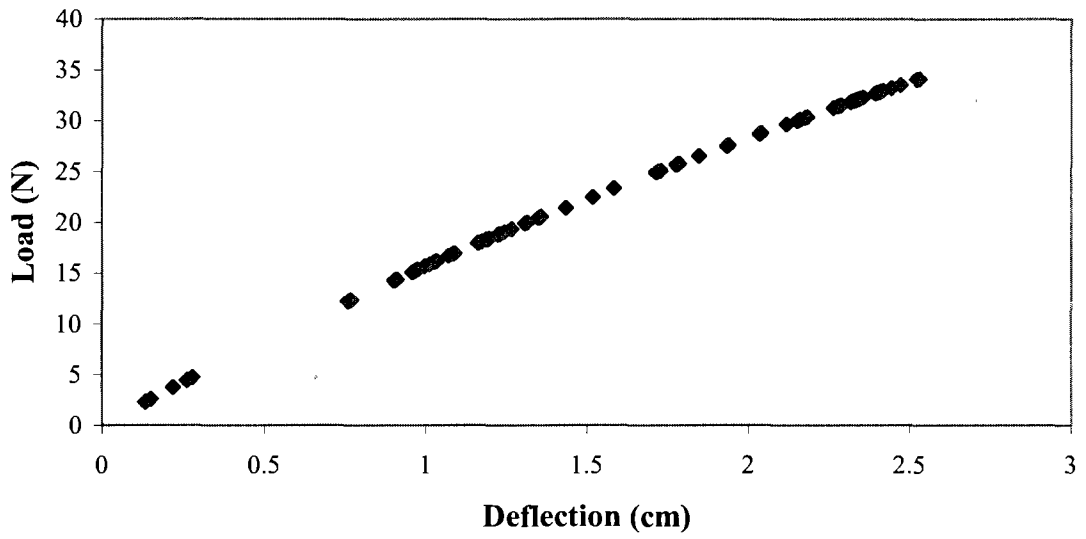
**Load vs. Deflection  
Woven Nacelle Specimen 3**



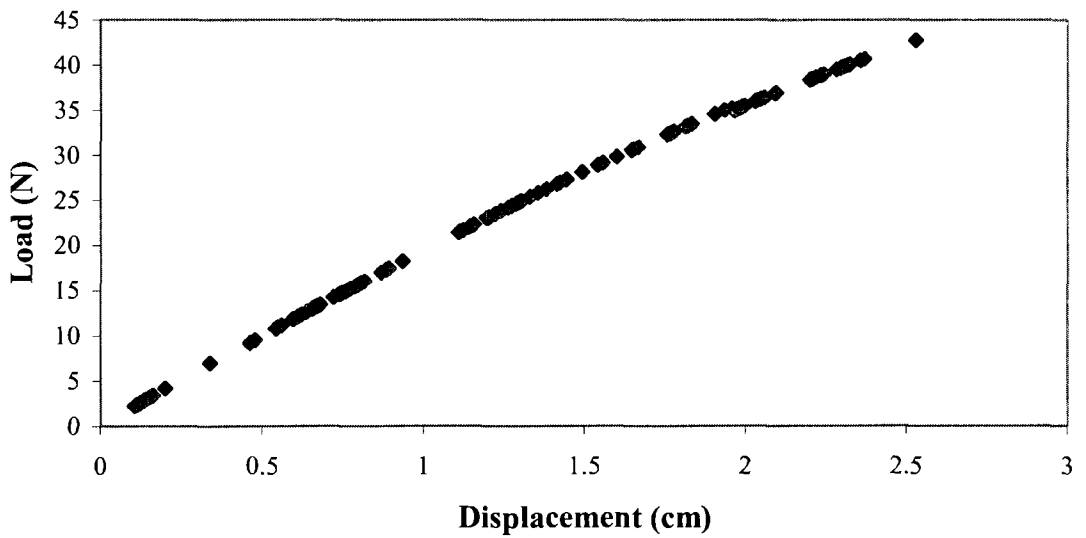
**Load vs. Deflection  
Woven Nacelle Specimen 4**



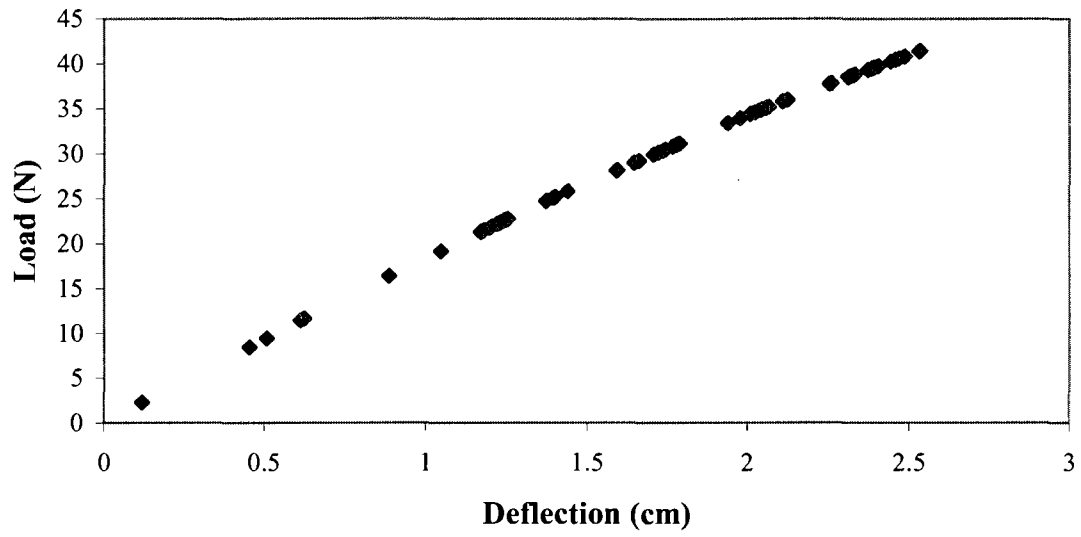
**Load vs. Deflection  
Prepreg Nacelle Specimen 2**



**Load vs. Deflection  
Prepreg Nacelle Specimen 3**



**Load vs. Deflection**  
**Prepreg Nacelle Specimen 4**



## APPENDIX VIII

### SAMPLE RADIOSS 9.0 REPORT FOR NACELLES

A sample Radioss report for the one inch deflection FEA simulations is shown here. The maximum displacement is in millimeters and the maximum 2-D element stress is in MPa. (Radioss replaces the OptiStruct 7 reports in HyperWorks 9.0. HyperWorks was upgraded to Version 9.0 in the spring of 2009 at the University of Nevada Las Vegas laboratories.)

# RADIOSS 9.0 Report

---

Problem submitted Fri Apr 10 15:18:42 2009

Input file C:/Documents and Settings/mstang96/Desktop/Thesis/FEA/Nacelle Skin Prepreg.fem

## Problem summary

---

- Problem parameters: *C:/Documents and Settings/mstang96/Desktop/Thesis/FEA/Nacelle Skin Prepreg.fem*
- Finite element model: *C:/Documents and Settings/mstang96/Desktop/Thesis/FEA/Nacelle Skin Prepreg.fem*
- Output files prefix: *Nacelle Skin Prepreg*

### ■ Finite element model information

Number of nodes: 15813  
Number of elements: 15586  
Number of degrees of freedom: 94710  
Number of non-zero stiffness terms: 2576229

#### • Elements

Number of QUAD4 elements: 15576  
Number of TRIA3 elements: 10

#### • Loads and boundaries

Number of FORCE sets: 1  
Number of SPC sets: 1

#### • Materials and properties

Number of PCOMP(G) cards: 1  
Number of MATB cards: 1

### ■ Subcases & loadcases information

#### • Static subcases

Subcase ID	SPC ID	Force ID	Weight
1	1	2	1.00

## Results summary

---

### ■ Subcase 1 - loadcol

- Maximum displacement is 25.4 at grid 63.
- Maximum 2-D element stress is 250. in element 1435.



## REFERENCES

- [1] Goebel, Greg “[17.0] Miniature UAVs”, *In the Public Domain*.  
[http://www.vectorsite.net/twuav\\_17.html](http://www.vectorsite.net/twuav_17.html).
- [2] Soutis, C., “Fibre reinforced composites in aircraft construction,” *Progress in Aerospace Sciences*, Volume 41, 2005, pp. 143-151.
- [3] Uzawa, K. et al., “Low cost fabrication of HOPE-X all-composite prototype structure,” *Advanced Composite Materials*, Volume 14, No. 3, 2005, pp. 289-304 .
- [4] Niitsu, M. et al., “HOPE-X: Development of the Japanese All-Composite Prototype Re-Entry Vehicle Structure,” *SAMPE Journal*, Volume 38, Issue 4, 2002, pp. 34-39.
- [5] Kotwani, K., “Design and Development of Fully Composite Mini Unmanned Aerial Vehicle (Mini-UAV).” 2003.
- [6] Chou, J.R., Hsiao, S.W., “Product design and prototype making for an electric scooter,” *Materials and Design*, Volume 26, 2005, pp. 439-449.
- [7] O’Donnchadha, B., Tansey, A., “A note on rapid metal composite tooling by selective laser sintering,” *Journal of Materials Processing Technology*, 2004, pp. 28-34.
- [8] Chang, F.K., Kutlu, Z., “Mechanical behavior of cylindrical composite tubes under transverse compressive loads,” *32<sup>nd</sup> International SAMPE Symposium and Exhibition*, Volume 32, 1987, pp. 698-707.
- [9] McLarty, D., “Selection of a Composite Tooling Material.” *34<sup>th</sup> International SAMPE Symposium and Exhibition*, Volume 34, Book 1 of 2, pp. 1294-1305, 1989.
- [10] Tomita, Y., Tempaku, M., “Effect of fiber strength on tensile fracture of unidirectional long carbon fiber-reinforced epoxy matrix composites”, *Materials Characterization*, Volume 38, Issue 2, Feb. 2006, pp. 91-96.
- [11] M. Kawai, M. Morishita, H. Satoh, S. Tomura, and K. Kemmochi, “Effects of end-tab shape on strain field of unidirectional carbon/epoxy composite specimens subjected to off-axis tension”, *Composites – Part A: Applied Science and Manufacturing*, Volume 28, Issue 3, 1997, pp. 267-275.

- [12] Akanda, S.R., Yuanxin, Z., Jeelani, S., "Effect of strain rate on tensile properties of carbon nanofiber-reinforced SC-15 epoxy", *Annual Technical Conference: Plastics Encounter at ANTEC 2007*, Conference Proceedings, 2007, pp. 1388-1392.
- [13] Mallick, P.K., *Fiber-Reinforced Composites: Materials, Manufacturing, and Design*, Marcel-Dekker Inc. 1993.
- [14] Kamrani, A., Nasr, E. A., *Rapid Prototyping: Theory and Practice*, Springer, 2006.
- [15] Beaman, J. J. et al., *A New Direction in Manufacturing with Research and Applications in Thermal Laser Processing*, kluwer Academic Publishers, 1997.
- [16] Chuk, R. N., Thomson, V. J., "A comparison of rapid prototyping techniques used for wind tunnel model fabrication", *Rapid Prototyping Journal*, Vol. 4 No. 4, 1998, pp. 185-196.
- [17] RedEye RPM. <http://www.redeyeondemand.com>.
- [18] Stratasys, Inc. <http://www.stratasys.com>.
- [19] 3D Systems. <http://www.3dsystems.com>
- [20] Solid Concepts. <http://www.solidconcepts.com>.
- [21] DSM Somos. <http://www.dsm.com>.
- [22] Nelson, S., O'Toole, B., Thota, J., "Characterization of a unidirectional carbon fiber/epoxy composite for prototype design", SAMPE 2008 Conference, Long Beach, CA.
- [23] NACA 4 Digits [sic] Series Profile Generator.  
<http://www.ppart.de/aerodynamics/profiles/NACA4.html>
- [24] "Moldless Composite Sandwich Homebuilt Aircraft Construction," Rutan Aircraft Factory, Inc., 1983.
- [25] "Carbon Cadillac: Human Powered Vehicle Design Report." ASME Human Powered Vehicle Competition, April 23-25, 2004, Corvallis, OR.
- [26] PBHT-30 [Internet]. [updated 2006 April]. Orange (CA): Coastal Enterprises; [cited 2008 Oct 6]. Available from: <http://www.precisionboard.com/Ind/pbht-30.pdf>

## VITA

Graduate College  
University of Nevada, Las Vegas

Kimberly Lynn Clark

### Home Address:

4191 South Pearl Street  
Las Vegas, Nevada 89121

### Degrees:

Bachelor of Science, Mechanical Engineering, 2006  
University of Nevada, Las Vegas

### Professional Memberships and Societies:

American Nuclear Society (ANS)  
American Society of Mechanical Engineers (ASME)  
Society for the Advancement of Material and Process Engineering (SAMPE)  
Tau Beta Pi Engineering Honor Society

### Special Honors and Awards:

Mildred P. Cotner Scholarship, 2001-2005  
O'Rourke Engineering Scholarship, 2005  
Dean's List 4 Semesters as Undergraduate  
Honor's College, UNLV 2001-2006

Thesis Title: Design and Fabrication of a Small Prototype Airframe Structure

### Thesis Examination Committee:

Chairperson, Dr. Brendan O'Toole, Ph.D.  
Committee Member, Dr. William Culbreth, Ph.D.  
Committee Member, Dr. Zhiyong Wang, Ph.D.  
Graduate Faculty Representative, Dr. Samaan Ladkany, Ph.D.